



**TIM LINDEN**

---

**THE RISE OF THE LEPTONS  
PULSAR EMISSION DOMINATES THE TEV GAMMA-RAY SKY**

Imperial College London Brown-Bag Talk

July 6, 2017



**THE OHIO STATE UNIVERSITY**  
CENTER FOR COSMOLOGY AND  
ASTROPARTICLE PHYSICS



**TIM LINDEN**

---

**THE RISE OF THE LEPTONS**  
**PULSAR EMISSION DOMINATES THE TEV GAMMA-RAY SKY**

**WITH: KATIE AUCHETTL, BEN BUCKMAN,  
JOSEPH BRAMANTE, ILIAS CHOLIS, KE FANG,  
DAN HOOPER, SHIRLEY LI**



**Start with a source of relativistic cosmic-rays**

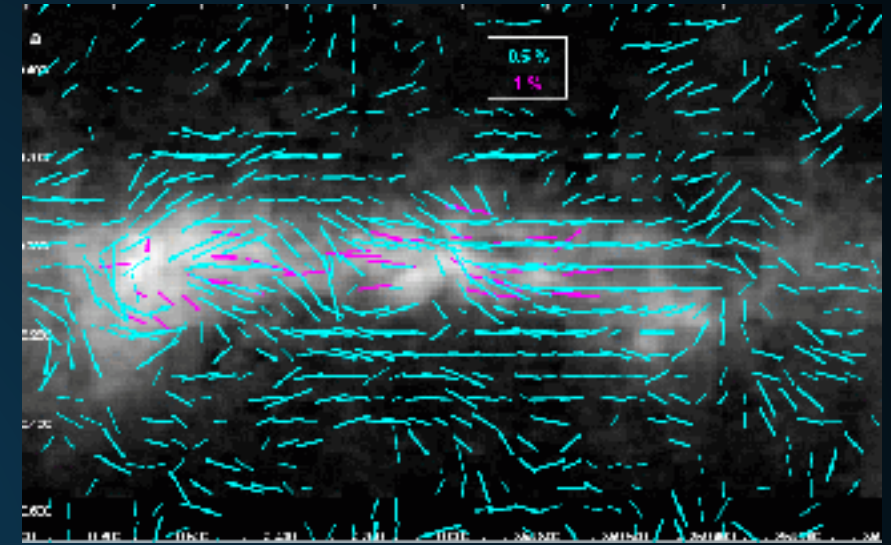
- ▶ **Supernova Explosions**
- ▶ **Supernova Remnants**
- ▶ **Pulsars**
- ▶ **Shocks/Mergers**

# COSMIC-RAY ACCELERATION AND PROPAGATION



Start with a source of relativistic cosmic-rays

cosmic rays propagate



$$\frac{\partial \psi}{\partial t} = q(\vec{r}, p) + \vec{\nabla} \cdot (D_{xx} \vec{\nabla} \psi - \vec{V} \psi) + \frac{\partial}{\partial p} p^2 D_{pp} \frac{\partial}{\partial p} \frac{1}{p^2} \psi - \frac{\partial}{\partial p} \left[ \dot{p} \psi - \frac{p}{3} (\vec{\nabla} \cdot \vec{V}) \psi \right] - \frac{1}{\tau_f} \psi - \frac{1}{\tau_r} \psi$$

Solved Numerically:  
e.g. Galprop

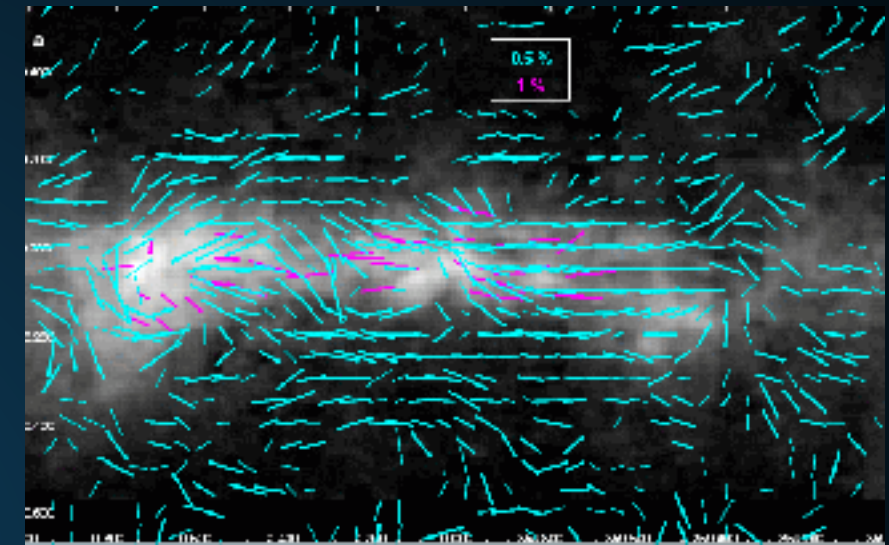
- ▶ If they propagate to Earth, can be detected:
- ▶ AMS-02/PAMELA
- ▶ CREAM/HEAT/CAPRICE

# COSMIC-RAY ACCELERATION AND PROPAGATION



Start with a source of relativistic cosmic-rays

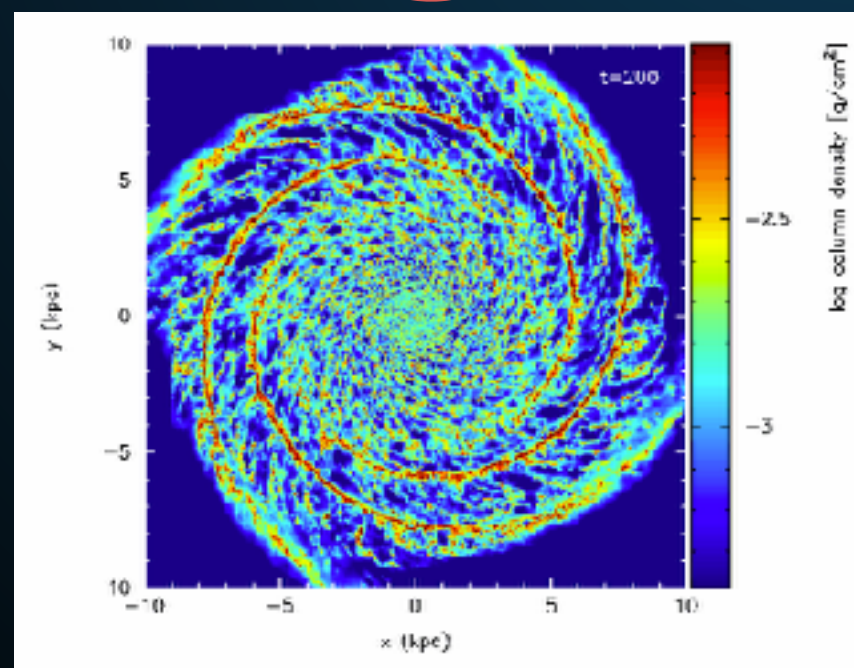
cosmic rays propagate



$$\frac{\partial \psi}{\partial t} = q(\vec{r}, p) + \vec{\nabla} \cdot (D_{xx} \vec{\nabla} \psi - \vec{V} \psi) + \frac{\partial}{\partial p} p^2 D_{pp} \frac{\partial}{\partial p} \frac{1}{p^2} \psi - \frac{\partial}{\partial p} \left[ \dot{p} \psi - \frac{p}{3} (\vec{\nabla} \cdot \vec{V}) \psi \right] - \frac{1}{\tau_f} \psi - \frac{1}{\tau_r} \psi$$

Solved Numerically:  
e.g. Galprop

Gas/ISRF



- ▶ Alternatively can collide with Galactic gas or the interstellar radiation field.

# COSMIC-RAY ACCELERATION AND PROPAGATION



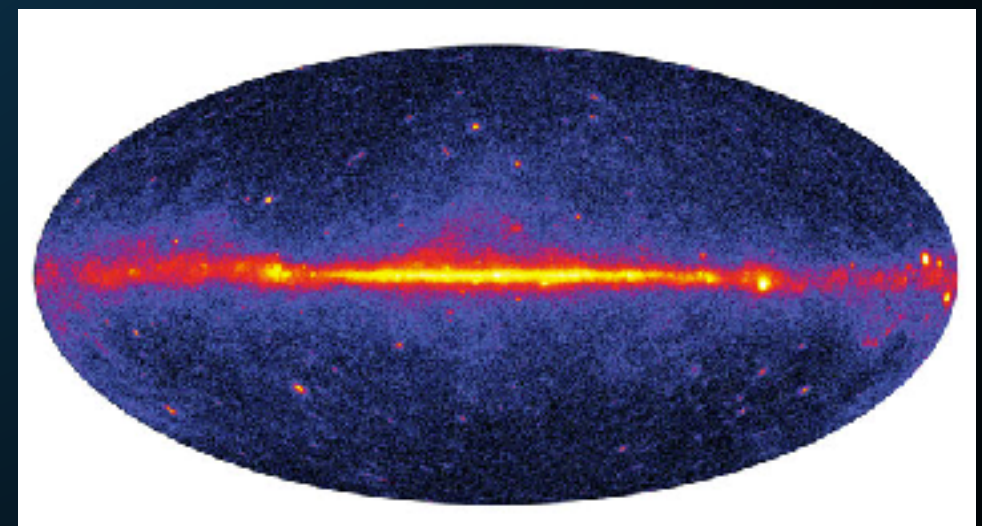
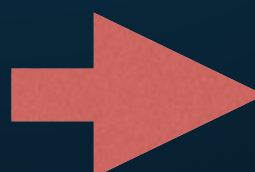
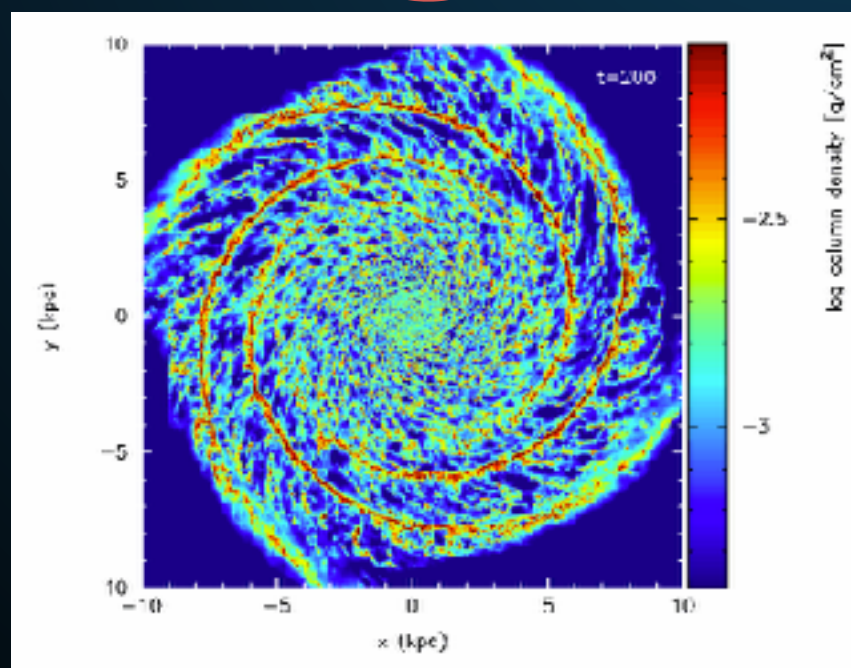
Start with a source of relativistic cosmic-rays

cosmic rays propagate

$$\frac{\partial \psi}{\partial t} = q(\vec{r}, p) + \vec{\nabla} \cdot (D_{xx} \vec{\nabla} \psi - \vec{V} \psi) + \frac{\partial}{\partial p} p^2 D_{pp} \frac{\partial}{\partial p} \frac{1}{p^2} \psi - \frac{\partial}{\partial p} \left[ \dot{p} \psi - \frac{p}{3} (\vec{\nabla} \cdot \vec{V}) \psi \right] - \frac{1}{\tau_f} \psi - \frac{1}{\tau_r} \psi$$

Solved Numerically:  
e.g. Galprop

Gas/ISRF



## TWO DIFFERENT SOURCES OF INFORMATION

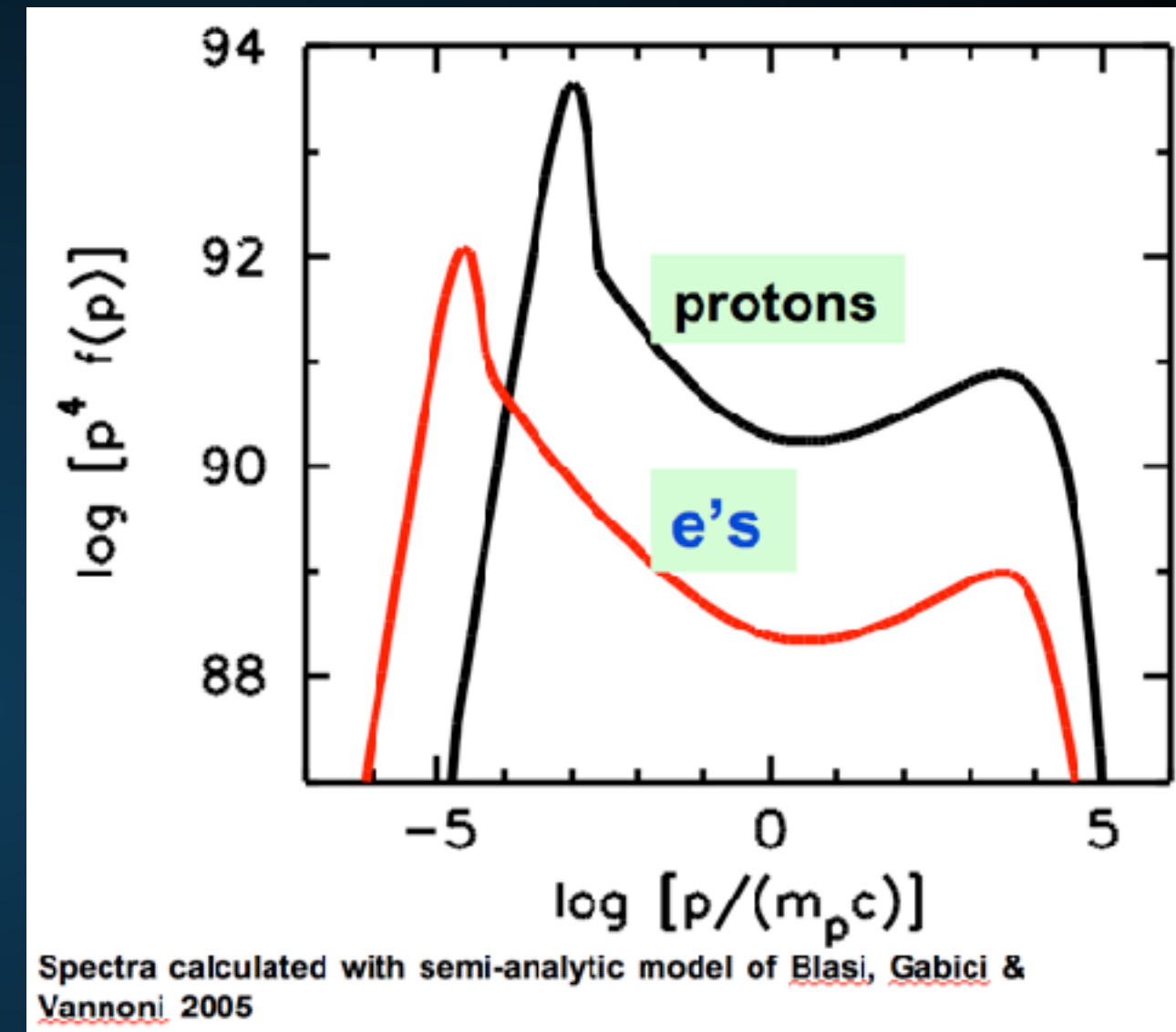
---

- ▶ This provides us two ways to learn about cosmic rays:
  - ▶ Investigating the cosmic-rays that directly hit satellites on Earth
    - ▶ Can directly detect cosmic-ray species
    - ▶ Only a local measurement
    - ▶ Solar Modulation
  - ▶ Investigating the gamma-ray signal from cosmic-ray interactions
    - ▶ Can understand propagation near sources
    - ▶ Don't directly know the cosmic-ray species, or even if the gamma-ray is galactic
    - ▶ Line of sight

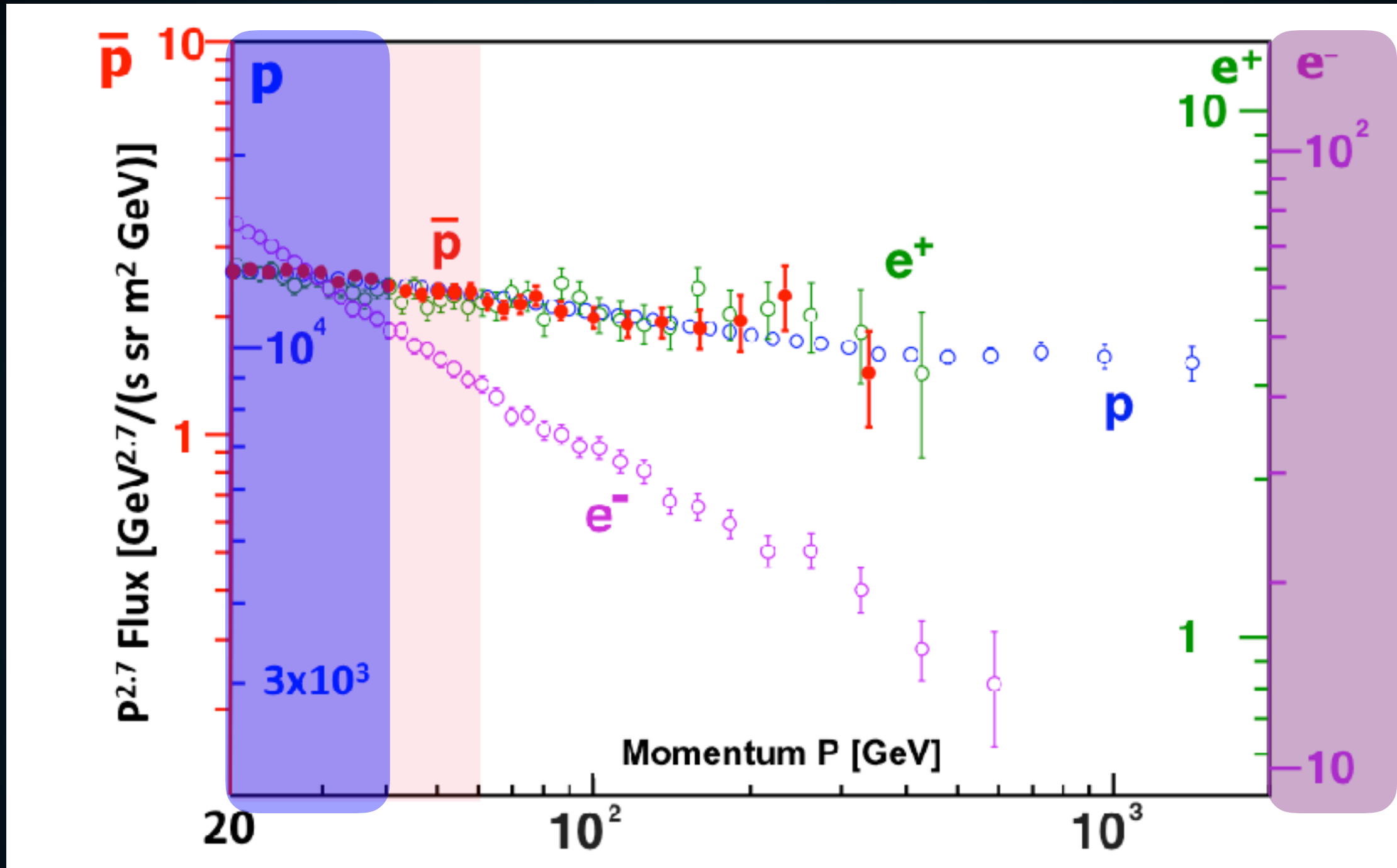
- ▶ Supernova remnants provide the only source energetic enough to explain the full energy spectrum of cosmic-ray protons up to PeV energies.

- ▶ First order Fermi acceleration naturally predicts protons dominate supernova energetics.

- ▶ Observationally confirmed by X-Ray observations of SNR synchrotron and gamma-ray measurements of hadronic interactions.

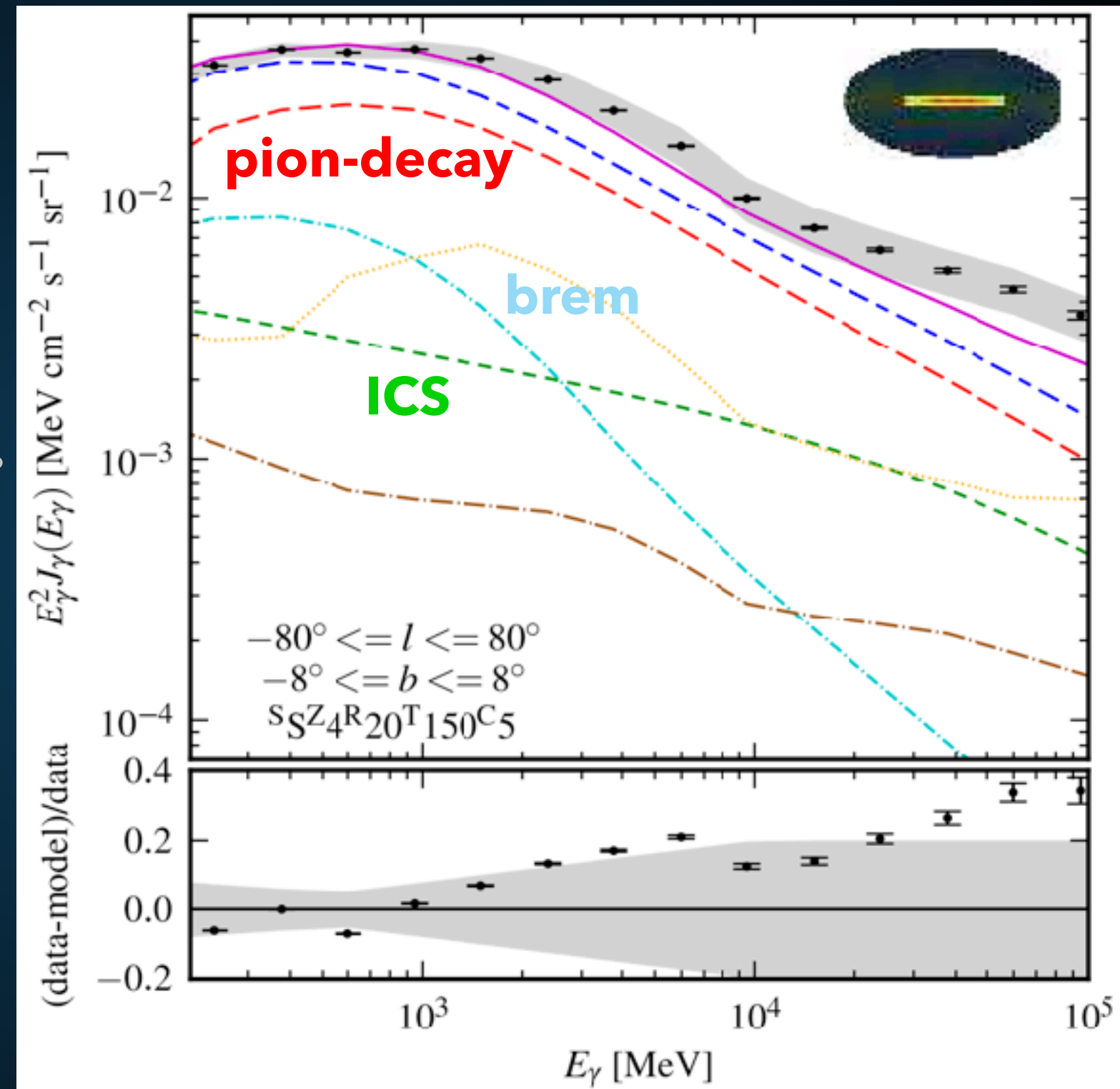


## LOCAL COSMIC-RAY OBSERVATIONS



- ▶ Protons are approximately 2-3 orders of magnitude more prevalent near the solar position.

- ▶ Models of GeV galactic diffuse emission indicate that hadronic emission mechanisms are highlight dominant.
- ▶ Models indicate a slightly larger leptonic fraction at high energies.



## A NEW PICTURE

---

- ▶ In this talk, I will instead argue that electrons and positrons dominate the Milky Way's energetics at TeV energies:
- ▶ 1.) Pulsars are responsible for the rising positron fraction observed by PAMELA/AMS-02
- ▶ 2.) Pulsars produce the majority of the bright TeV sources observed by CTA/HAWC/HESS etc.
- ▶ 3.) Pulsars produce the majority of the TeV gamma-ray emission observed from the Milky Way

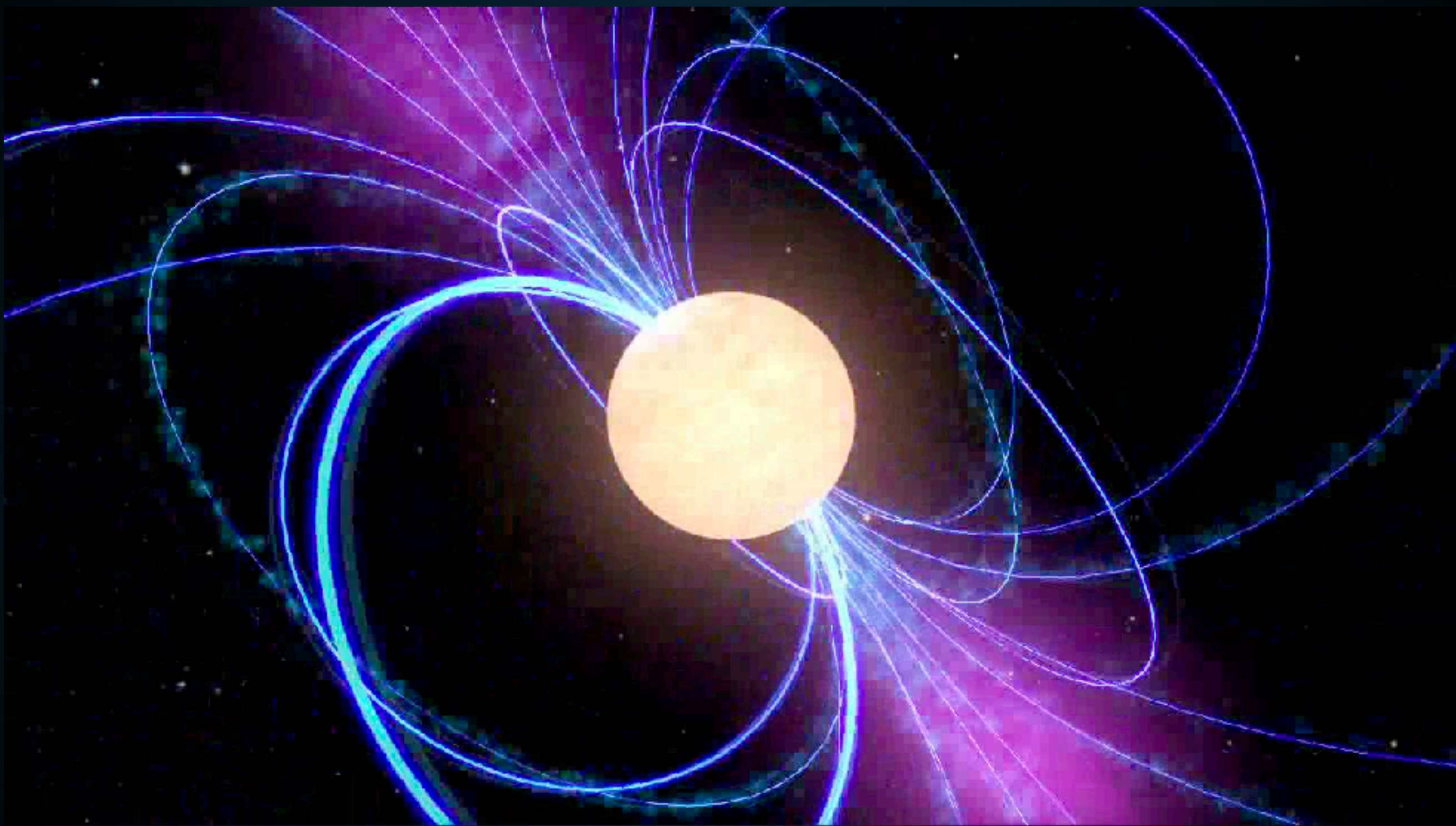
## A VERY SIMPLE MODEL OF PULSAR EMISSION

---

**Pulsars as high-energy particle accelerators**

## PULSARS AS ASTROPHYSICAL ACCELERATORS

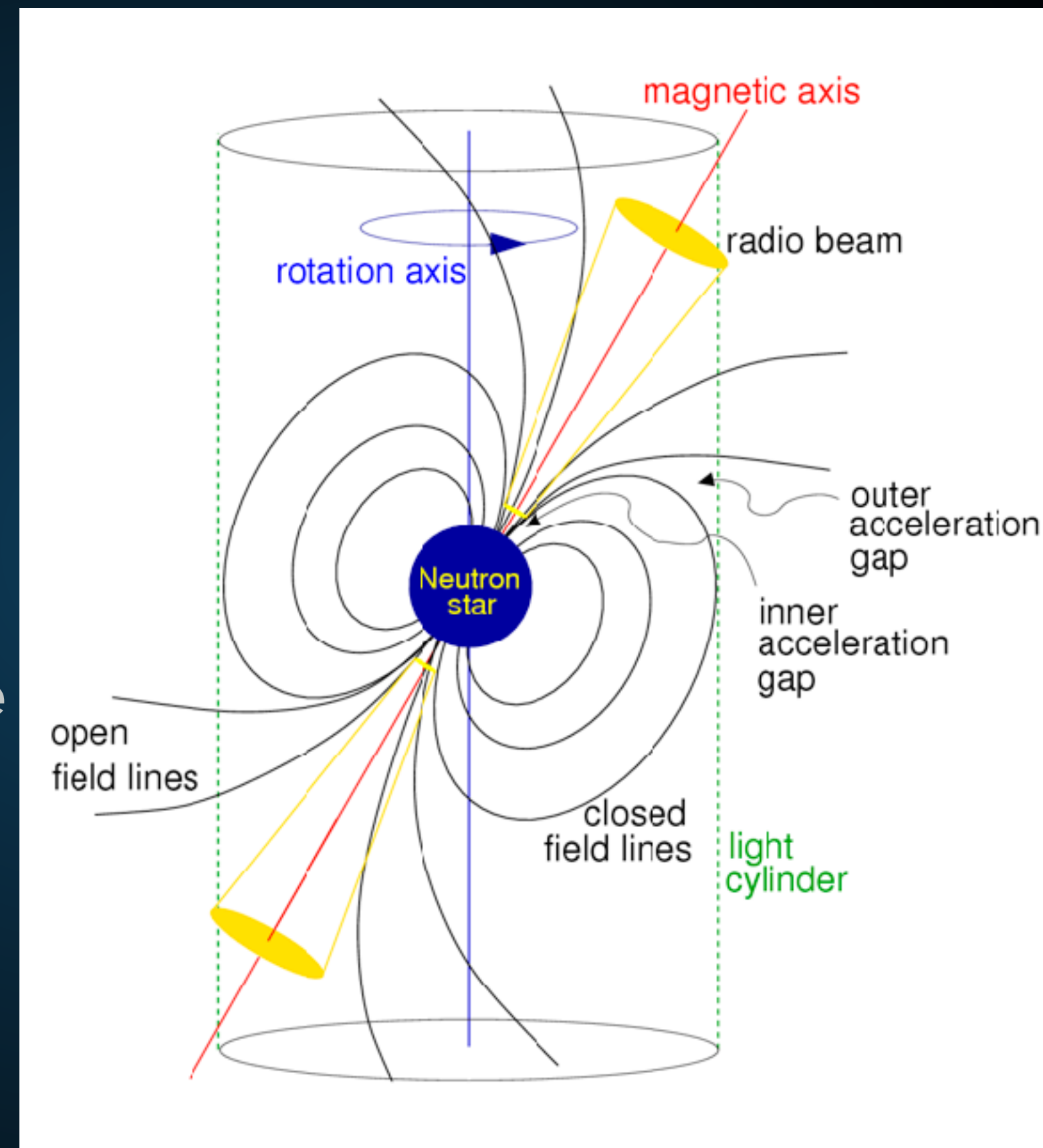
---



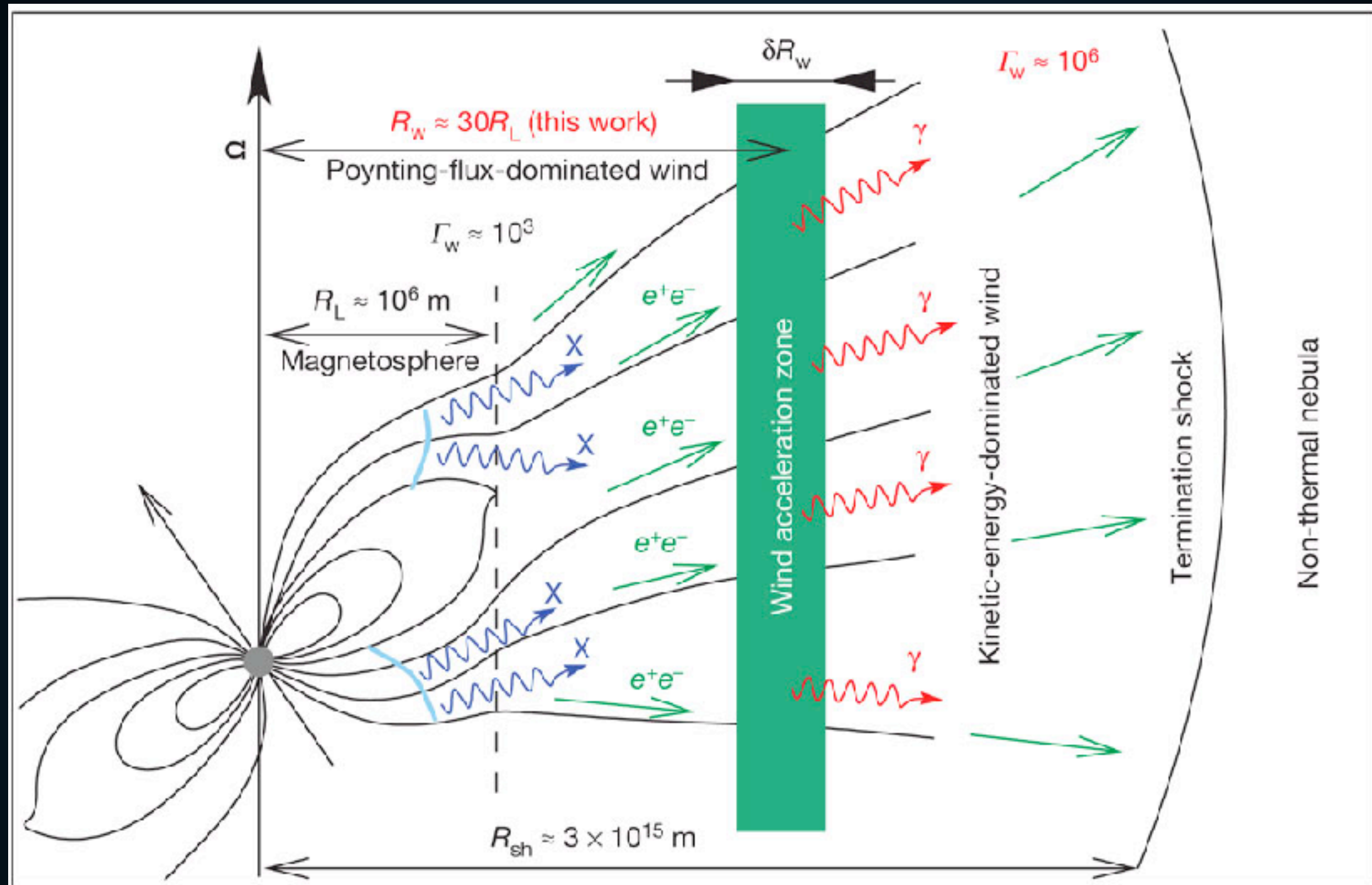
- ▶ Rotational Kinetic Energy of the neutron star is the ultimate power source of all emission in this problem.

# PULSARS AS ASTROPHYSICAL ACCELERATORS

- ▶ **radio beam**
- ▶ **gamma-ray beam**
- ▶  **$e^+e^-$  acceleration in pulsar magnetosphere**
- ▶  **$e^+e^-$  acceleration at termination shock**

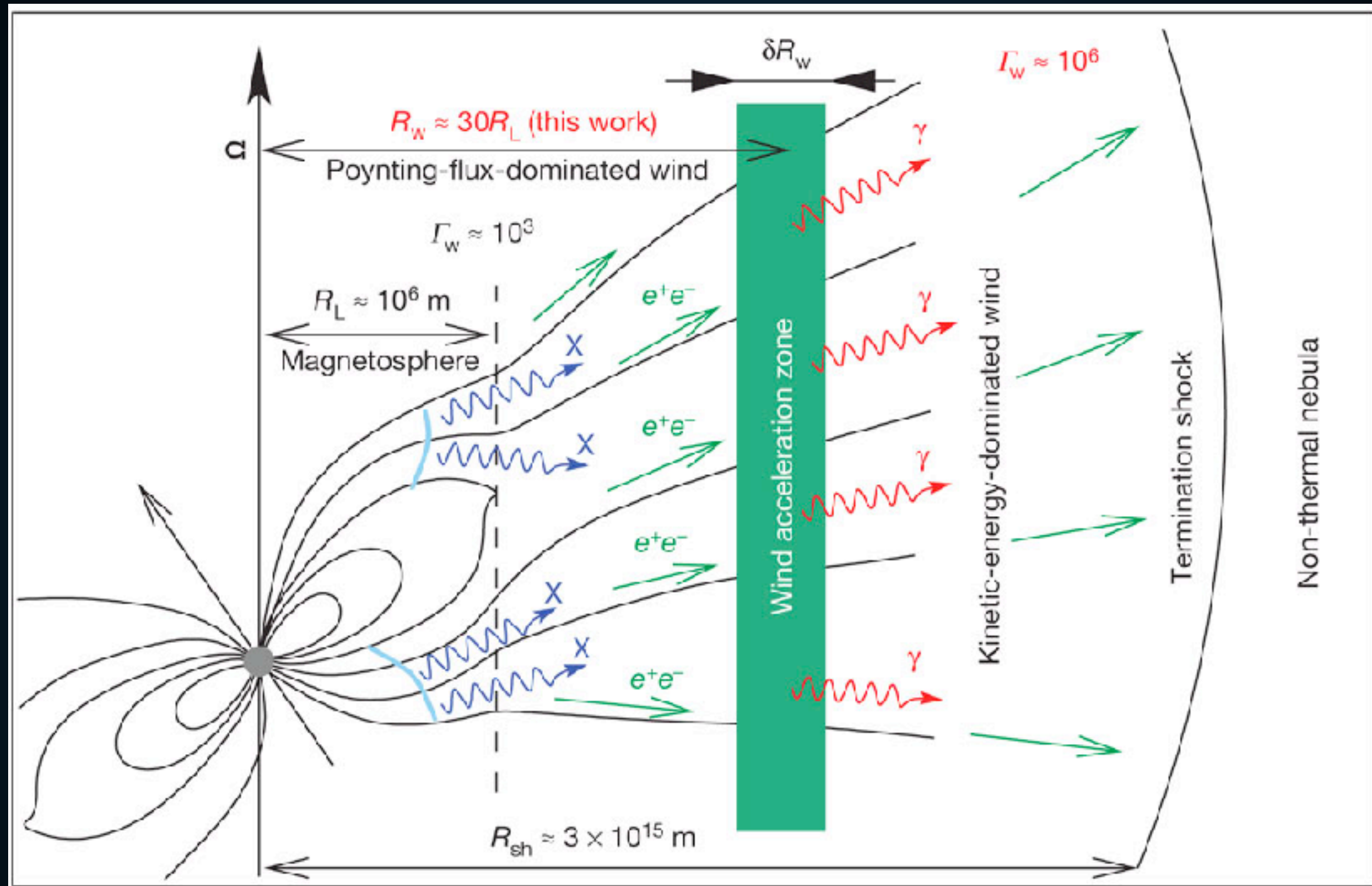


# PRODUCTION OF ELECTRON AND POSITRON PAIRS



- ▶ Electrons boiled off the pulsar surface produce  $e^+e^-$  pairs
- ▶ Pair multiplicity is high, but model dependent.

# PRODUCTION OF ELECTRON AND POSITRON PAIRS



- ▶ Final e<sup>+</sup>e<sup>-</sup> spectrum is model dependent.
- ▶ Understanding this is important for MSPs.

# REACCELERATION IN THE PULSAR WIND NEBULA



Blandford & Ostriker (1978)  
Hoshino et al. (1992)  
Coroniti (1990)  
Sironi & Spitkovsky (2011)

- ▶ **PWN termination shock:**
  - ▶ **Voltage Drop  $> 30$  PV**
  - ▶  **$e^+e^-$  energy  $> 1$  PeV  
(known from synchrotron)**
- ▶ **Resets  $e^+e^-$  spectrum.**
- ▶ **Many Possible Models:**
  - ▶ **1st Order Fermi-Acceleration**
  - ▶ **Magnetic Reconnection**
  - ▶ **Shock-Driven Reconnection**

## IN THIS TALK

---

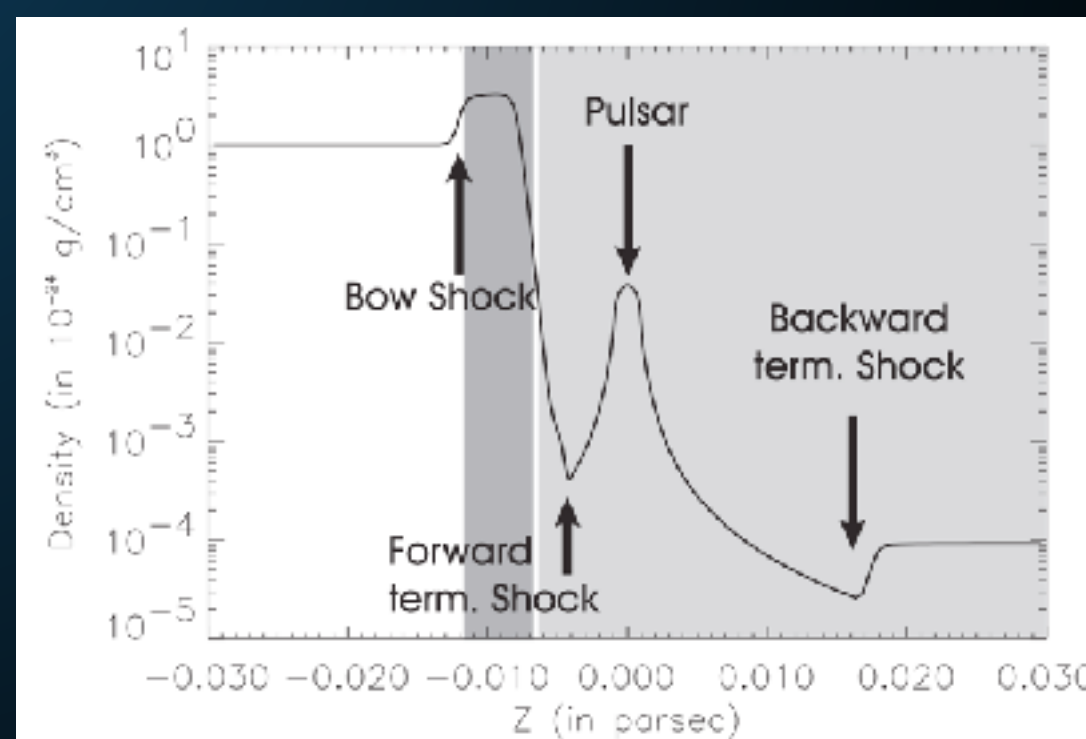
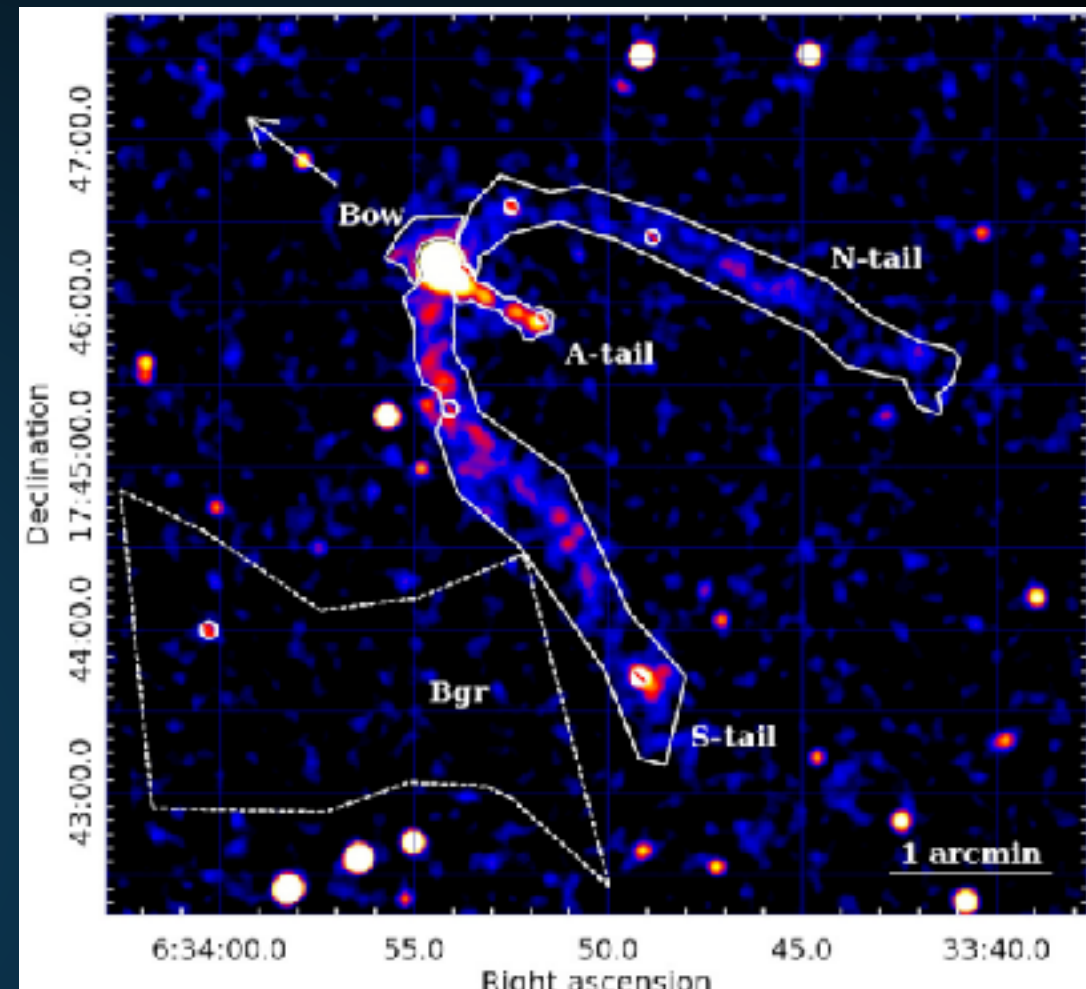
- ▶ Will remain agnostic to source of relativistic e+e-
- ▶ Will assume a simple power-law spectrum with an exponential cutoff:

$$\frac{dN}{dE} = E^{-\alpha} \exp(-E/E_{\text{cut}})$$

- ▶ Extent of radio and X-Ray PWN is approximately 1 pc.
- ▶ Termination shock produced when ISM energy density overwhelms and stops the relativistic pulsar wind.

$$R_{\text{PWN}} \simeq 1.5 \left( \frac{\dot{E}}{10^{35} \text{ erg/s}} \right)^{1/2} \times \left( \frac{n_{\text{gas}}}{1 \text{ cm}^{-3}} \right)^{-1/2} \left( \frac{v}{100 \text{ km/s}} \right)^{-3/2} \text{ pc}$$

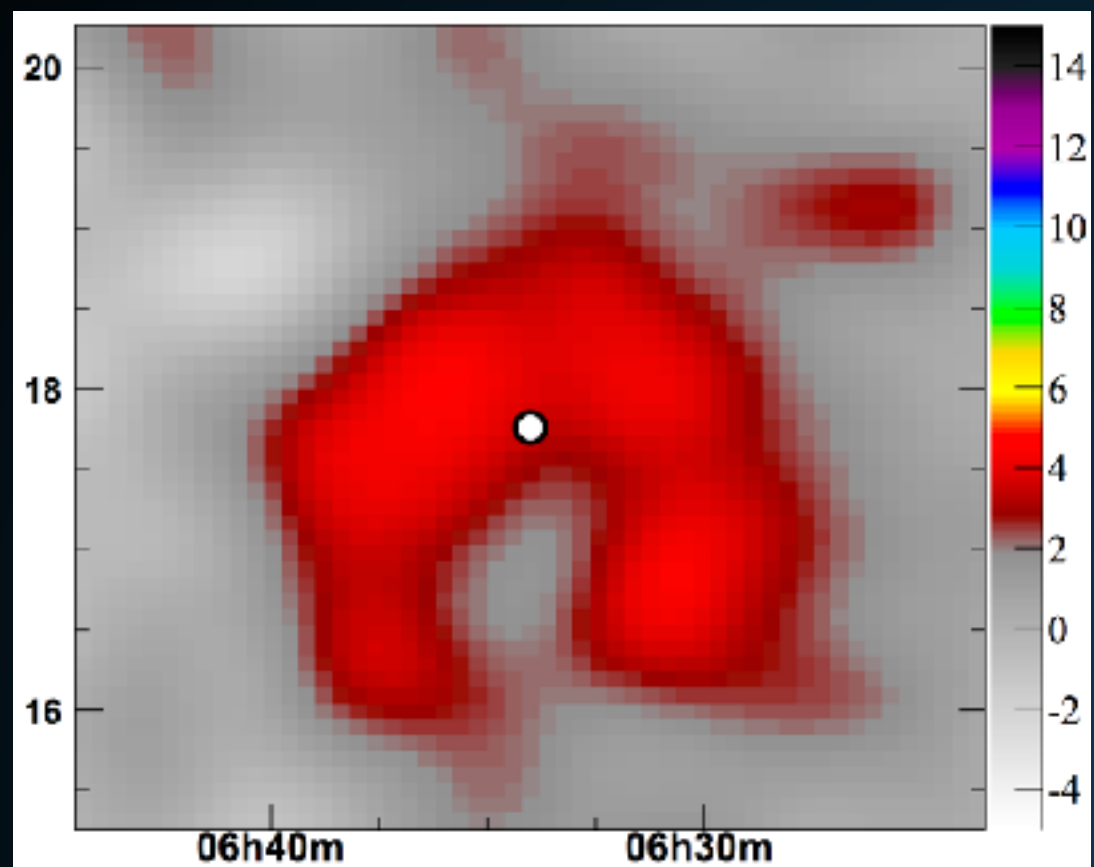
- ▶ **NOTE: The radial extent of PWN is explained by a known physical mechanism.**



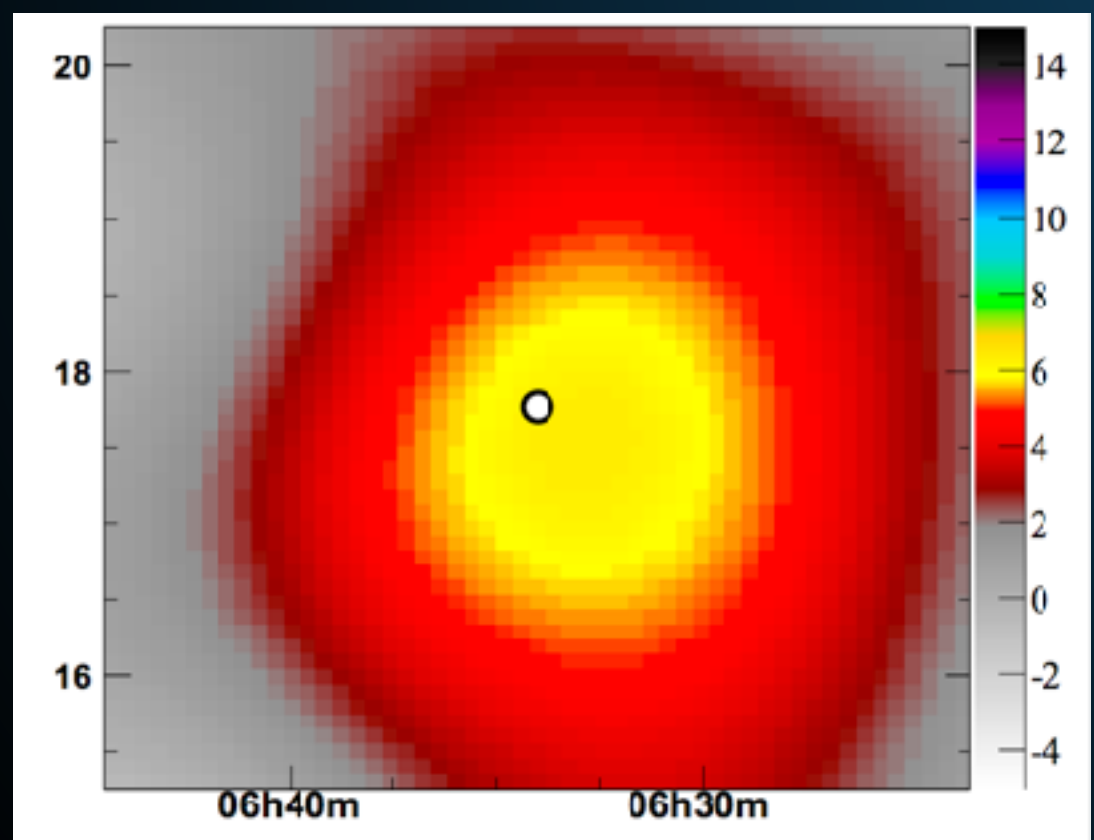
## TEV PULSAR OBSERVATIONS

---

**TeV observations inform pulsar models**



- ▶ Milagro observes very extended emission from Geminga ( $2.6^{+0.7}_{-0.9} \text{°}$ )
- ▶ Corresponds to  $\sim 10 \text{ pc}$  assuming Geminga distance is 250 pc.



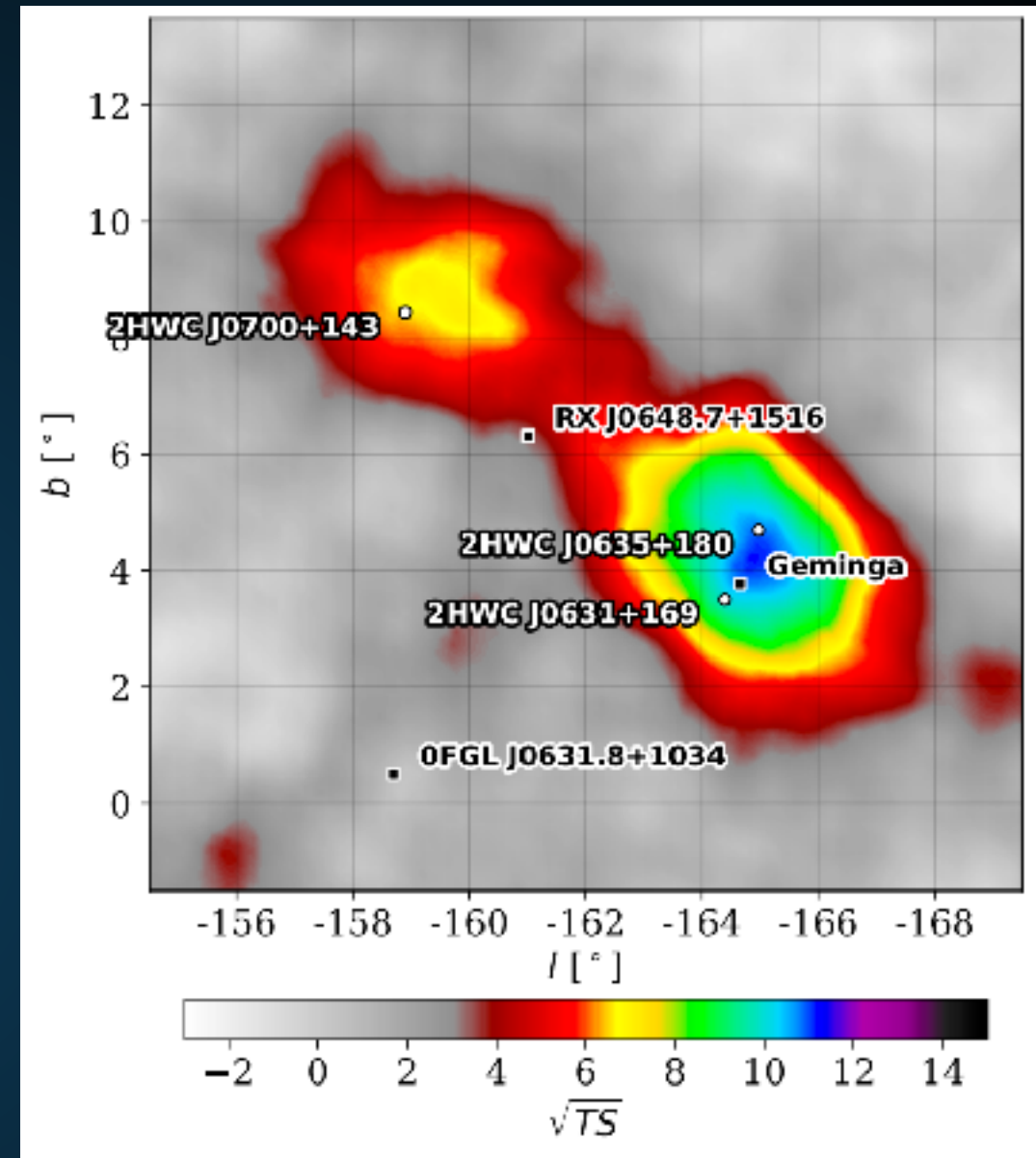
- ▶ Note: Large distance uncertainty on Geminga:

▶  $250^{+230}_{-80} \text{ pc}$

# HAWC OBSERVATIONS OF GEMINGA AND MONOGEM

Name	Tested radius [°]	Index	$F_7 \times 10^{16}$ [TeV $^{-1}$ cm $^{-2}$ s $^{-1}$ ]	TeVCat
2HWC J0534-220	-	-2.58 ± 0.01	184.7 ± 2.4	Crab
2HWC J0631+169	-	-2.57 ± 0.15	6.7 ± 1.5	Geminga
"	2.0	-2.23 ± 0.08	48.7 ± 6.9	Geminga
2HWC J0635+180	-	-2.56 ± 0.16	6.5 ± 1.5	Geminga
2HWC J0700+143	1.0	-2.17 ± 0.16	13.8 ± 4.2	-
"	2.0	-2.03 ± 0.14	23.0 ± 7.3	-

- ▶ HAWC confirms Geminga observation.



- ▶ Also sees Monogem at high significance and spatial extension.
- ▶ Spatial extension for both systems is ~2°.

**Table 1** HGPS sources considered as firmly identified pulsar wind nebulae in this paper.

HGPS name	ATNF name	Canonical name	$\lg \dot{E}$	$\tau_c$ (kyr)	$d$ (kpc)	PSR offset (pc)	$\Gamma$	$R_{\text{PWN}}$ (pc)	$L_{1-10 \text{ TeV}}$ ( $10^{33} \text{ erg s}^{-1}$ )
J1813–178 <sup>[1]</sup>	J1813–1749		37.75	5.60	4.70	< 2	$2.07 \pm 0.05$	$4.0 \pm 0.3$	$19.0 \pm 1.5$
J1833–105	J1833–1034	G21.5–0.9 <sup>[2]</sup>	37.53	4.85	4.10	< 2	$2.42 \pm 0.19$	< 4	$2.6 \pm 0.5$
J1514–591	B1509–58	MSH 15–52 <sup>[3]</sup>	37.23	1.56	4.40	< 4	$2.26 \pm 0.03$	$11.1 \pm 2.0$	$52.1 \pm 1.8$
J1930+188	J1930+1852	G54.1+0.3 <sup>[4]</sup>	37.08	2.89	7.00	< 10	$2.6 \pm 0.3$	< 9	$5.5 \pm 1.8$
J1420–607	J1420–6048	Kookaburra (K2) <sup>[5]</sup>	37.00	13.0	5.61	$5.1 \pm 1.2$	$2.20 \pm 0.05$	$7.9 \pm 0.6$	$44 \pm 3$
J1849–000	J1849–0001	IGR J18490–0000 <sup>[6]</sup>	36.99	42.9	7.00	< 10	$1.97 \pm 0.09$	$11.0 \pm 1.9$	$12 \pm 2$
J1846–029	J1846–0258	Kes 75 <sup>[2]</sup>	36.91	0.728	5.80	< 2	$2.41 \pm 0.09$	< 3	$6.0 \pm 0.7$
J0835–455	B0833–45	Vela X <sup>[7]</sup>	36.84	11.3	0.280	$2.37 \pm 0.18$	$1.89 \pm 0.03$	$2.9 \pm 0.3$	$0.83 \pm 0.11^*$
J1837–069 <sup>[8]</sup>	J1838–0655		36.74	22.7	6.60	$17 \pm 3$	$2.54 \pm 0.04$	$41 \pm 4$	$204 \pm 8$
J1418–609	J1418–6058	Kookaburra (Rabbit) <sup>[5]</sup>	36.69	10.3	5.00	$7.3 \pm 1.5$	$2.26 \pm 0.05$	$9.4 \pm 0.9$	$31 \pm 3$
J1356–645 <sup>[9]</sup>	J1357–6429		36.49	7.31	2.50	$5.5 \pm 1.4$	$2.20 \pm 0.08$	$10.1 \pm 0.9$	$14.7 \pm 1.4$
J1825–137 <sup>[10]</sup>	B1823–13		36.45	21.4	3.93	$33 \pm 6$	$2.38 \pm 0.03$	$32 \pm 2$	$116 \pm 4$
J1119–614	J1119–6127	G292.2–0.5 <sup>[11]</sup>	36.36	1.61	8.40	< 11	$2.64 \pm 0.12$	$14 \pm 2$	$23 \pm 4$
J1303–631 <sup>[12]</sup>	J1301–6305		36.23	11.0	6.65	$20.5 \pm 1.8$	$2.33 \pm 0.02$	$20.6 \pm 1.7$	$96 \pm 5$

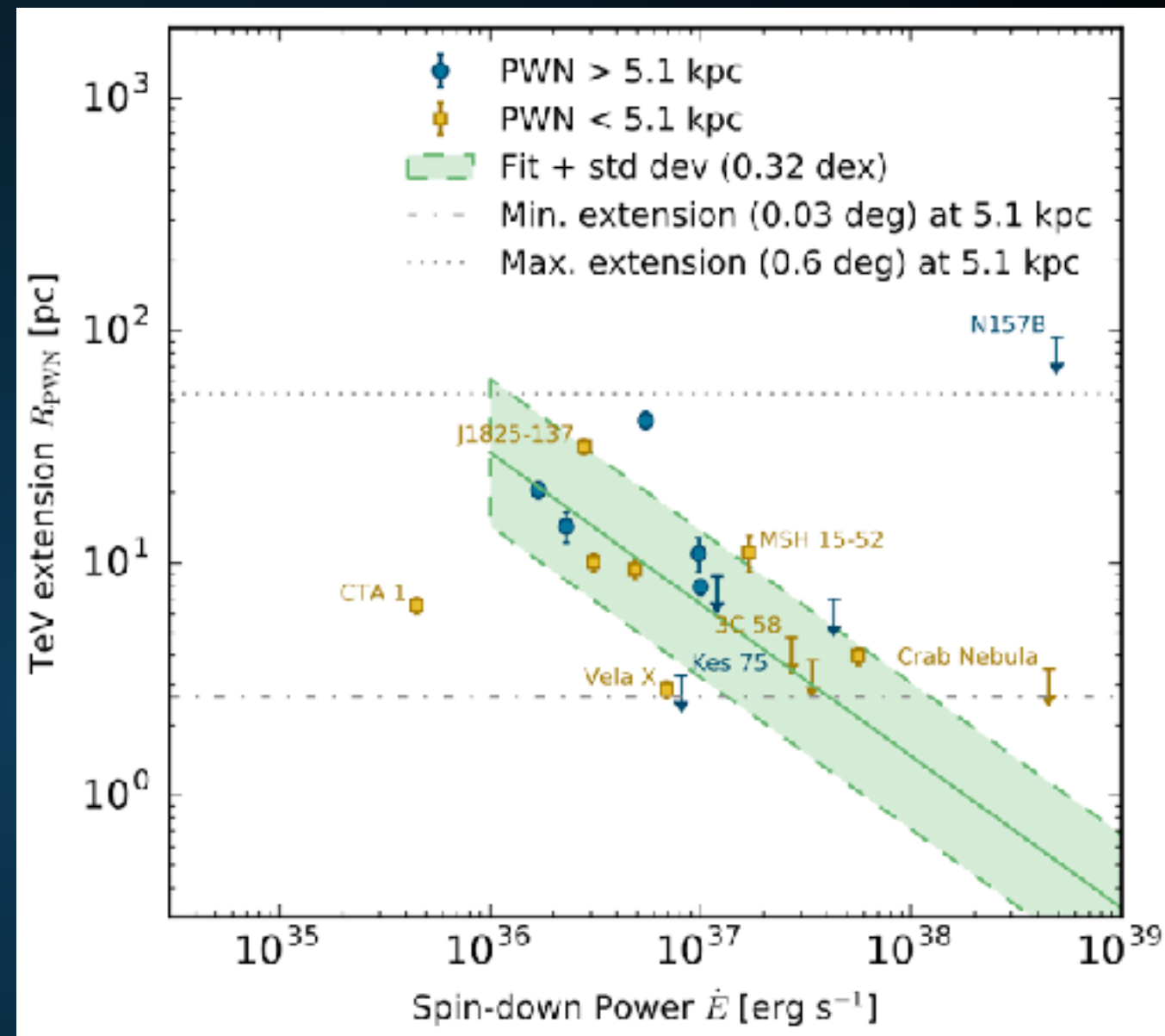
- ▶ **HESS finds a large population of “TeV PWN”**
- ▶ **HESS systems have a higher spin down power, but are more distant.**

Table 4 Candidate pulsar wind nebulae from the pre-selection.

HGPS name	ATNF name	$\lg \dot{E}$	$\tau_c$	$d$	PSR offset	$\Gamma$	$R_{\text{PWN}}$	$L_{1-10 \text{ TeV}}$
			(kyr)	(kpc)	(pc)		(pc)	( $10^{33} \text{ erg s}^{-1}$ )
J1616–508 (1)	J1617–5055	37.20	8.13	6.82	< 26	$2.34 \pm 0.06$	$28 \pm 4$	$162 \pm 9$
J1023–575	J1023–5746	37.04	4.60	8.00	< 9	$2.36 \pm 0.05$	$23.2 \pm 1.2$	$67 \pm 5$
J1809–193 (1)	J1811–1925	36.81	23.3	5.00	$29 \pm 7$	$2.38 \pm 0.07$	$35 \pm 4$	$53 \pm 3$
J1857+026	J1856+0245	36.66	20.6	9.01	$21 \pm 6$	$2.57 \pm 0.06$	$41 \pm 9$	$118 \pm 13$
J1640–465	J1640–4631 (1)	36.64	3.35	12.8	< 20	$2.55 \pm 0.04$	$25 \pm 8$	$210 \pm 12$
J1641–462	J1640–4631 (2)	36.64	3.35	12.8	$50 \pm 5$	$2.50 \pm 0.11$	< 14	$17 \pm 4$
J1708–443	B1706–44	36.53	17.5	2.60	$17 \pm 3$	$2.17 \pm 0.08$	$12.7 \pm 1.4$	$6.6 \pm 0.9$
J1908+063	J1907+0602	36.45	19.5	3.21	$21 \pm 3$	$2.26 \pm 0.06$	$27.2 \pm 1.5$	$28 \pm 2$
J1018–589A	J1016–5857 (1)	36.41	21.0	8.00	$47.5 \pm 1.6$	$2.24 \pm 0.13$	< 4	$8.1 \pm 1.4$
J1018–589B	J1016–5857 (2)	36.41	21.0	8.00	$25 \pm 7$	$2.20 \pm 0.09$	$21 \pm 4$	$23 \pm 5$
J1804–216	B1800–21	36.34	15.8	4.40	$18 \pm 5$	$2.69 \pm 0.04$	$19 \pm 3$	$42.5 \pm 2.0$
J1809–193 (2)	J1809–1917	36.26	51.3	3.55	< 17	$2.38 \pm 0.07$	$25 \pm 3$	$26.9 \pm 1.5$
J1616–508 (2)	B1610–50	36.20	7.42	7.94	$60 \pm 7$	$2.34 \pm 0.06$	$32 \pm 5$	$220 \pm 12$
J1718–385	J1718–3825	36.11	89.5	3.60	$5.4 \pm 1.6$	$1.77 \pm 0.06$	$7.2 \pm 0.9$	$4.6 \pm 0.8$
J1026–582	J1028–5819	35.92	90.0	2.33	$9 \pm 2$	$1.81 \pm 0.10$	$5.3 \pm 1.6$	$1.7 \pm 0.5$
J1832–085	B1830–08 (1)	35.76	147	4.50	$23.3 \pm 1.5$	$2.38 \pm 0.14$	< 4	$1.7 \pm 0.4$
J1834–087	B1830–08 (2)	35.76	147	4.50	$32.3 \pm 1.9$	$2.61 \pm 0.07$	$17 \pm 3$	$25.8 \pm 2.0$
J1858+020	J1857+0143	35.65	71.0	5.75	$38 \pm 3$	$2.39 \pm 0.12$	$7.9 \pm 1.6$	$7.1 \pm 1.5$
J1745–303	B1742–30 (1)	33.93	546	0.200	$1.42 \pm 0.15$	$2.57 \pm 0.06$	$0.62 \pm 0.07$	$0.014 \pm 0.003$
J1746–308	B1742–30 (2)	33.93	546	0.200	< 1.1	$3.3 \pm 0.2$	$0.56 \pm 0.12$	$0.009 \pm 0.003$

- ▶ HESS finds a large population of “TeV PWN”
- ▶ HESS systems have a higher spin down power, but are more distant.

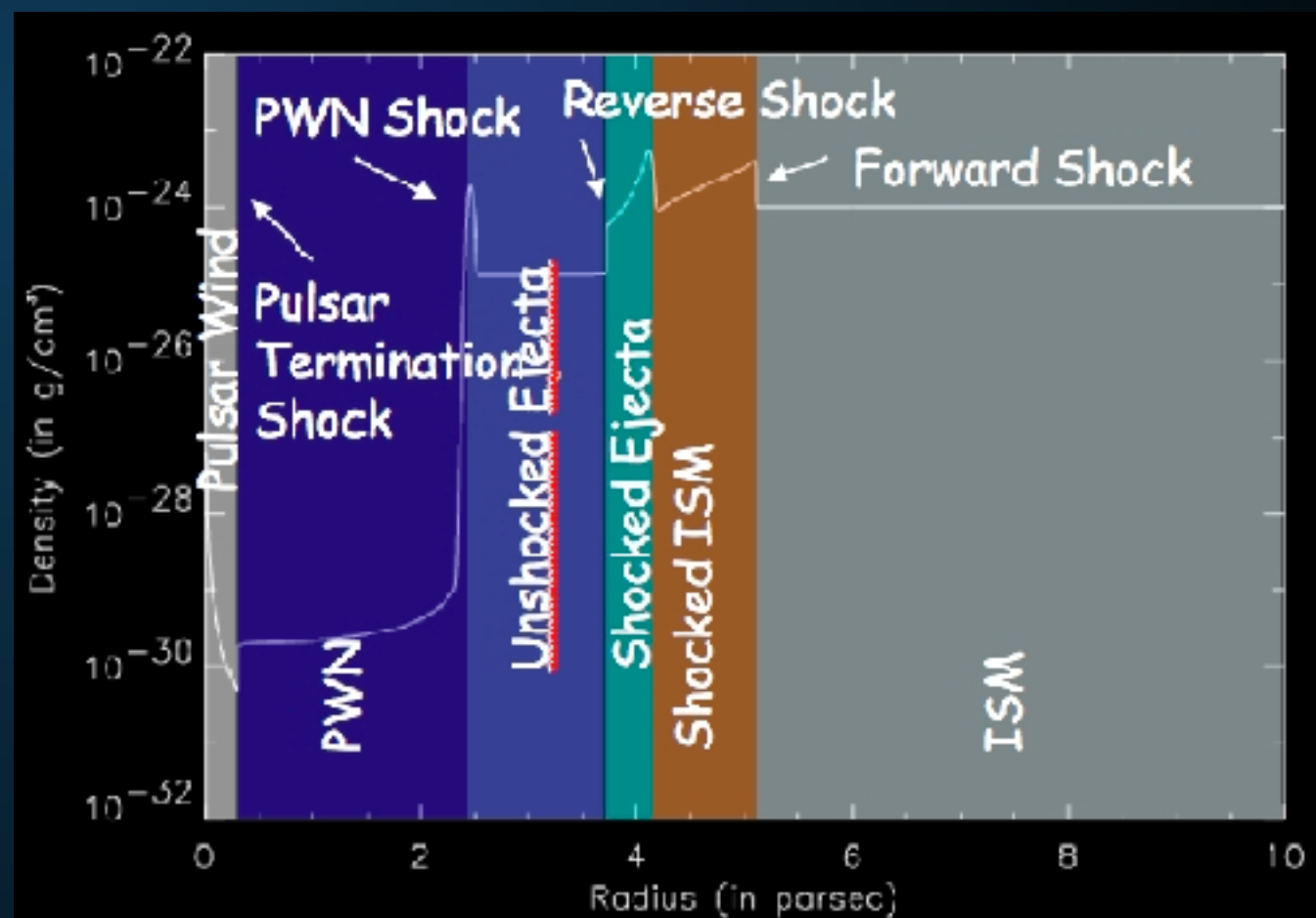
- ▶ TeV PWN are much larger.
- ▶ Particularly true in low-energy systems.



**NOTE:** This has the opposite energy dependence as the X-Ray PWN.

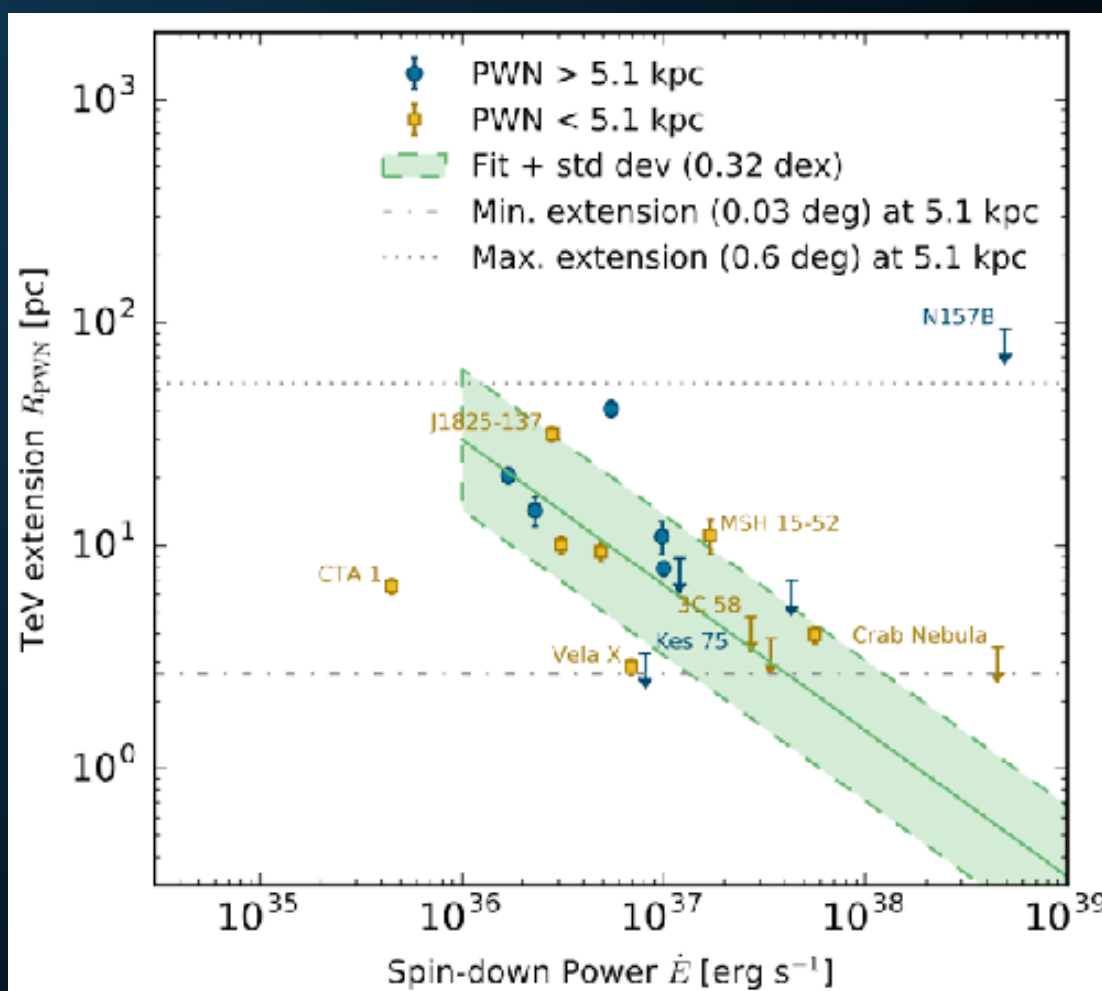
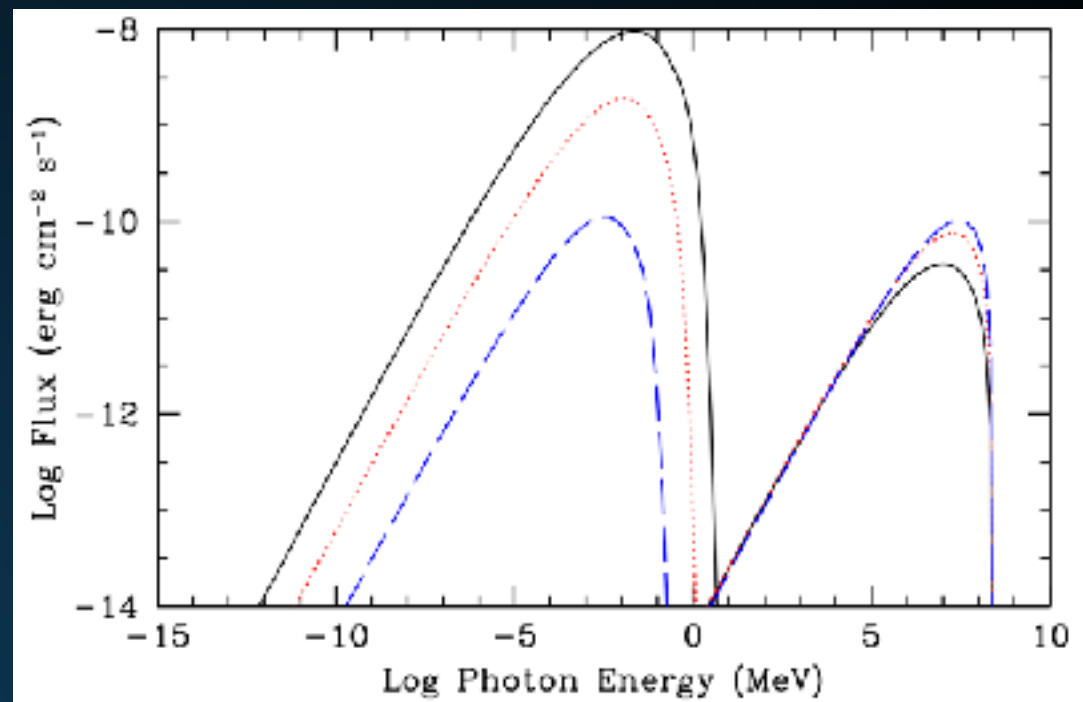
$$R_{\text{PWN}} \simeq 1.5 \left( \frac{\dot{E}}{10^{35} \text{ erg/s}} \right)^{1/2} \times \left( \frac{n_{\text{gas}}}{1 \text{ cm}^{-3}} \right)^{-1/2} \left( \frac{v}{100 \text{ km/s}} \right)^{-3/2} \text{ pc}$$

- ▶ TeV halos are a new feature
  - ▶ 3 orders of magnitude larger than PWN in volume
  - ▶ Opposite energy dependence
- ▶ PWN are morphologically connected to the physics of the termination shock
- ▶ TeV halos need a similar morphological description.



# AN ALTERNATIVE EXPLANATION

- ▶ Maybe TeV electrons propagate farther?
- ▶ Energy loss time-scale:  $E^{-1}$ .
- ▶ Propagation Distance in t:  $E^{0.16}$ .
- ▶ Size of Halo:  $E^{-0.33}$ .
- ▶ Moving from PeV to  $\sim 50$  TeV electrons leads to 10x larger radius.



## GEMINGA - A TEMPLATE FOR TEV HALOS

---

- ▶ Will now use Geminga as a standard template for TeV halos.
  - ▶ Bright (nearby)
  - ▶ High latitude (low background)
  - ▶ Middle-Aged (no associated SNR)
- ▶ Would get same (actually slightly better) results if we used Monogem.

## INVERSE COMPTON SCATTERING WITH THE ISM

- It is not energetically possible for Geminga to produce the magnetic field or ISRF that these electrons interact with.

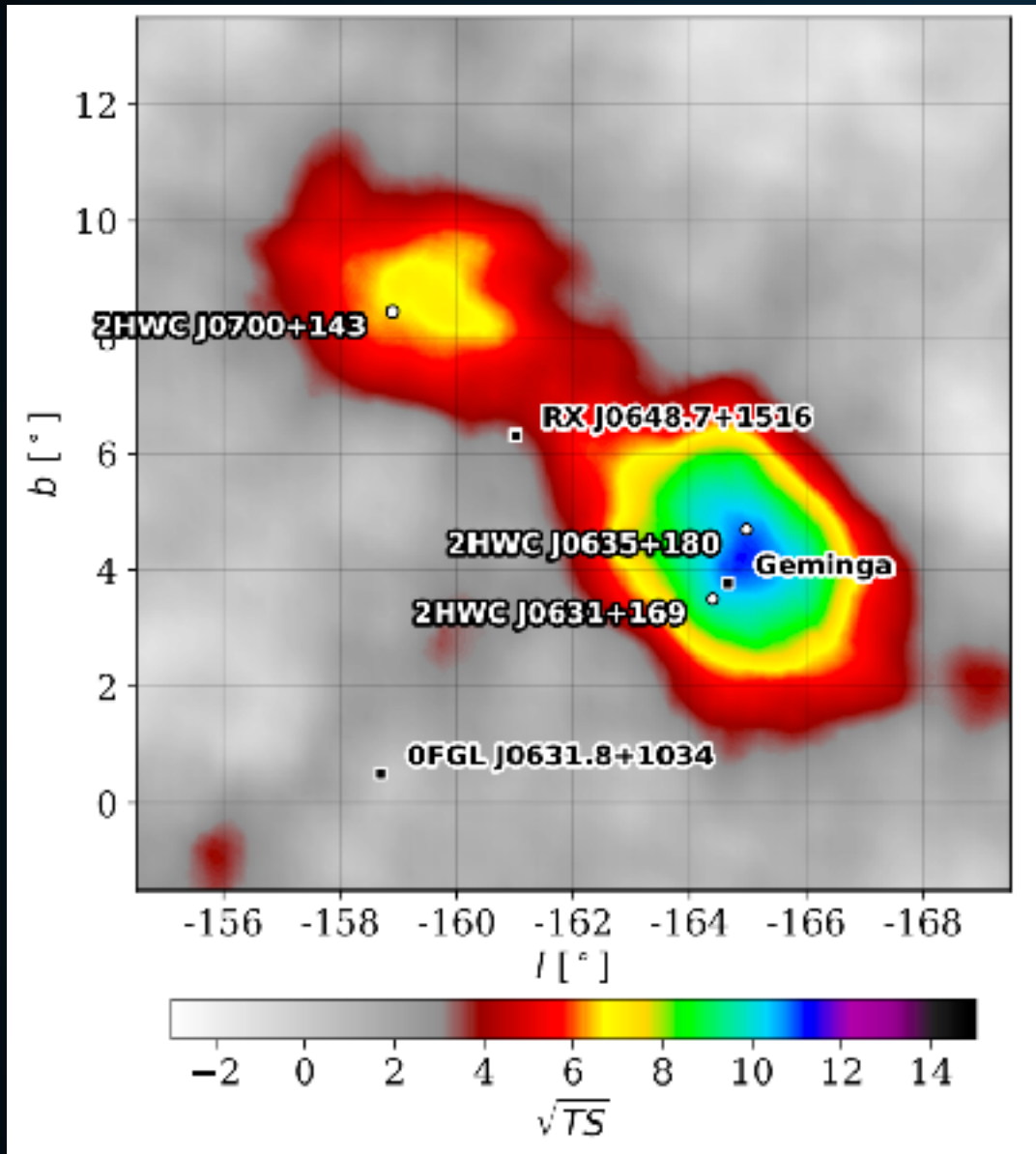
$$U = \frac{1}{8\pi} \beta^2 = \frac{(10 \mu G)^2}{8\pi}$$
$$= 4 \times 10^{-12} \frac{\text{erg}}{\text{cm}^3}$$
$$\int_0^{10 \mu G} U dV = 5 \times 10^{47} \text{ erg}$$
$$\hookrightarrow \text{Magnetic Flux} \approx 5 \times 10^{38} \frac{\text{erg s}}{\text{s}}$$

$$\text{ISRF} = I \frac{\text{eV}}{\text{cm}^3}$$
$$\int \text{ISRF} dV = 8 \times 10^{47} \text{ erg}$$
$$\hookrightarrow \text{Flux} = 8 \times 10^{38} \frac{\text{erg s}}{\text{s}}$$

- We can use typical ISM values ( $5 \mu G$ ;  $1 \text{ eV cm}^{-3}$ ) to characterize interactions.
- Nearly equal energy to synchrotron and ICS.

## TWO CONTRASTING OBSERVABLES

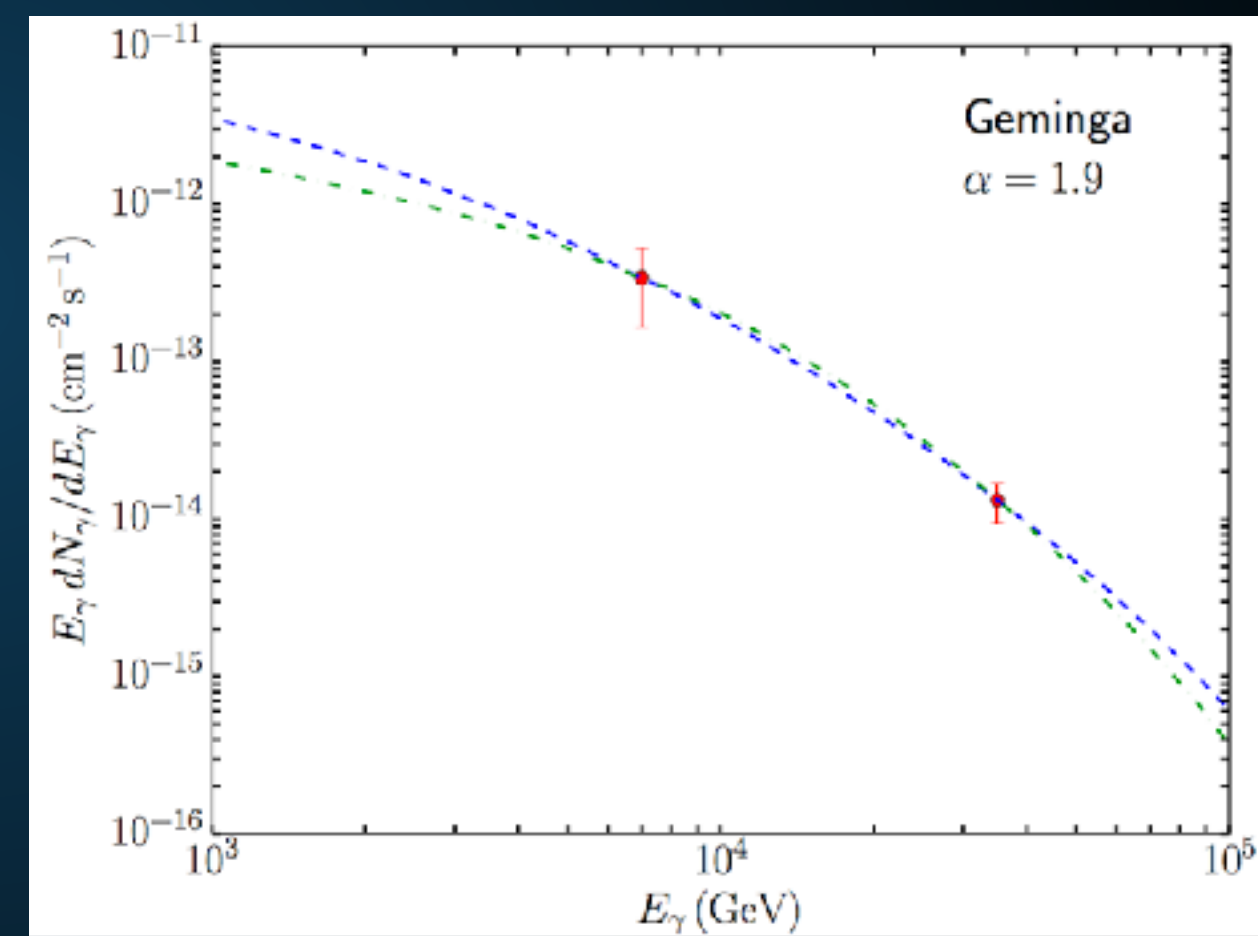
### Geminga is Bright



Indicative of significant  
electron cooling

### Geminga has a hard-spectrum

Name	Tested radius [°]	Index	$F_\gamma \times 10^{15}$ [TeV $^{-1}$ cm $^{-2}$ s $^{-1}$ ]	TeVCat
2HWC J0631+169	-	-2.57 $\pm$ 0.15	6.7 $\pm$ 1.5	Geminga
"	2.0	-2.23 $\pm$ 0.08	48.7 $\pm$ 6.9	Geminga
2HWC J0635+180	-	-2.56 $\pm$ 0.16	6.5 $\pm$ 1.5	Geminga



Indicative of minimal  
electron cooling

## TOTAL POWER OF TEV HALOS

---

- ▶ Measured Geminga flux translates to an intensity:  
 $2.86 \times 10^{31} \text{ erg s}^{-1}$  at 7 TeV
- ▶ For the best-fit spectrum, this requires an  $e^+e^-$  injection:  
 $3.8 \times 10^{33} \text{ erg s}^{-1}$
- ▶ Total Spindown Power of Geminga is:  
 $3.4 \times 10^{34} \text{ erg s}^{-1}$
- ▶ Roughly 10% conversion efficiency to  $e^+e^-$  !

## COSMIC-RAY DIFFUSION IN A TEV HALO

- ▶ Energy constraints demand that ~30 TeV electrons lose the majority of their energy before exiting TeV halo.

$$\tau = 3.1 \times 10^4 \text{ yr} \left( \frac{E_e}{10 \text{ TeV}} \right)^{-1}$$

- ▶ This strongly constrains the efficiency of particle propagation near the halo.

$$D = \frac{L^2}{6\tau} = \frac{(10 \text{ pc})^2}{6(3.1 \times 10^4 \text{ yr})} = \frac{(3.08 \times 10^{19} \text{ cm})^2}{5.86 \times 10^{12} \text{ s}}$$

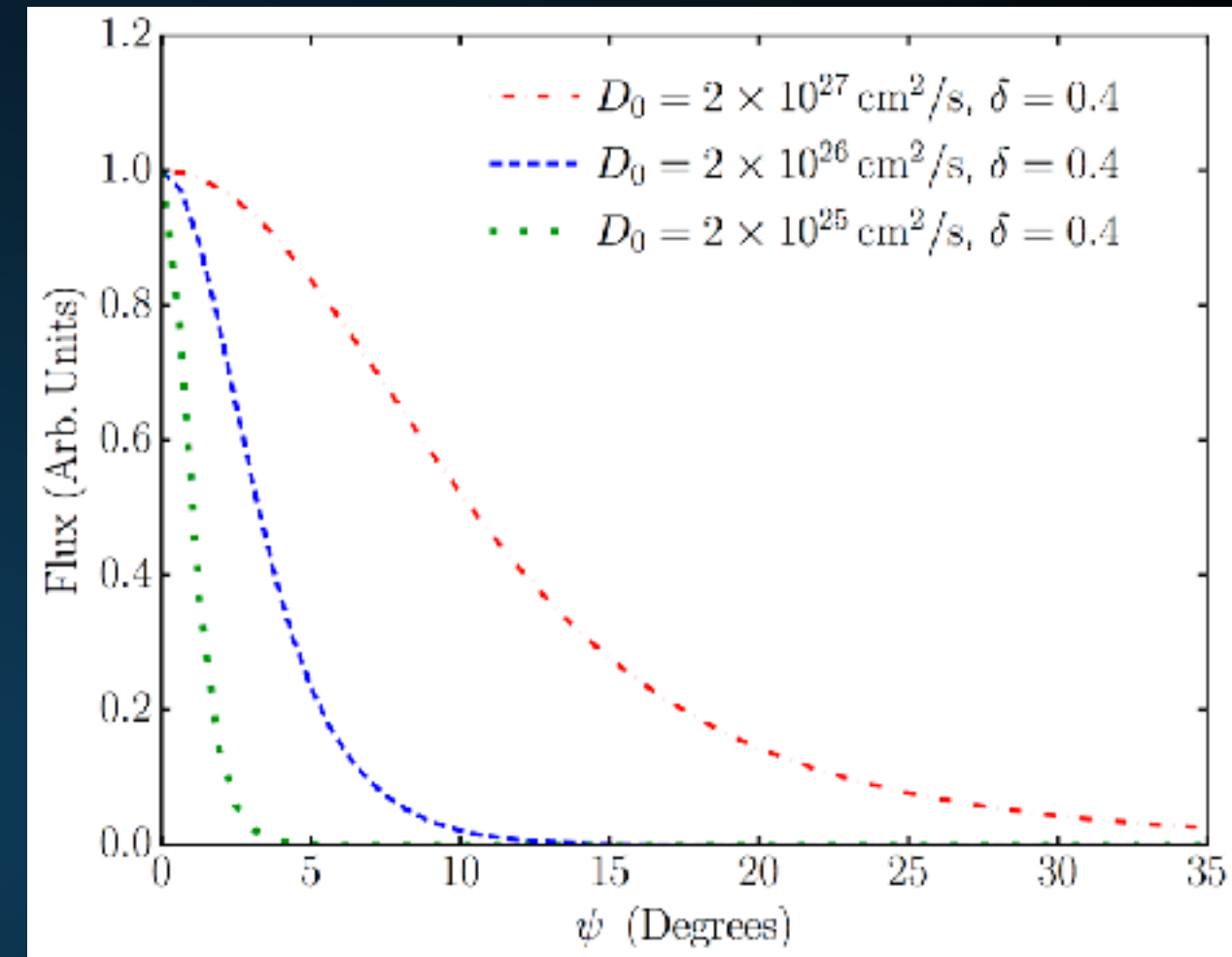
$$D = 1.6 \times 10^{26} \frac{\text{cm}^2}{\text{s}}$$

- ▶ Provides strong evidence for new morphological feature.

# COSMIC-RAY DIFFUSION IN A TEV HALO

- ▶ Actual source of particle propagation is unknown:

- ▶ Diffusion
- ▶ Advection



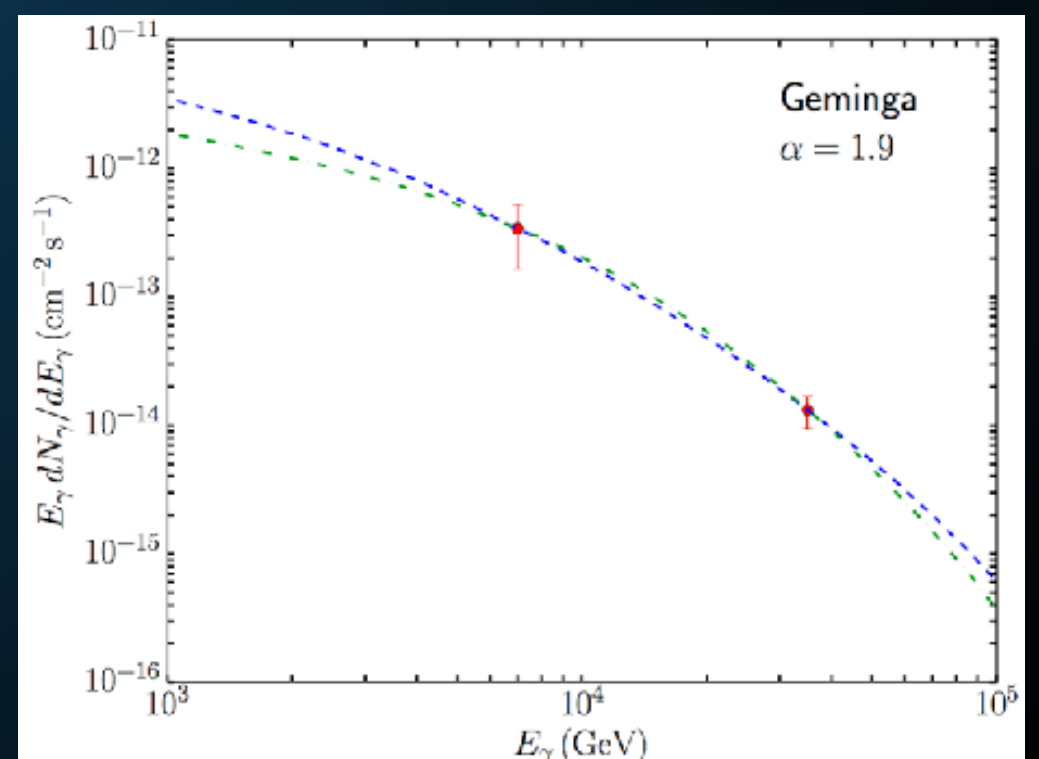
- ▶ Particle propagation near pulsars must be orders of magnitude less efficient than typical for the ISM.
- ▶ Continues far outside the termination shock of a pulsar with no SNR.

## SPECTRUM OF TEV HALOS

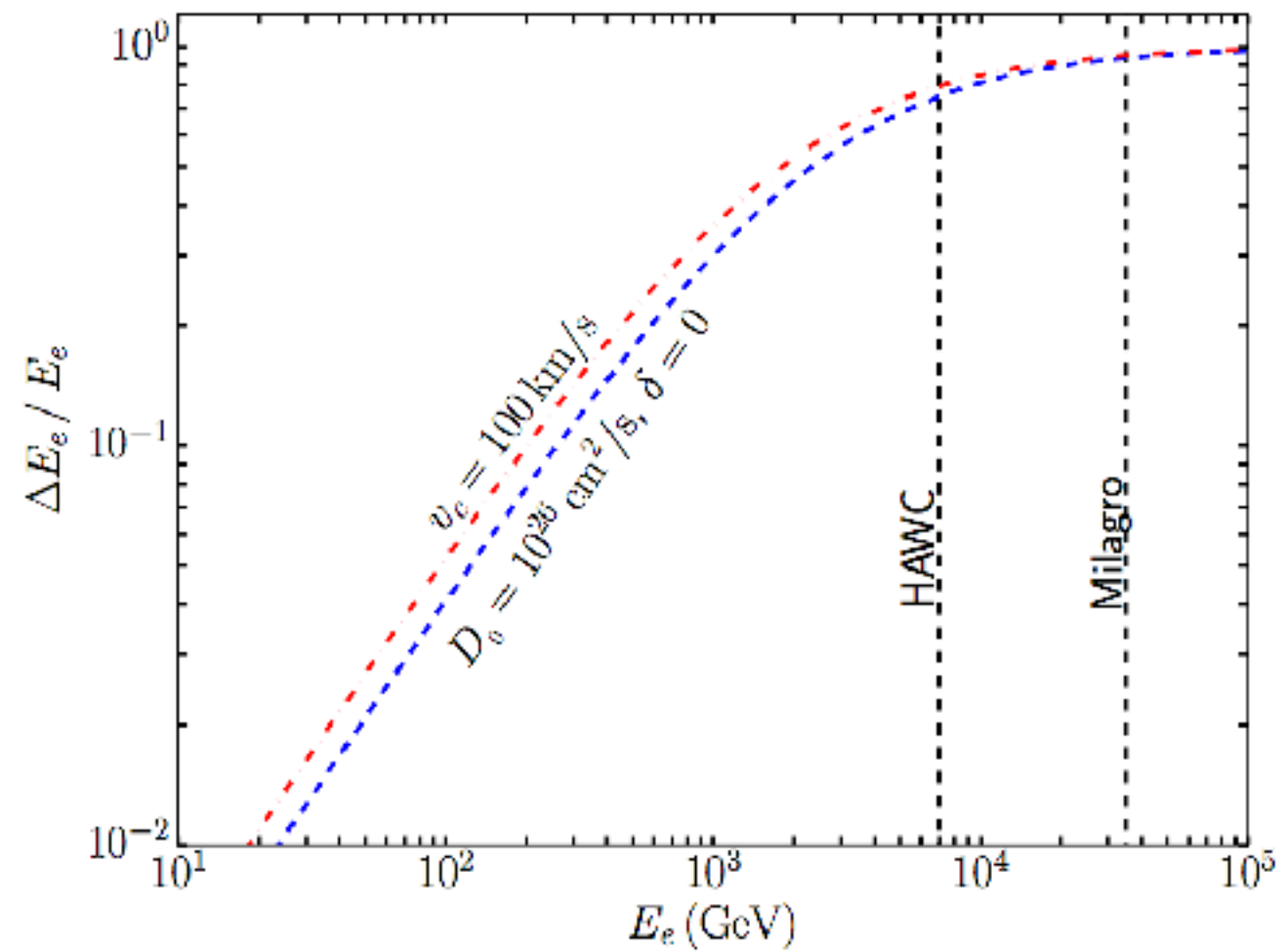
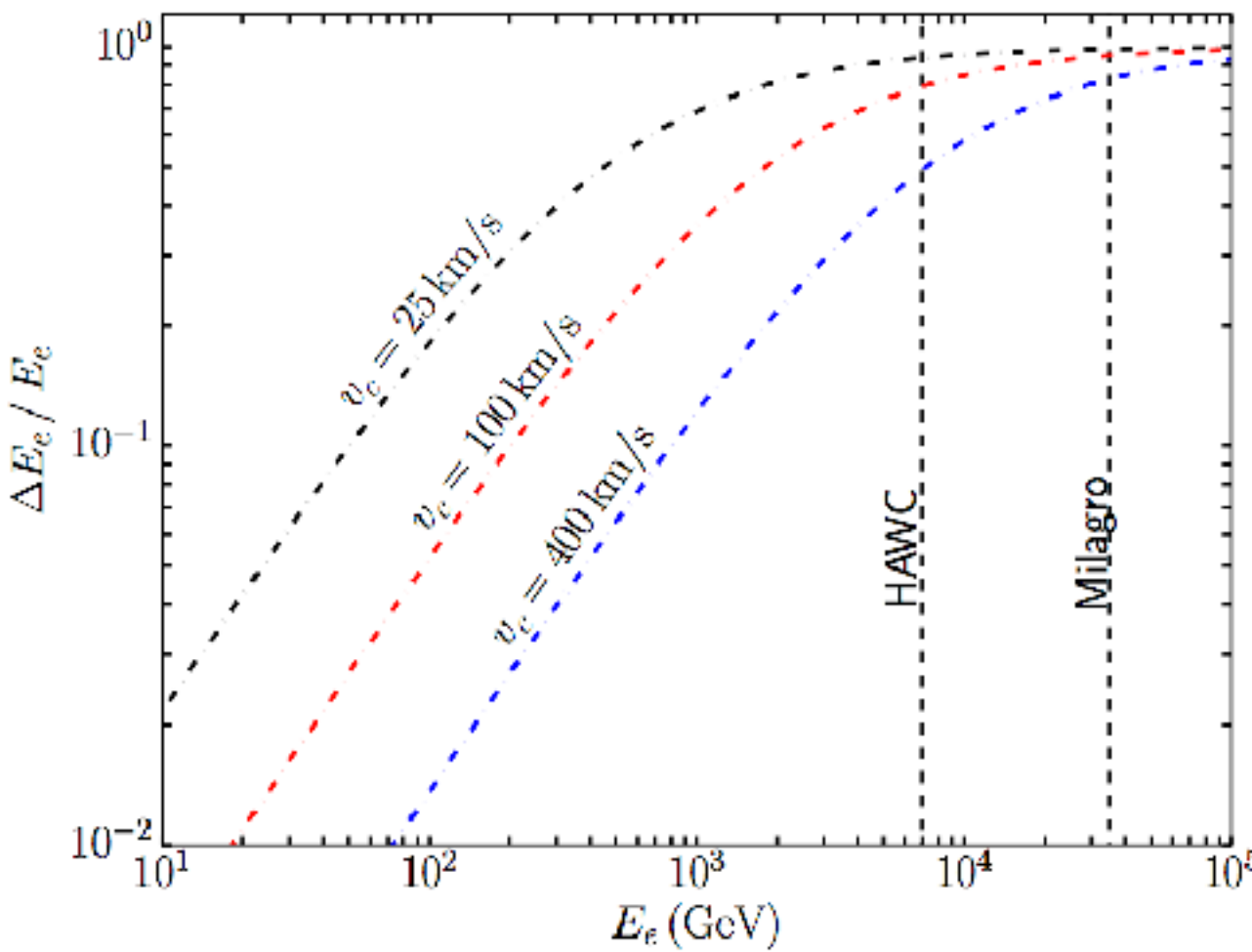
- ▶ **Geminga has a hard gamma-ray spectrum**

Name	Tested radius [°]	Index	$F_7 \times 10^{15}$ [TeV $^{-1}$ cm $^{-2}$ s $^{-1}$ ]	TeVCat
2HWC J0631+169	-	$-2.57 \pm 0.15$	$6.7 \pm 1.5$	Geminga
"	2.0	$-2.23 \pm 0.08$	$48.7 \pm 6.9$	Geminga
2HWC J0635+180	-	$-2.56 \pm 0.16$	$6.5 \pm 1.5$	Geminga

- ▶ **Electrons cannot be completely cooled, or else gamma-ray spectrum would be too soft (Klein-Nishina effects)**
- ▶ **Combined with Milagro observation at 30 TeV, this requires:**
  - ▶  **$-1.9 < \alpha < -1.5$**
  - ▶  **$E_{\text{cut}} \approx 50 \text{ TeV}$**



## WHAT ABOUT THE LOW-ENERGY ELECTRONS?



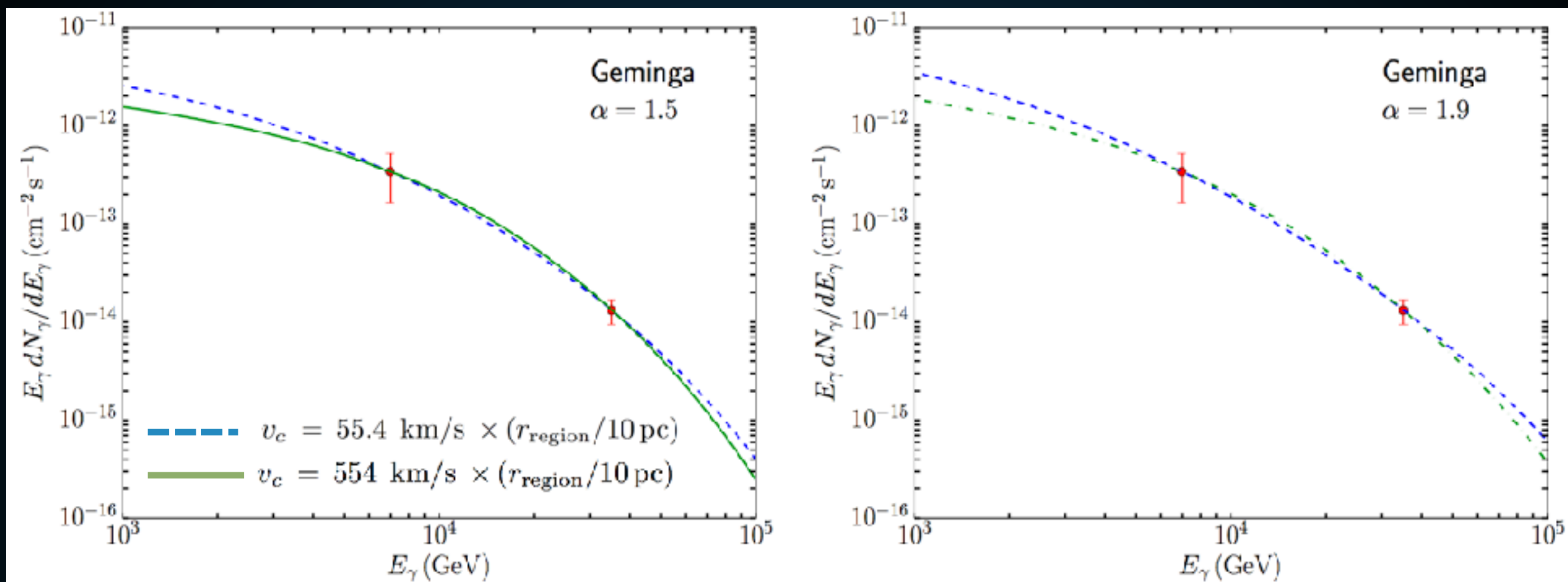
- ▶ Low-energy electrons lose energy slower, must escape.
- ▶ This is true in both convective and most diffusive (Kolmogorov, Kraichnian) scenarios.

## BOHMIAN DIFFUSION

$$\tau_{\text{Diff}} \propto \frac{l^2}{D_0 E^\delta} \quad \tau_{\text{loss}} \propto E^{-1}$$
$$\left( \frac{\Delta E}{E} \right) \propto \frac{\tau_{\text{Diff}}}{\tau_{\text{loss}}} \propto E^{1-\delta}$$

- More generically, low-energy electrons can only be confined if the diffusion is Bohmian (diffusion coefficient scales as  $E^1$ .)

## GEMINGA SPECTRUM INDICATIVE OF CONVECTION



- ▶ However, Bohmian diffusion is incompatible with the gamma-ray spectrum.
- ▶ If low-energy electrons are cooled, the spectrum at 7 TeV should be significantly softer.

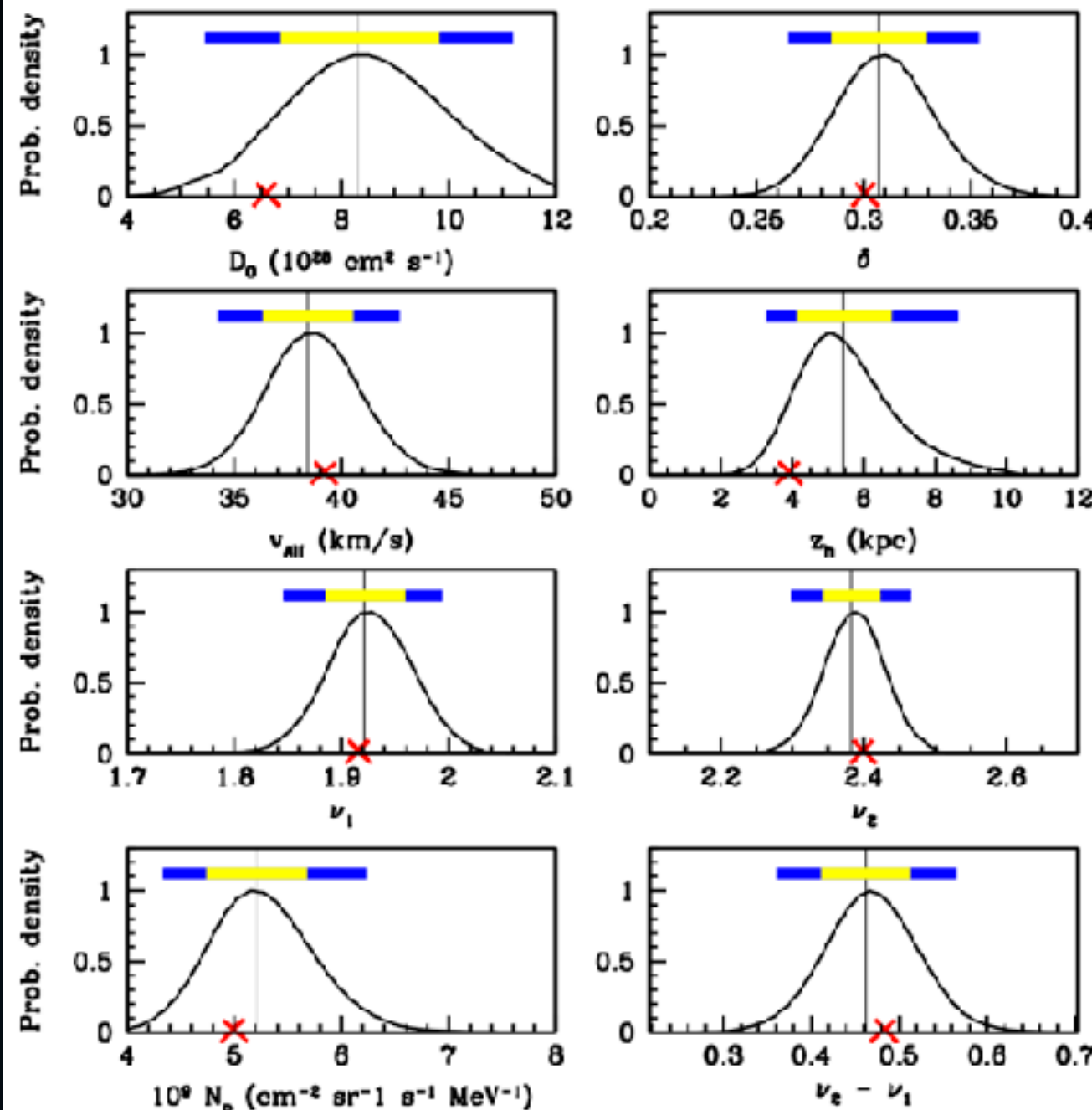
## AN UPPER LIMIT ON THE TEV HALO SIZE

---

- ▶ These arguments only set a lower limit on the TeV halo size.
- ▶ What if TeV halos are much larger, but the TeV electrons die at  $\sim 10$  pc?
- ▶ Will need to answer this question on the population level.

- ▶ **New Assumption: Geminga is typical of a 100-400 kyr pulsar.**
- ▶ **Two Nearest Systems Observed: Geminga, Monogem**
- ▶ **Indications of many similar HESS sources.**

# EFFECT OF TEV HALOS ON ISM PROPAGATION

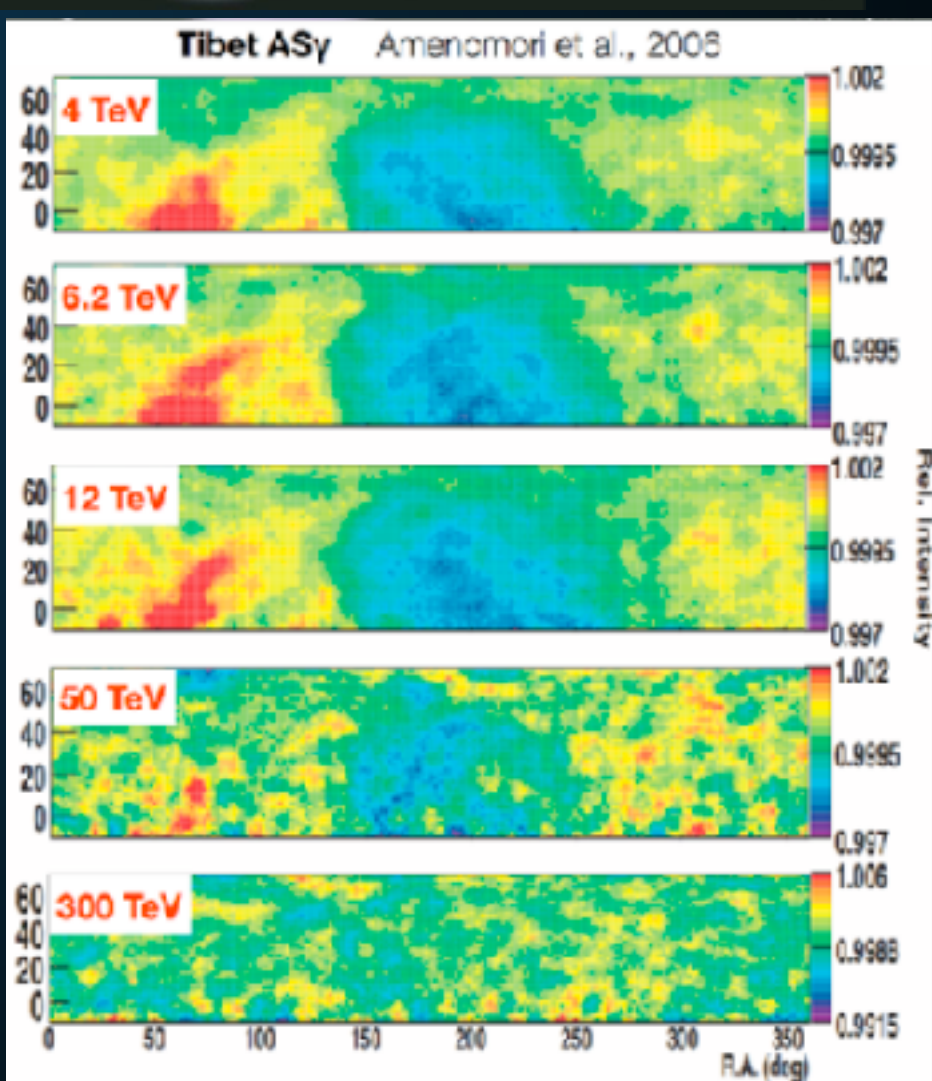


- ▶ Multiple cosmic-ray observations indicate that the average diffusion constant is  $\sim 5 \times 10^{28} \text{ cm}^2 \text{s}^{-1}$
- ▶ Inhibited cosmic-ray propagation in TeV halos must not substantially affect this number.

$$\begin{aligned}
 f &\sim \frac{N_{\text{region}} \times \frac{4\pi}{3} r_{\text{region}}^3}{\pi R_{\text{MW}}^2 \times 2z_{\text{MW}}} \\
 &\sim 0.25 \times \left( \frac{r_{\text{region}}}{100 \text{ pc}} \right)^3 \left( \frac{\dot{N}_{\text{SN}}}{0.03 \text{ yr}^{-1}} \right) \left( \frac{\tau_{\text{region}}}{10^6 \text{ yr}} \right) \left( \frac{20 \text{ kpc}}{R_{\text{MW}}} \right)^2 \left( \frac{200 \text{ pc}}{z_{\text{MW}}} \right)
 \end{aligned}$$

# CAN WE BE INSIDE A TEV HALO?

- ▶ We probably cannot be inside a TeV halo without affecting cosmic-ray anisotropies.
- ▶ If we are at the center of a TeV halo, it must be huge.
- ▶ Would make understanding the  $e^+e^-$  flux even more difficult.



---

**Implication I:**

**Most TeV gamma-ray sources are TeV halos.**

# TEV HALOS ARE A GENERIC FEATURE OF PULSARS

2HWC Name	ATNF Name	Distance (kpc)	Angular Separation	Projected Separation	Expected Flux ( $\times 10^{-15}$ )	Actual Flux ( $\times 10^{-15}$ )	Flux Ratio	Expected Extension	Actual Extension	Age (kyr)	Chance Overlap
J0700+143	B0656+14	0.29	0.18°	0.91 pc	43.0	23.0	1.87	2.0°	1.73°	111	0.0
J0631+169	J0633+1746	0.25	0.89°	3.88 pc	48.7	48.7	1.0	2.0°	2.0°	342	0.0
J1912+099	J1913+1011	4.61	0.34°	27.36 pc	13.0	36.6	0.36	0.11°	0.7°	169	0.30
J2031+415	J2032+4127	1.70	0.11°	3.26 pc	5.59	61.6	0.091	0.29°	0.7°	181	0.002
J1831-098	J1831-0952	3.68	0.04°	2.57 pc	7.70	95.8	0.080	0.14°	0.9°	128	0.006

- ▶ 5 / 39 sources in the 2HWC catalog are correlated with bright, middle-aged (100 – 400 kyr) pulsars.

2HWC Name	ATNF Name	Distance (kpc)	Angular Separation	Projected Separation	Expected Flux ( $\times 10^{-15}$ )	Actual Flux ( $\times 10^{-15}$ )	Flux Ratio	Expected Extension	Actual Extension	Age (kyr)	Chance Overlap
J1930+188	J1930+1852	7.0	0.03°	3.67 pc	23.2	9.8	2.37	0.07°	0.0°	2.89	0.002
J1814-173	J1813-1749	4.7	0.54°	44.30 pc	243	152	1.60	0.11°	1.0°	5.6	0.61
J2019+367	J2021+3651	1.8	0.27°	8.48 pc	99.8	58.2	1.71	0.28°	0.7°	17.2	0.04
J1928+177	J1928+1746	4.34	0.03°	2.27 pc	8.08	10.0	0.81	0.11°	0.0°	82.6	0.002
J1908+063	J1907+0602	2.58	0.36°	16.21 pc	40.0	85.0	0.47	0.2°	0.8°	19.5	0.26
J2020+403	J2021+4026	2.15	0.18°	6.75 pc	2.48	18.5	0.134	0.23°	0.0°	77	0.01
J1857+027	J1856+0245	6.32	0.12°	13.24 pc	11.0	97.0	0.11	0.08°	0.9°	20.6	0.06
J1825-134	J1826-1334	3.61	0.20°	12.66 pc	20.5	249	0.082	0.14°	0.9°	21.4	0.14
J1837-065	J1838-0655	6.60	0.38°	43.77 pc	12.0	341	0.035	0.08°	2.0°	22.7	0.48
J1837-065	J1837-0604	4.78	0.50°	41.71 pc	8.3	341	0.024	0.10°	2.0°	33.8	0.68
J2006+341	J2004+3429	10.8	0.42°	80.07 pc	0.48	24.5	0.019	0.04°	0.9°	18.5	0.08

- ▶ 12 others with young pulsars (2.36 chance overlaps)
- ▶ Young pulsars may be contaminated by SNR.

## STEP I: TEV HALOS ARE A GENERIC FEATURE OF PULSARS

2HWC Name	ATNF Name	Distance (kpc)	Angular Separation	Projected Separation	Expected Flux ( $\times 10^{-15}$ )	Actual Flux ( $\times 10^{-15}$ )	Flux Ratio	Expected Extension	Actual Extension	Age (kyr)	Chance Overlap
J0700+143	B0656+14	0.29	0.18°	0.91 pc	43.0	23.0	1.87	2.0°	1.73°	111	0.0
J0631+169	J0633+1746	0.25	0.89°	3.88 pc	48.7	48.7	1.0	2.0°	2.0°	342	0.0
J1912+099	J1913+1011	4.61	0.34°	27.36 pc	13.0	36.6	0.36	0.11°	0.7°	169	0.30
J2031+415	J2032+4127	1.70	0.11°	3.26 pc	5.59	61.6	0.091	0.29°	0.7°	181	0.002
J1831-098	J1831-0952	3.68	0.04°	2.57 pc	7.70	95.8	0.080	0.14°	0.9°	128	0.006

- ▶ There are 57 middle-aged pulsars in the HAWC field of view.
- ▶ Can produce a ranked list of the spin-down flux of these systems (spin-down luminosity divided by distance squared).
- ▶ If TeV halo luminosity is correlated to spin-down power, these should be among the brightest systems.

## STEP I: TEV HALOS ARE A GENERIC FEATURE OF PULSARS

ATNF Name	Dec. ( $^{\circ}$ )	Distance (kpc)	Age (kyr)	Spindown Lum. ( $\text{erg s}^{-1}$ )	Spindown Flux ( $\text{erg s}^{-1} \text{ kpc}^{-2}$ )	2HWC
J0633+1746	17.77	0.25	342	3.2e34	4.1e34	2HWC J0631+169
B0656+14	14.23	0.29	111	3.8e34	3.6e34	2HWC J0700+143
B1951+32	32.87	3.00	107	3.7e36	3.3e34	—
J1740+1000	10.00	1.23	114	2.3e35	1.2e34	—
J1913+1011	10.18	4.61	169	2.9e36	1.1e34	2HWC J1912+099
J1831-0952	-9.86	3.68	128	1.1e36	6.4e33	2HWC J1831-098
J2032+4127	41.45	1.70	181	1.7e35	4.7e33	2HWC J2031+415
B1822-09	-9.58	0.30	232	4.6e33	4.1e33	—
B1830-08	-8.45	4.50	147	5.8e35	2.3e33	—
J1913+0904	9.07	3.00	147	1.6e35	1.4e33	—
B0540+23	23.48	1.56	253	4.1e34	1.4e33	—

- ▶ **The five pulsars associated with TeV emission are among the seven brightest sources.**
- ▶ **Private communication with the HAWC collaboration reveals that the missing two sources are currently  $2\text{-}3\sigma$  excesses!**

## TEV HALOS: THE FIRST ORDER MODEL

---

$$\phi_{\text{TeV halo}} = \left( \frac{\dot{E}_{\text{psr}}}{\dot{E}_{\text{Geminga}}} \right) \left( \frac{d_{\text{Geminga}}^2}{d_{\text{psr}}^2} \right) \phi_{\text{Geminga}}$$

$$\theta_{\text{TeV halo}} = \left( \frac{d_{\text{Geminga}}}{d_{\text{psr}}} \right) \theta_{\text{Geminga}}$$

- ▶ **Assume that every pulsar converts an equivalent fraction of its spin-down power into the TeV halo flux.**
- ▶ **Can then calculate the TeV flux and extension of every TeV halo based on its spin-down power, and the observations of Geminga.**
- ▶ **Note: Using Monogem would increases fluxes by nearly a factor of 2.**

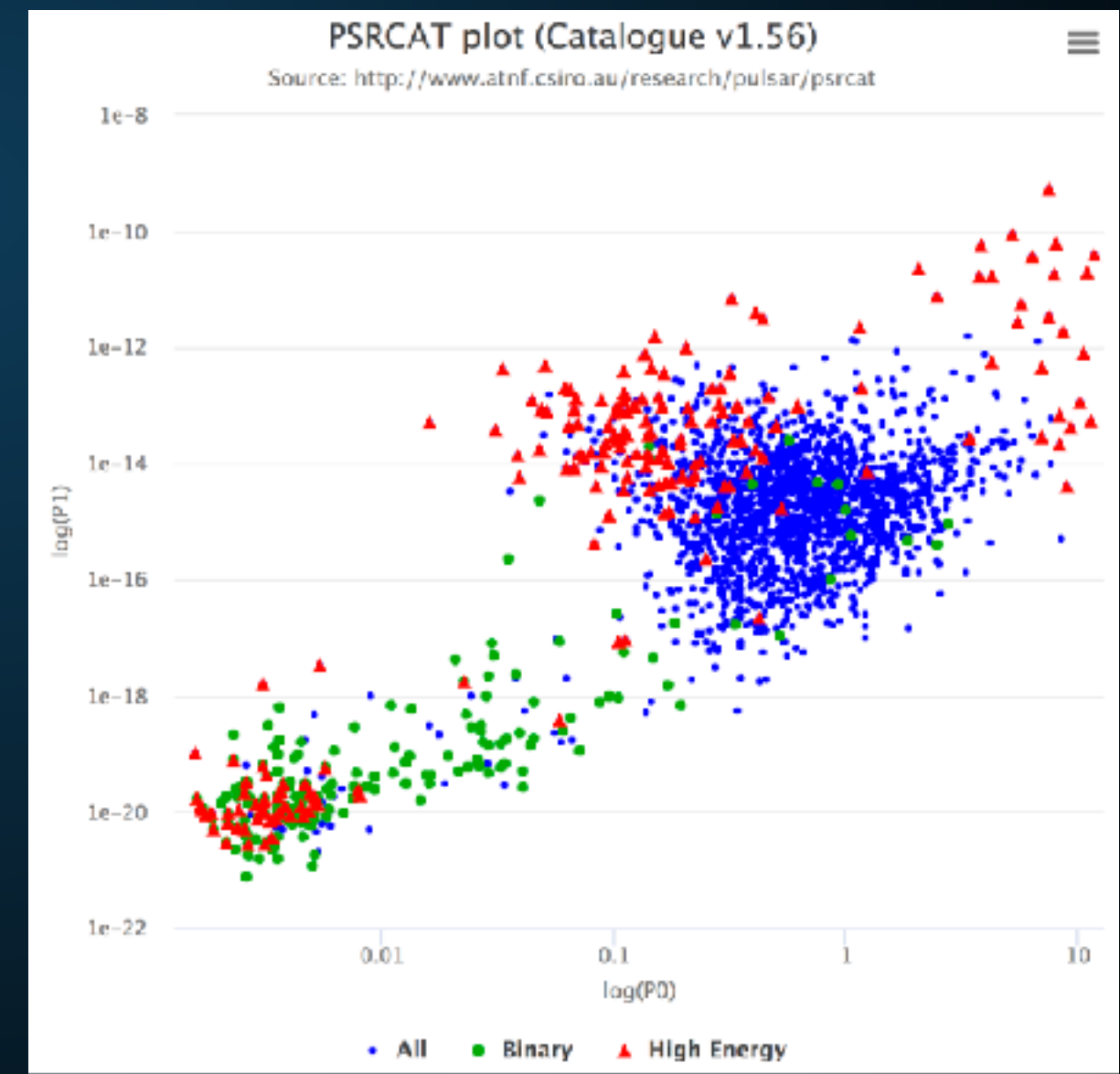
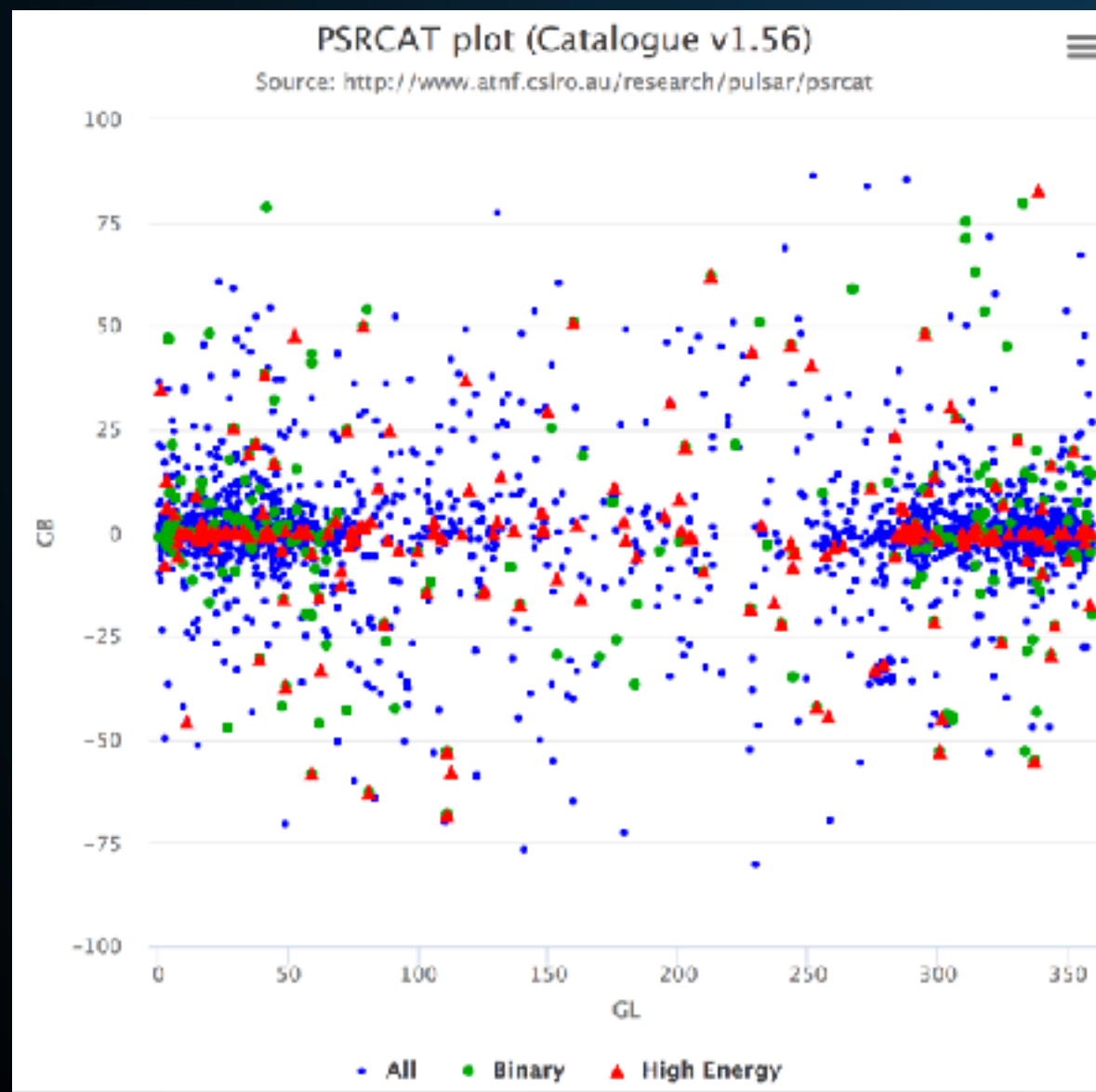
## HAWC SENSITIVITY AFTER 10 YEARS

ATNF Name	Dec. ( $^{\circ}$ )	Distance (kpc)	Age (kyr)	Spindown Lum. ( $\text{erg s}^{-1}$ )	Spindown Flux ( $\text{erg s}^{-1} \text{kpc}^{-2}$ )	2HWC
J0633+1746	17.77	0.25	342	3.2e34	4.1e34	2HWC J0631+169
B0656+14	14.23	0.29	111	3.8e34	3.6e34	2HWC J0700+143
B1951+32	32.87	3.00	107	3.7e36	3.3e34	—
J1740+1000	10.00	1.23	114	2.3e35	1.2e34	—
J1913+1011	10.18	4.61	169	2.9e36	1.1e34	2HWC J1912+099
J1831-0952	-9.86	3.68	128	1.1e36	6.4e33	2HWC J1831-098
J2032+4127	41.45	1.70	181	1.7e35	4.7e33	2HWC J2031+415
B1822-09	-9.58	0.30	232	4.6e33	4.1e33	—
B1830-08	-8.45	4.50	147	5.8e35	2.3e33	—
J1913+0904	9.07	3.00	147	1.6e35	1.4e33	—
B0540+23	23.48	1.56	253	4.1e34	1.4e33	—

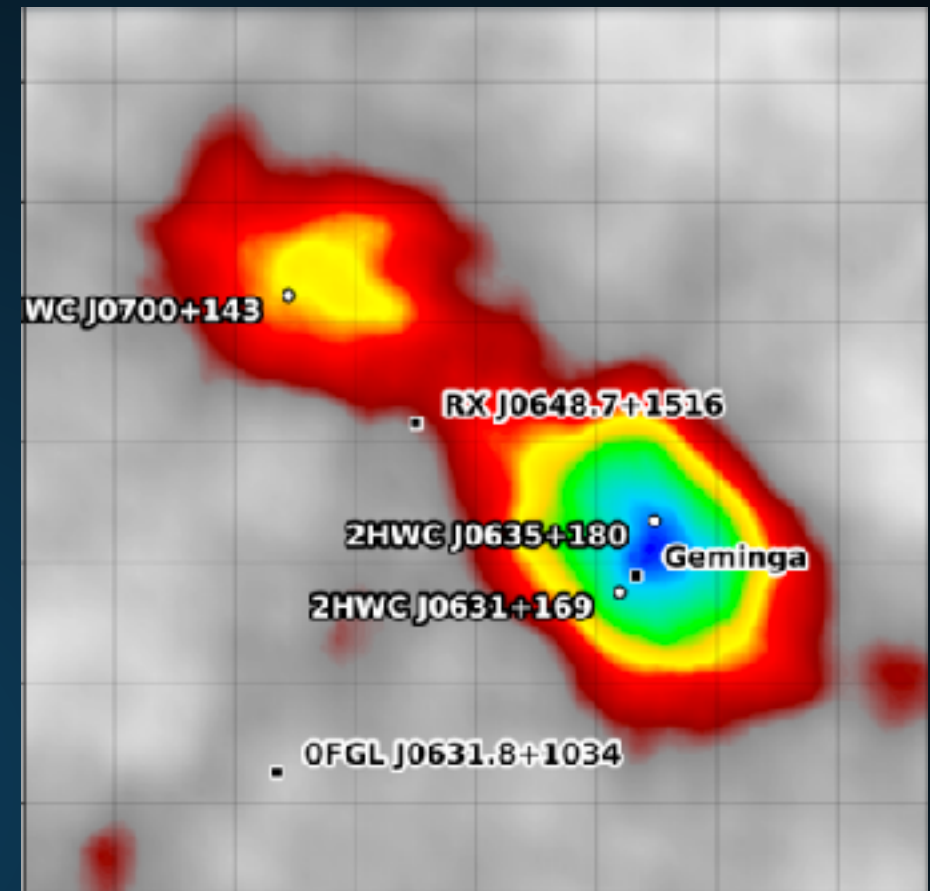
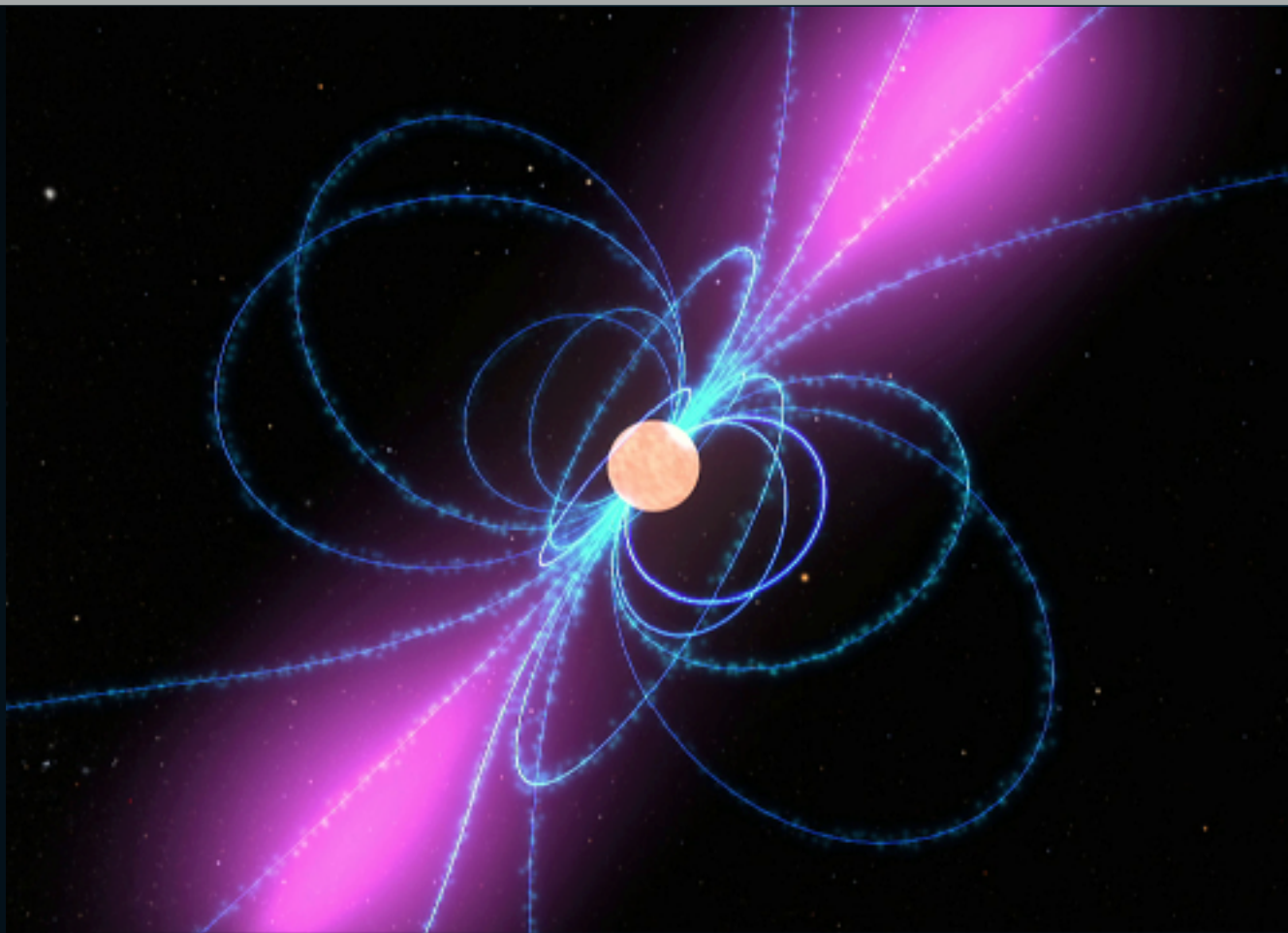
- ▶ HAWC will eventually reach a flux sensitivity of 0.02 Geminga
- ▶ Will observe
  - ▶ TeV halos from a dozen middle-aged ATNF pulsars.
  - ▶ TeV halos from ~40 additional young pulsars.

# A PLETHORA OF (RADIO) PULSARS

- ▶ Pulsations detected from 2613 systems.
- ▶ Vast majority in radio.



## USING TEV HALOS TO DISCOVER PULSARS



- ▶ Multi-wavelength emission from pulsar is beamed.
- ▶ 30 kyr propagation time of TeV halo implies the emission is isotropic.
- ▶ Can find off-beam pulsars by detecting the TeV halo.

- ▶ Tauris and Manchester (1998) calculated the beaming angle from a population of young and middle-aged pulsars.

$$f = \left[ 1.1 \left( \log_{10} \left( \frac{\tau}{100 \text{ Myr}} \right) \right)^2 + 15 \right] \%$$

- ▶ This varies between 15-30%.
- ▶ 1/f pulsars are unseen in radio surveys.

# MISSING TEV HALOS

2HWC Name	ATNF Name	Distance (kpc)	Angular Separation	Projected Separation	Expected Flux ( $\times 10^{-15}$ )	Actual Flux ( $\times 10^{-15}$ )	Flux Ratio	Expected Extension	Actual Extension	Age (kyr)	Chance Overlap
J0700+143	B0656+14	0.29	0.18°	0.91 pc	43.0	23.0	1.87	2.0°	1.73°	111	0.0
J0631+169	J0633+1746	0.25	0.89°	3.88 pc	48.7	48.7	1.0	2.0°	2.0°	342	0.0
J1912+099	J1913+1011	4.61	0.34°	27.36 pc	13.0	36.6	0.36	0.11°	0.7°	169	0.30
J2031+415	J2032+4127	1.70	0.11°	3.26 pc	5.59	61.6	0.091	0.29°	0.7°	181	0.002
J1831-098	J1831-0952	3.68	0.04°	2.57 pc	7.70	95.8	0.080	0.14°	0.9°	128	0.006

2HWC Name	ATNF Name	Distance (kpc)	Angular Separation	Projected Separation	Expected Flux ( $\times 10^{-15}$ )	Actual Flux ( $\times 10^{-15}$ )	Flux Ratio	Expected Extension	Actual Extension	Age (kyr)	Chance Overlap
J1930+188	J1930+1852	7.0	0.03°	3.67 pc	23.2	9.8	2.37	0.07°	0.0°	2.89	0.002
J1814-173	J1813-1749	4.7	0.54°	44.30 pc	243	152	1.60	0.11°	1.0°	5.6	0.61
J2019+367	J2021+3651	1.8	0.27°	8.48 pc	99.8	58.2	1.71	0.28°	0.7°	17.2	0.04
J1928+177	J1928+1746	4.34	0.03°	2.27 pc	8.08	10.0	0.81	0.11°	0.0°	82.6	0.002
J1908+063	J1907+0602	2.58	0.36°	16.21 pc	40.0	85.0	0.47	0.2°	0.8°	19.5	0.26
J2020+403	J2021+4026	2.15	0.18°	6.75 pc	2.48	18.5	0.134	0.23°	0.0°	77	0.01
J1857+027	J1856+0245	6.32	0.12°	13.24 pc	11.0	97.0	0.11	0.08°	0.9°	20.6	0.06
J1825-134	J1826-1334	3.61	0.20°	12.66 pc	20.5	249	0.082	0.14°	0.9°	21.4	0.14
J1837-065	J1838-0655	6.60	0.38°	43.77 pc	12.0	341	0.035	0.08°	2.0°	22.7	0.48
J1837-065	J1837-0604	4.78	0.50°	41.71 pc	8.3	341	0.024	0.10°	2.0°	33.8	0.68
J2006+341	J2004+3429	10.8	0.42°	80.07 pc	0.48	24.5	0.019	0.04°	0.9°	18.5	0.08

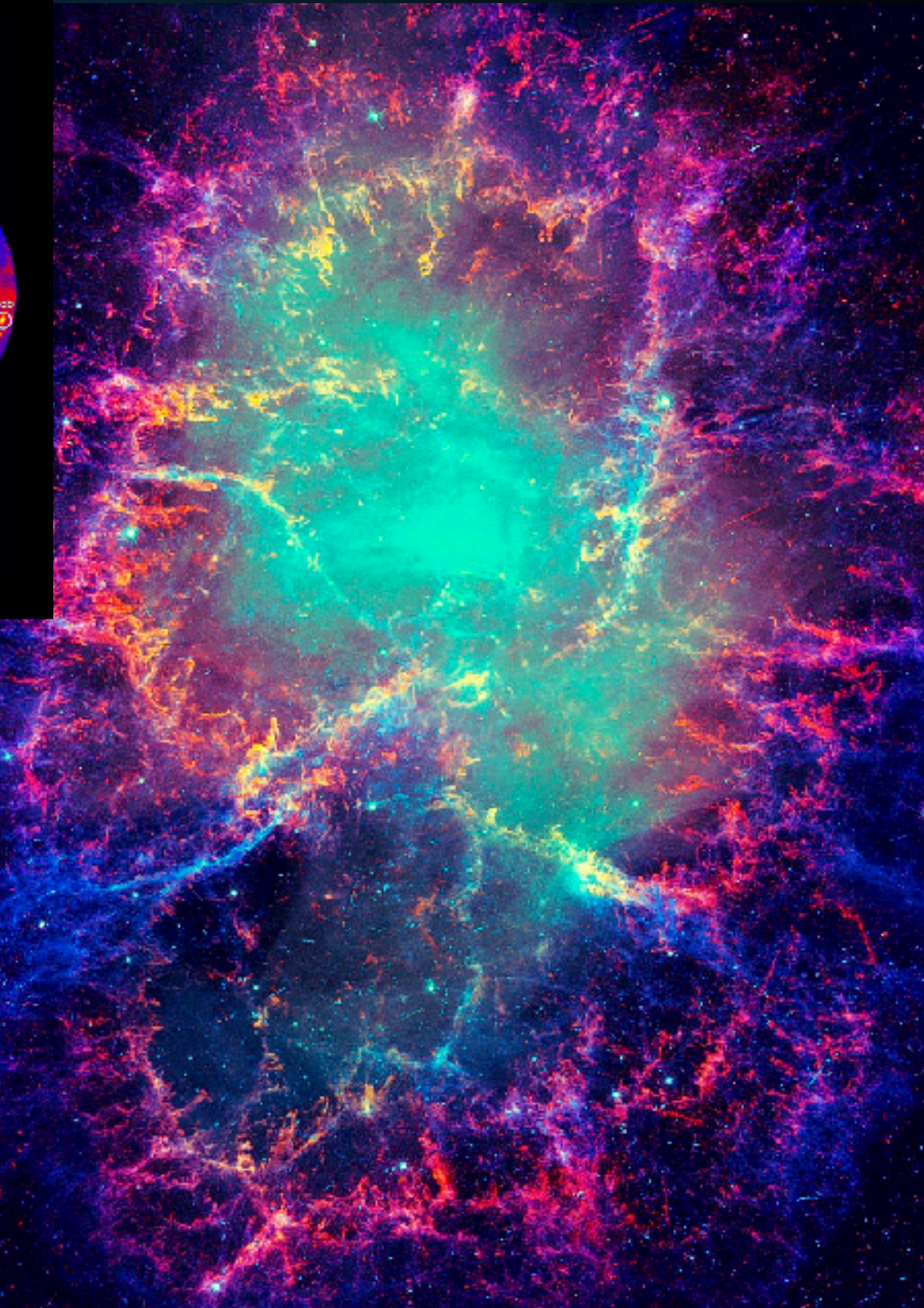
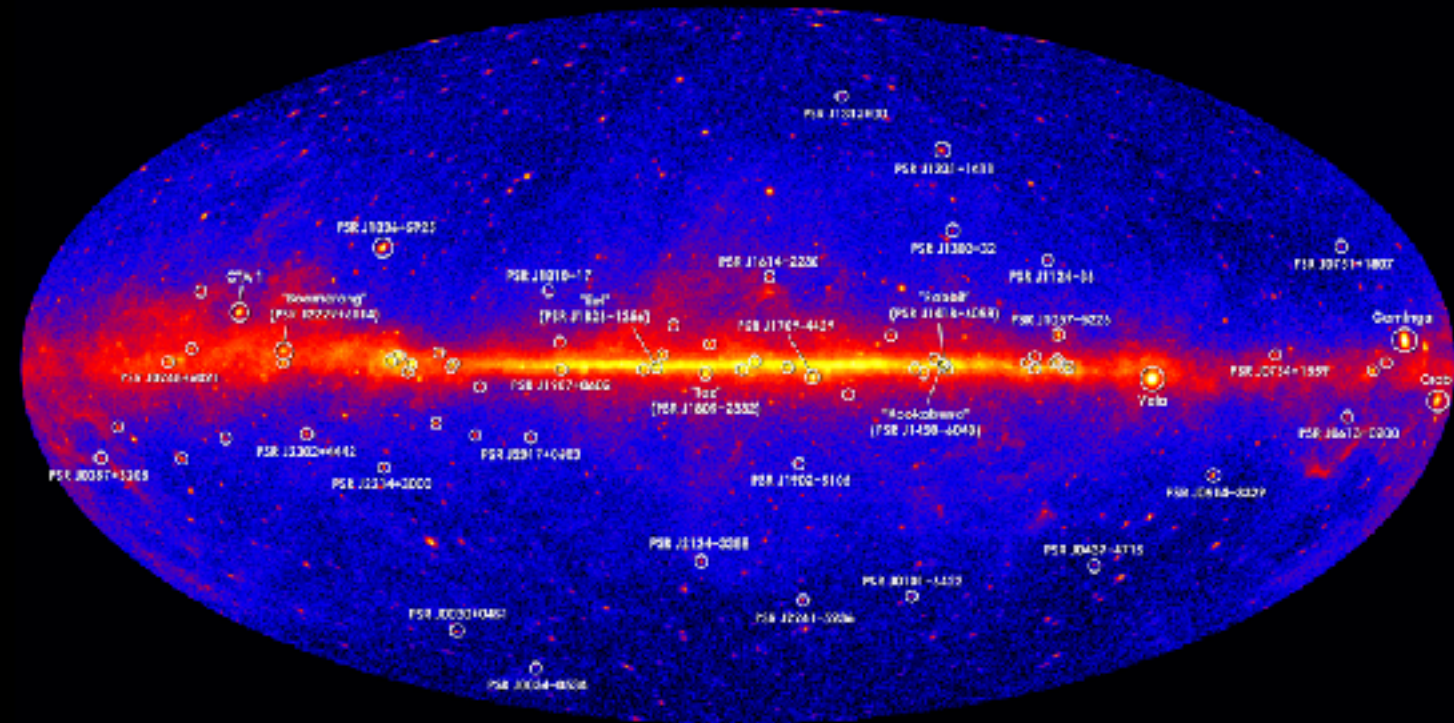
- ▶ The beaming fractions predicts that  $56^{+15}_{-11}$  TeV halos are currently observed by HAWC.
- ▶ However, only 39 total HAWC sources
- ▶ Chance overlaps, SNR contamination must be taken into account.

## EVENTUAL TEV HALO DETECTIONS

ATNF Name	Dec. ( $^{\circ}$ )	Distance (kpc)	Age (kyr)	Spindown Lum. ( $\text{erg s}^{-1}$ )	Spindown Flux ( $\text{erg s}^{-1} \text{ kpc}^{-2}$ )	2HWC
J0633+1746	17.77	0.25	342	3.2e34	4.1e34	2HWC J0631+169
B0656+14	14.23	0.29	111	3.8e34	3.6e34	2HWC J0700+143
B1951+32	32.87	3.00	107	3.7e36	3.3e34	—
J1740+1000	10.00	1.23	114	2.3e35	1.2e34	—
J1913+1011	10.18	4.61	169	2.9e36	1.1e34	2HWC J1912+099
J1831-0952	-9.86	3.68	128	1.1e36	6.4e33	2HWC J1831-098
J2032+4127	41.45	1.70	181	1.7e35	4.7e33	2HWC J2031+415
B1822-09	-9.58	0.30	232	4.6e33	4.1e33	—
B1830-08	-8.45	4.50	147	5.8e35	2.3e33	—
J1913+0904	9.07	3.00	147	1.6e35	1.4e33	—
B0540+23	23.48	1.56	253	4.1e34	1.4e33	—

- ▶ 10 year HAWC observations should detect  $37^{+17}_{-13}$  TeV halos surrounding middle-aged pulsars.
- ▶ These numbers correspond to most of the TeV sources detectable by HAWC.

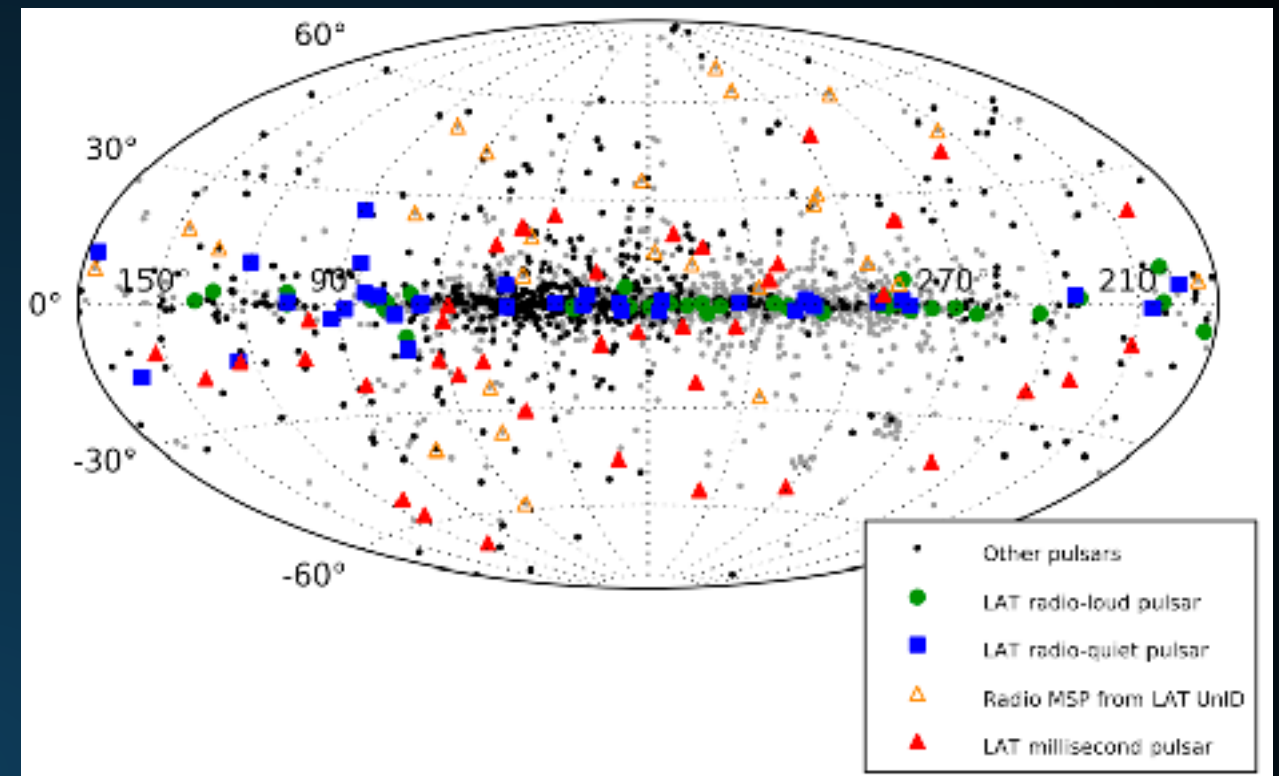
# HOW MANY OF THESE SOURCES ARE NEW?



- ▶ How many of these sources have been discovered?
  - ▶ gamma-ray pulsars
  - ▶ X-Ray PWN
  - ▶ Current ACTs

## FERMI-LAT DETECTIONS

- ▶ Fermi-LAT has detected 54 new pulsars
  - ▶ 35 younger than 100 kyr
  - ▶ Only 5/35 in HAWC field of view
- ▶ Fermi-LAT has detected only ~5 of these 37 systems.

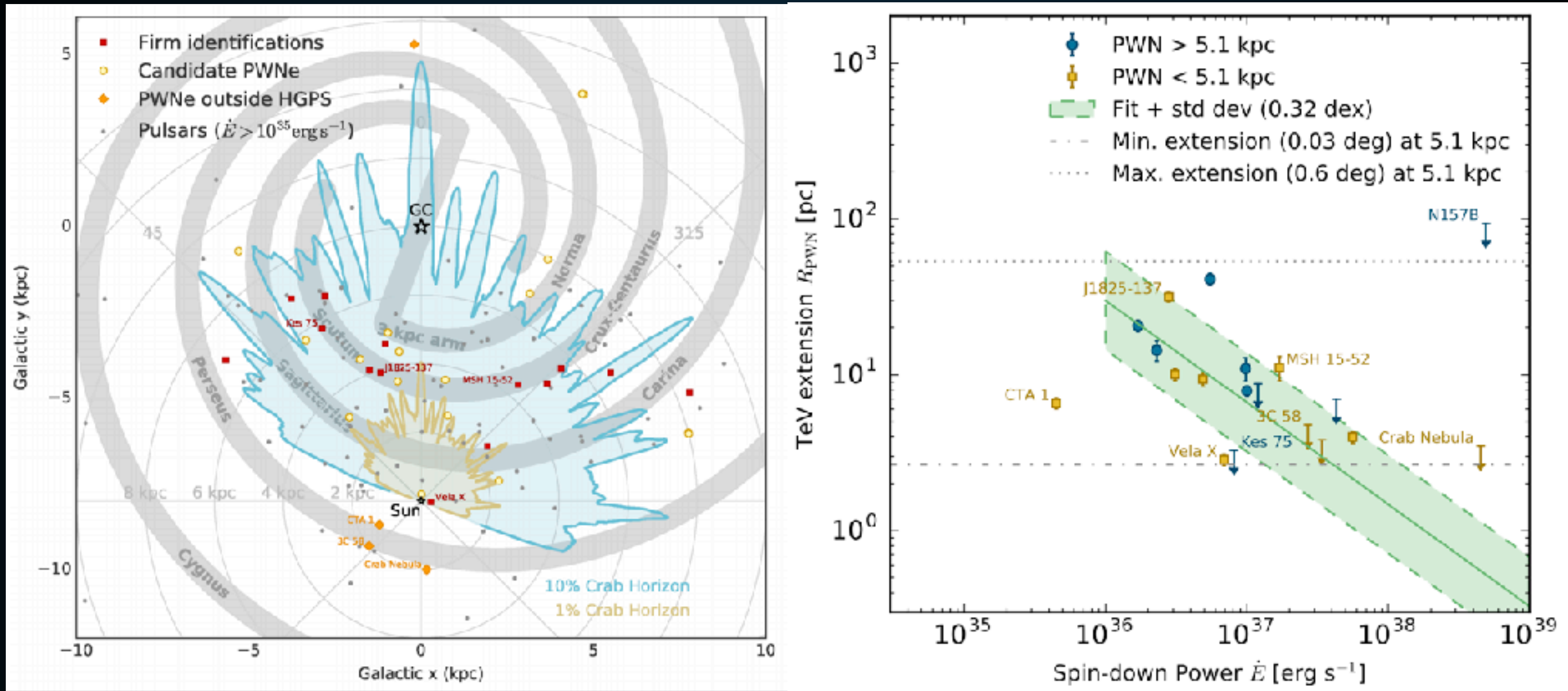


# X-RAY PWN DETECTIONS

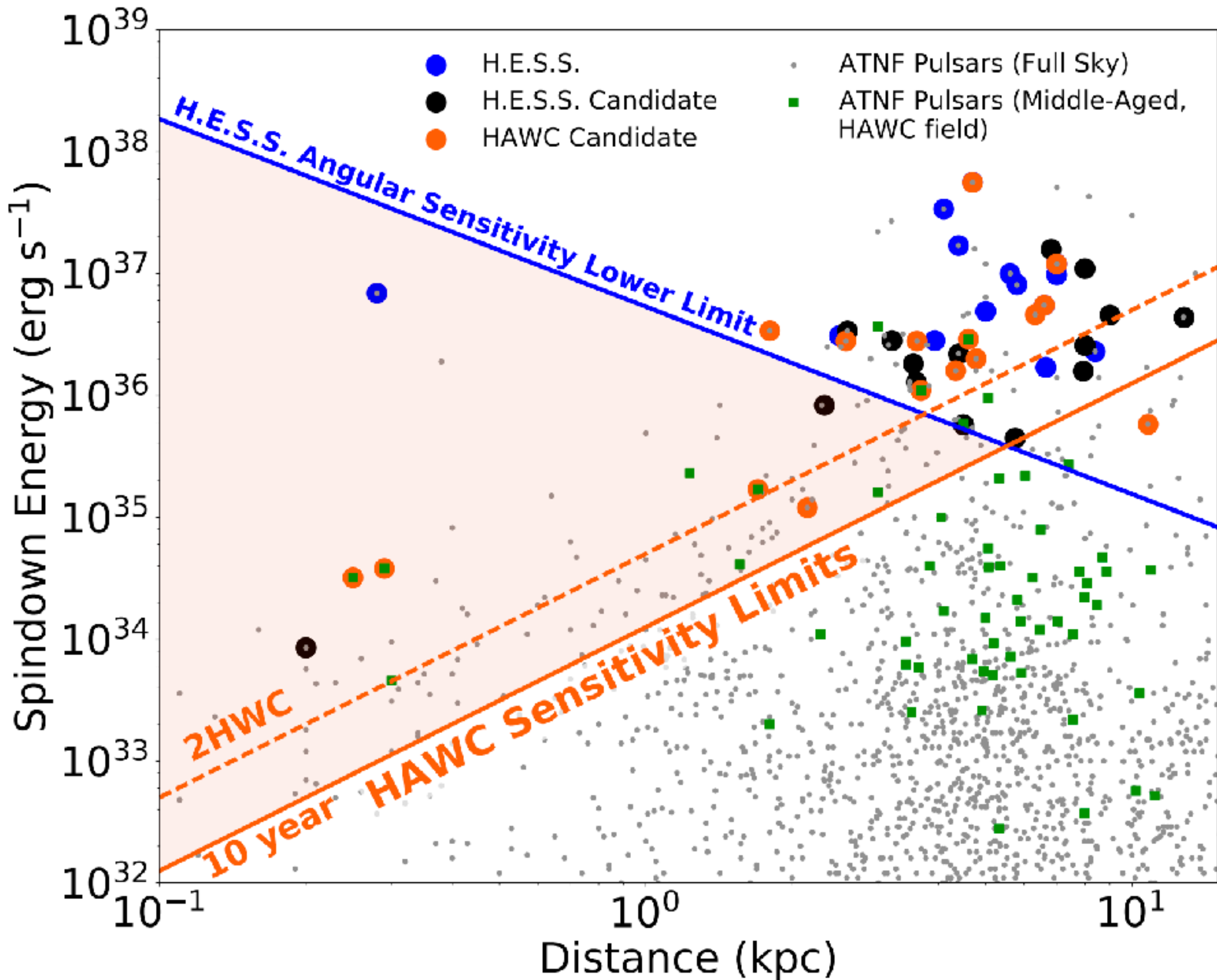
PWNe With No Detected Pulsar					
Gname	other name(s)	R	X	Q	G
G0.13-0.11				?	notes
G0.9+0.1				N	notes
G7.4-2.0	GeV J1809-2327, Tazzie			Y	notes
G16.7+0.1				N	notes
G18.5-0.4	GeV J1825-1310, Ecl			Y	notes
G20.0-0.2				N	notes
G24.7+0.6				N	notes
G27.8+0.6				N	notes
G39.2-0.3	3C 396			Y	notes
G63.7+1.1				N	notes
G74.9+1.2	CTB 87			Y	notes
G119.5+10.2	CTA 1			Y	notes
G189.1+3.0	IC 443			?	notes
G279.8-35.8	B0453-685			N	notes
G291.0-0.1	MSH 11-62			Y	notes
G293.8+0.6				N	notes
G313.3+0.1	Rabbit			Y	notes
G318.9+0.4				N	notes
G322.5-0.1				N	notes
G326.3-1.8	MSH 15-56			N	notes
G327.1-1.1				N	notes
G328.4+0.2	MSH 15-57			N	notes
G358.6-17.2	RX J1856.5-3754	N	N	N	notes
G359.89-0.08				Y	notes

- ▶ X-Ray PWN have detected only ~6 of these 37 systems.

# HESS/VERITAS DETECTIONS



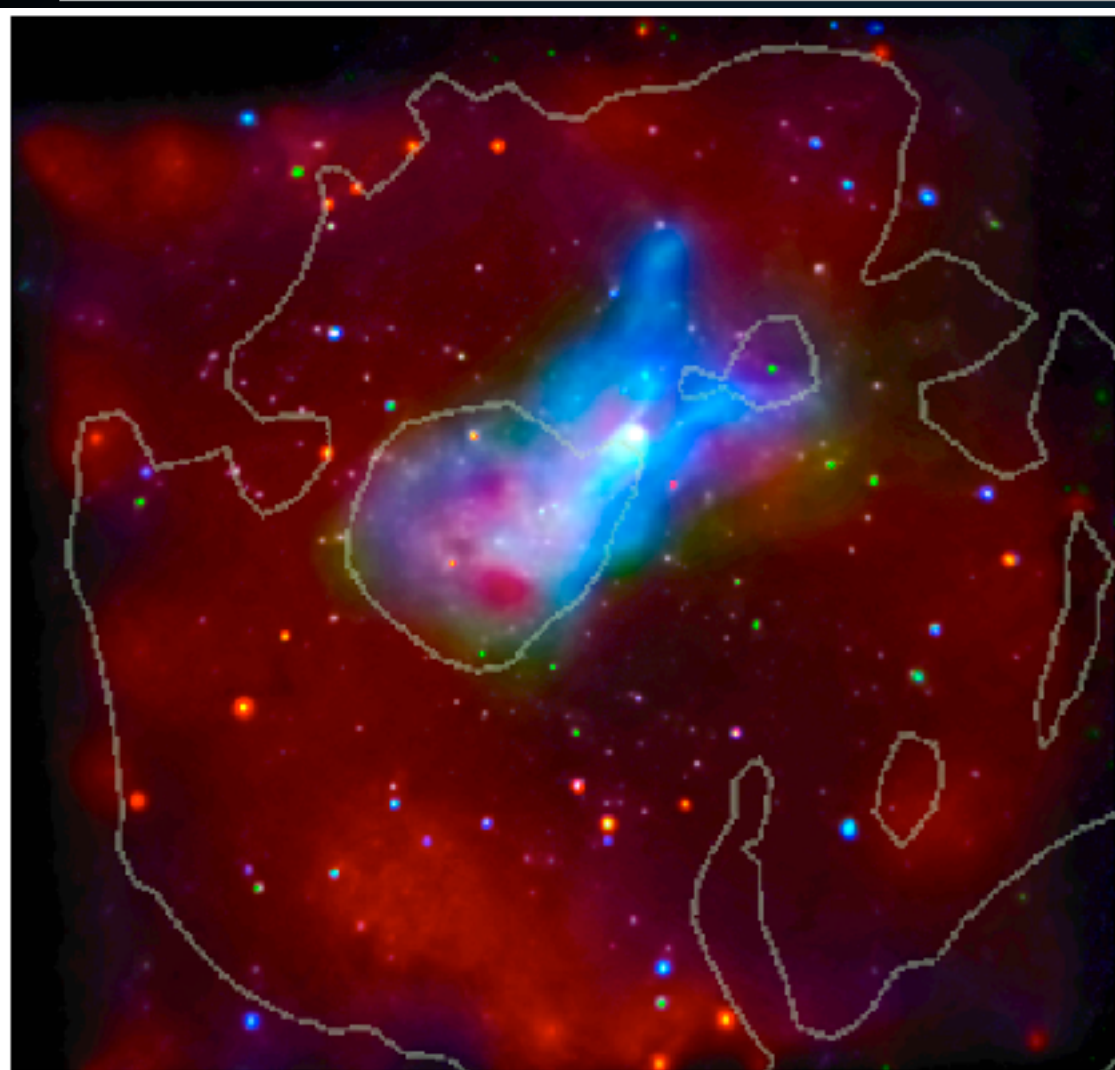
- ▶ Targeted ACTs are sensitive to the flux from TeV halos.
- ▶ ACTs are not sensitive to sources extended  $>0.5^\circ$ .
- ▶ Large parameter space available only to HAWC.



## CONFIRMING TEV HALOS

---

- ▶ Several Methods to confirm TeV halo detections:
  - ▶ X-Ray halos
  - ▶ X-Ray PWN



- ▶ Possible Detection! (G327-1.1)
- ▶ Young Pulsar (17.4 kyr)
- ▶ Two PWN
- ▶ Diffuse PWN has significantly softer spectrum

Region	Area (arcsec <sup>2</sup> )	Cts (1000)	N <sub>H</sub> (10 <sup>22</sup> cm <sup>-2</sup> )	Photon Index	Amplitude (10 <sup>-4</sup> )	kT (keV)	τ (10 <sup>12</sup> s cm <sup>-3</sup> )	Norm. (10 <sup>-3</sup> )	F <sub>1</sub> (10 <sup>-12</sup> )	F <sub>2</sub>	Red. $\chi^2$
1 Compact Source	84.657	6.34	1.93 <sup>+0.08</sup> <sub>-0.08</sub>	1.61 <sup>+0.08</sup> <sub>-0.07</sub>	1.05 <sup>+0.11</sup> <sub>-0.10</sub>	...	...	...	0.45	...	0.80
2 Cometary PWN	971.22	7.75	1.93	1.62 <sup>+0.08</sup> <sub>-0.07</sub>	1.47 <sup>+0.16</sup> <sub>-0.14</sub>	...	...	...	1.09	...	...
3 Trail East	537.42	2.13	1.93	1.84 <sup>+0.12</sup> <sub>-0.12</sub>	0.44 <sup>+0.07</sup> <sub>-0.06</sub>	...	...	...	0.27	...	...
4 Trail West	766.56	3.12	1.93	1.80 <sup>+0.11</sup> <sub>-0.11</sub>	0.61 <sup>+0.09</sup> <sub>-0.08</sub>	...	...	...	0.39	...	...
5 Trail 1	424.45	1.98	1.93	1.76 <sup>+0.12</sup> <sub>-0.12</sub>	0.39 <sup>+0.05</sup> <sub>-0.05</sub>	...	...	...	0.26	...	...
6 Trail 2	588.19	2.13	1.93	1.95 <sup>+0.11</sup> <sub>-0.11</sub>	0.49 <sup>+0.07</sup> <sub>-0.06</sub>	...	...	...	0.28	...	...
7 Trail 3	994.92	2.99	1.93	2.09 <sup>+0.10</sup> <sub>-0.10</sub>	0.78 <sup>+0.09</sup> <sub>-0.08</sub>	...	...	...	0.42	...	...
8 Trail 4	839.48	2.38	1.93	2.28 <sup>+0.12</sup> <sub>-0.12</sub>	0.74 <sup>+0.09</sup> <sub>-0.09</sub>	...	...	...	0.37	...	...
9 Prong East	828.58	1.66	1.93	1.72 <sup>+0.14</sup> <sub>-0.14</sub>	0.30 <sup>+0.06</sup> <sub>-0.05</sub>	...	...	...	0.27	...	...
10 Prong West	971.22	2.06	1.93	1.85 <sup>+0.14</sup> <sub>-0.14</sub>	0.44 <sup>+0.08</sup> <sub>-0.07</sub>	...	...	...	1.09	...	...
11 Diffuse PWN*	20007	27.7	1.93	2.11 <sup>+0.04</sup> <sub>-0.05</sub>	6.91 <sup>+0.37</sup> <sub>-0.74</sub>	0.23 <sup>+0.14</sup> <sub>-0.05</sub>	0.21 <sup>+0.88</sup> <sub>-0.16</sub>	6.0 <sup>+16</sup> <sub>-4.0</sub>	3.68	17.7	0.82
12 Relic PWN*	26787	17.2	1.93	2.58 <sup>+0.07</sup> <sub>-0.10</sub>	6.51 <sup>+0.53</sup> <sub>-0.71</sub>	0.23	0.21	6.9 <sup>+18</sup> <sub>-5.5</sub>	3.14	20.3	...
13 Total	31474	41.9	1.93 <sup>+0.23</sup> <sub>-0.20</sub>	2.38 <sup>+0.19</sup> <sub>-0.19</sub>	7.22 <sup>+0.49</sup> <sub>-0.74</sub>	0.23	0.21	6.9 <sup>+18</sup> <sub>-5.5</sub>	3.21	17.7	...

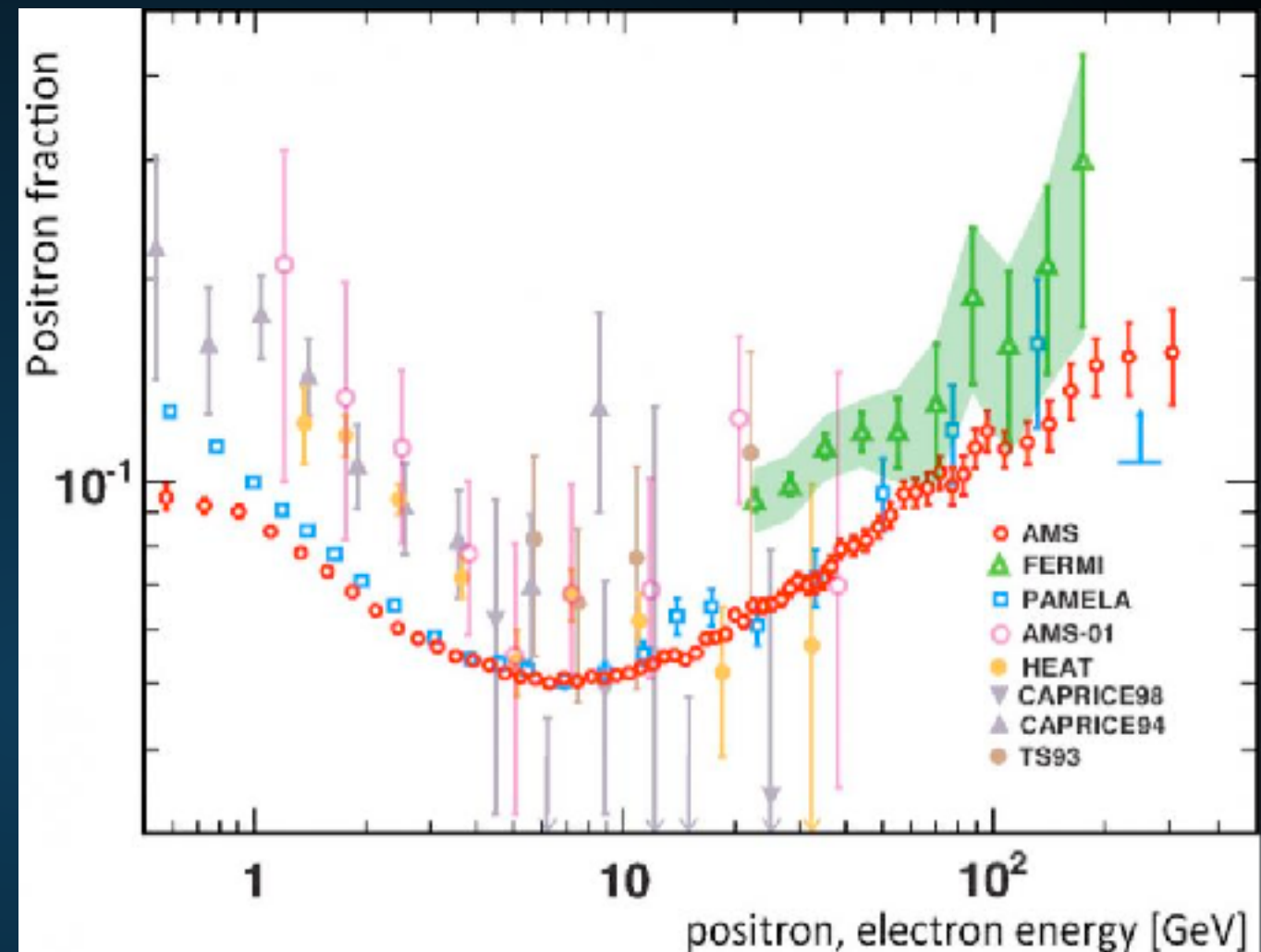
---

# Implication II: The Positron Excess

# THE POSITRON EXCESS

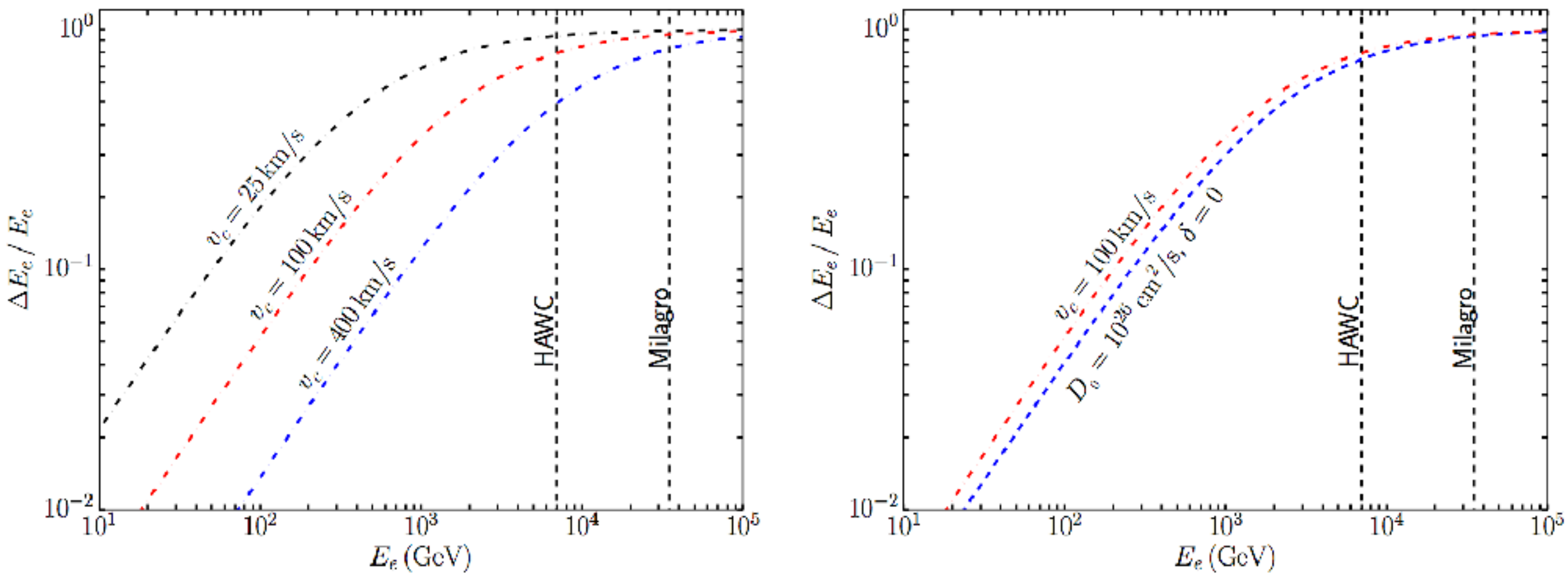
- ▶ **Rising fraction of cosmic-ray positrons at energies above 10 GeV**

- ▶ **Standard Cosmic-Ray Secondary Production predicts the positron fraction falls as  $\sim E^{-0.4}$ .**



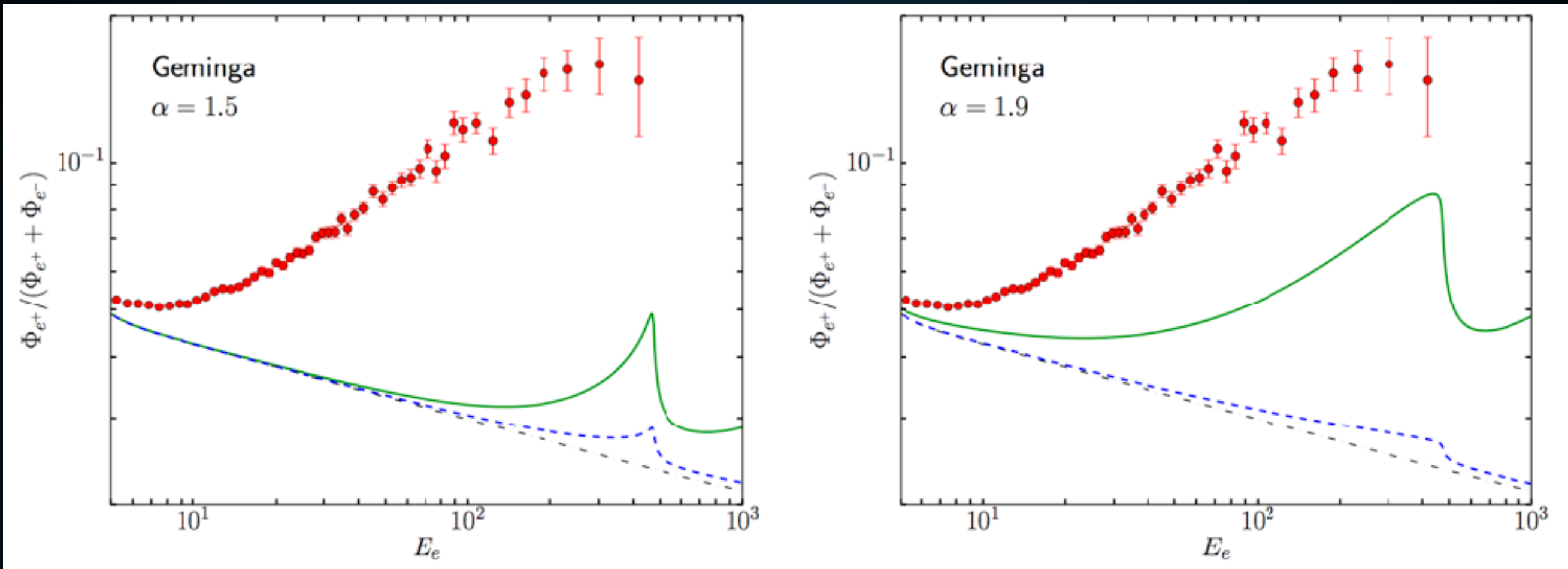
- ▶ **Indicates a new primary source of high energy  $e^+e^-$  pairs.**

## IMPLICATION I: THE POSITRON EXCESS



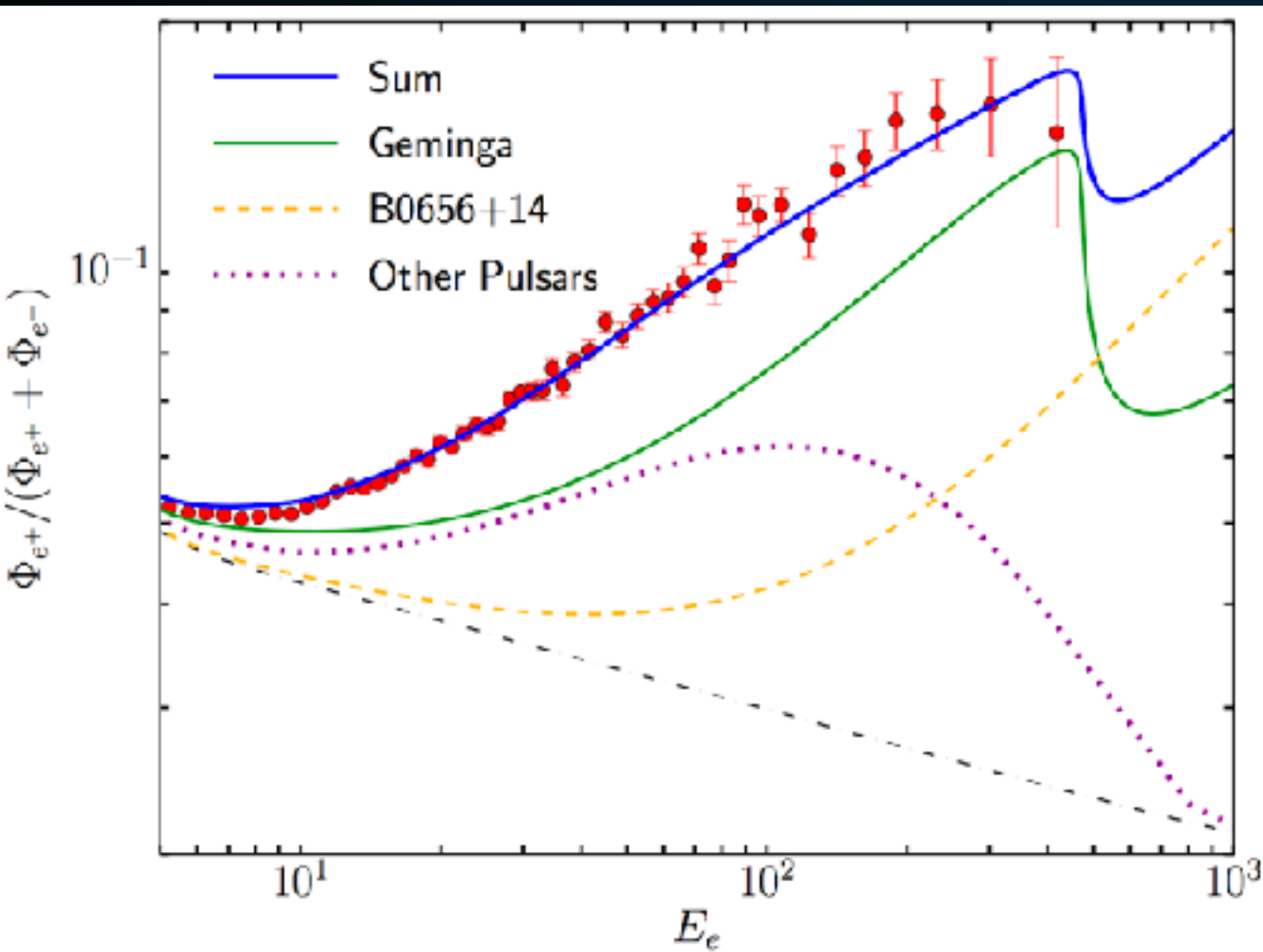
- ▶ What do the low-energy  $e^+e^-$  do?
- ▶ Large flux (10% of spin-down power)
- ▶ Hard Spectrum
- ▶ Most escape

# THE POSITRON FRACTION FROM TEV HALOS



- ▶ **Geminga can individually produce nearly half of the positron excess.**
- ▶ **Models not fit to the data - this contribution must exist.**

# THE POSITRON FRACTION FROM TEV HALOS



\*Braking index slightly changed to fit model to data.

- ▶ Total Contribution from:
  - ▶ Geminga
  - ▶ Monogem
  - ▶ Average of other young pulsars

- ▶ Reasonable models can be exactly fit to the excess.

---

# **Implication III:**

## **Most TeV gamma-rays are leptonic**

## Hadronic Emission

$$E_{p, \text{SN}} = 10^{50} \text{ erg}$$

$$\frac{dN_{p,\text{SN}}}{dE} = 4 \times 10^{51} E^{-2} e^{-E/1\text{PeV}} \text{ GeV}^{-1}$$

$$\boxed{\phi_{\gamma, \pi_0} \propto E^{-2.7} \rightarrow 4 \times 10^{51} E^{-2.7} e^{-E/1\text{PeV}}}$$

## Leptonic Emission

$$KE_{\text{pulsar}} = 10^{49} \text{ erg}$$

$$e^+ e^-_{\text{pulsar}} \approx 10^{48} \text{ erg}$$

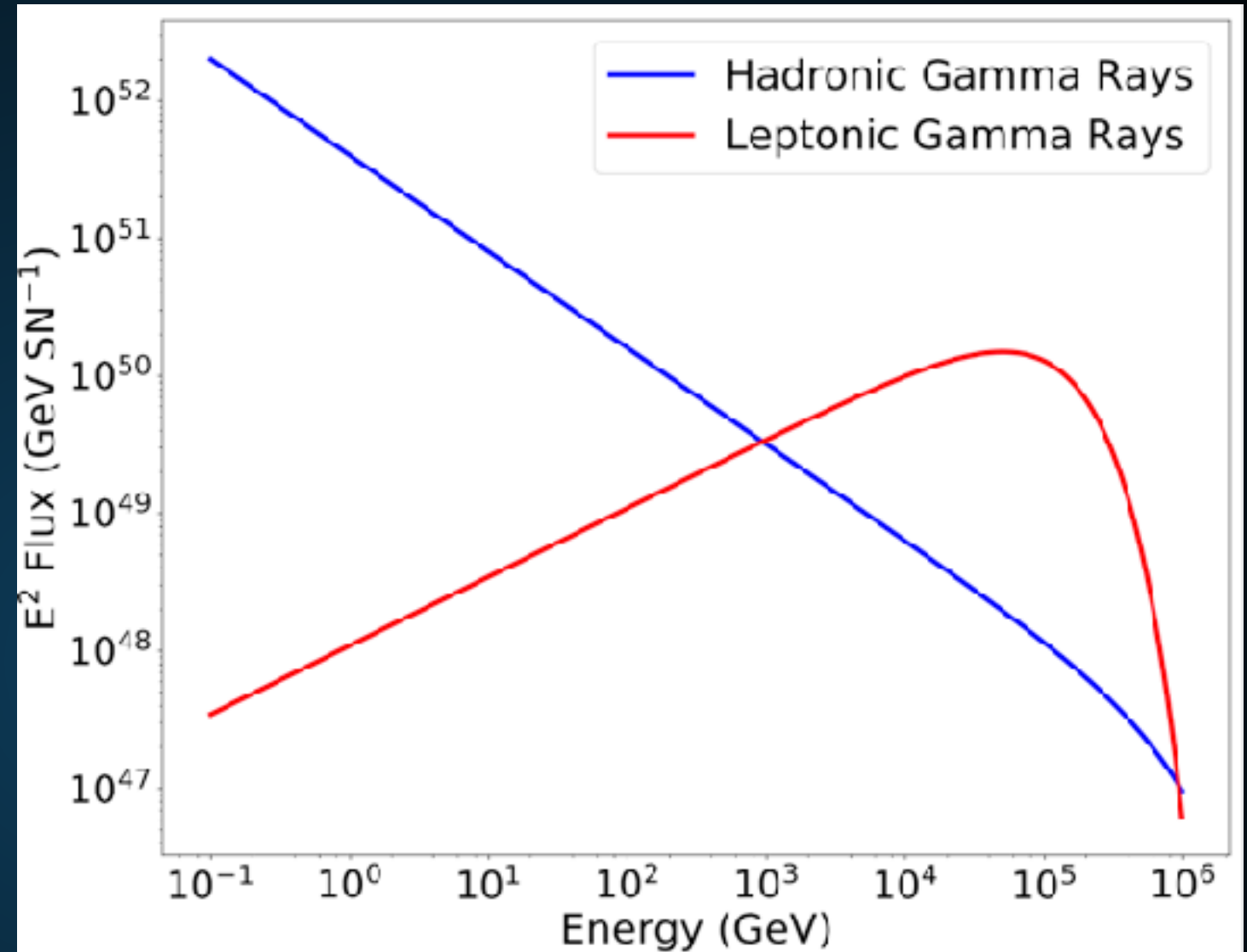
$$\frac{dN_{e^+ e^-, p}}{dE} = 1.1 \times 10^{48} E^{-1.5} e^{-E/100\text{TeV}}$$

$$\boxed{\phi_{\gamma, \text{ICS}} = 1.1 \times 10^{48} E^{-1.5} e^{-E/100\text{TeV}}}$$

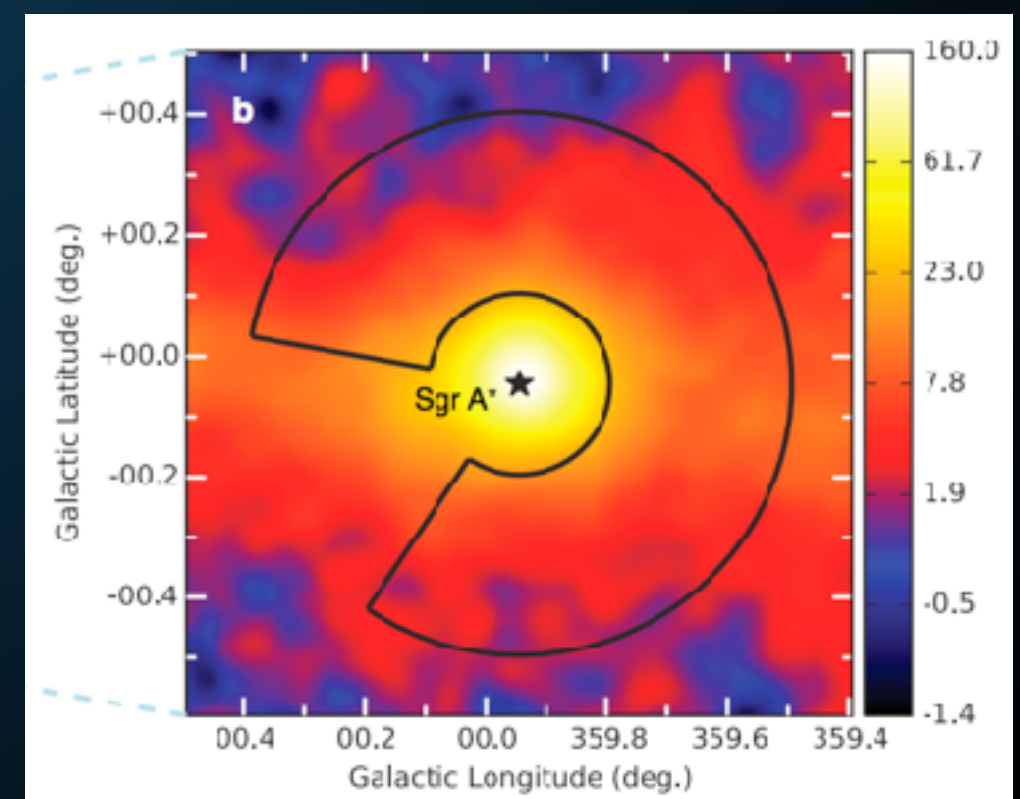
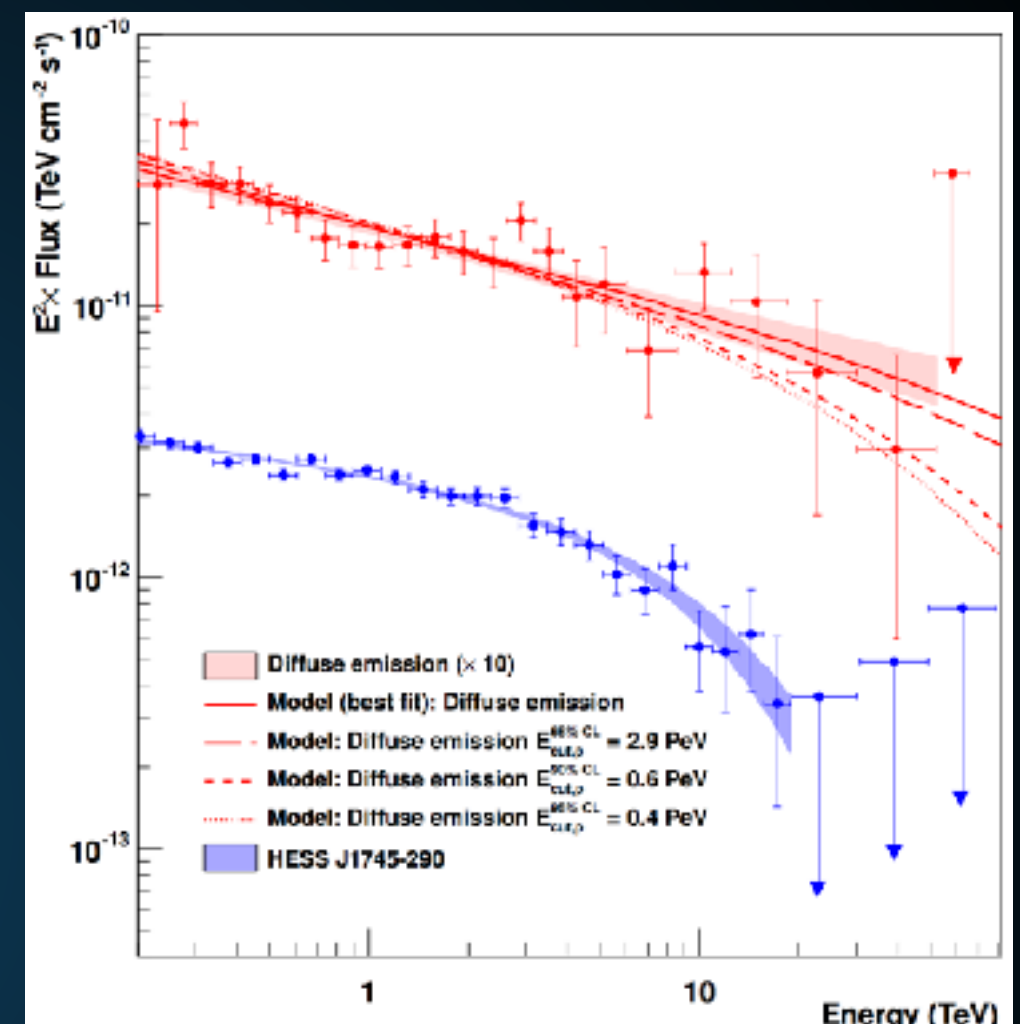
- ▶ Traditionally believe that hadronic cosmic-rays are dominant.
- ▶ Two effects at high energies:
  - ▶ Hard primary electron injection spectra
  - ▶ Milky Way is calorimetric to TeV leptons

## TOTAL HIGH-ENERGY EMISSION FROM SNR AND PULSAR

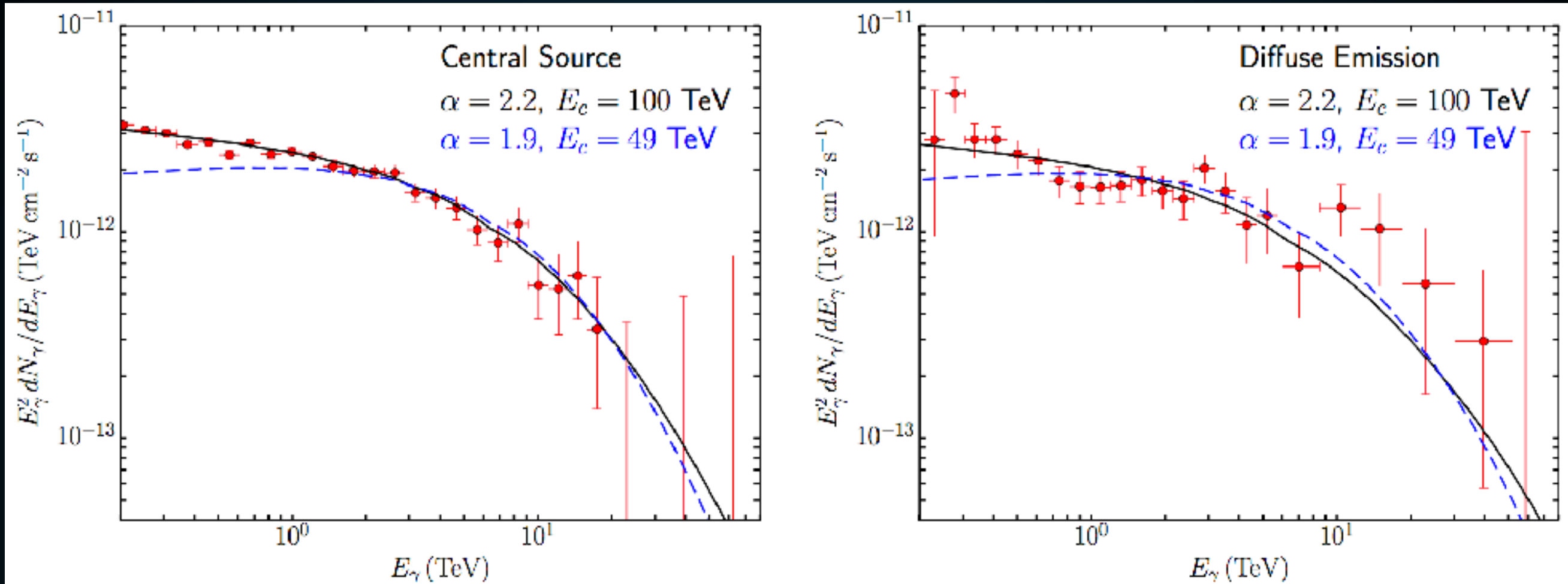
- ▶ At high energies, leptonic gamma-rays become dominant.
- ▶ There are many TeV halos in the Milky Way
- ▶ Dim TeV halos will be observed as a new diffuse gamma-ray emission component.



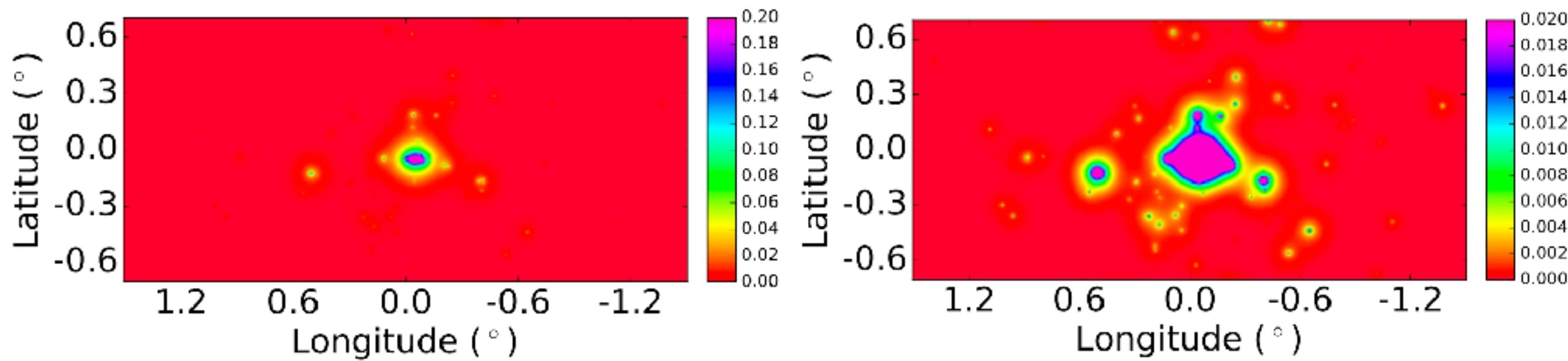
- ▶ HESS observations indicate diffuse ~50 TeV emission from the Galactic center
- ▶ If this emission is hadronic, it indicates PeV particle acceleration in the GC
- ▶ Spherical symmetry hints at Galactic Center source.



# TEV HALOS PRODUCE THE PEVATRON SPECTRUM

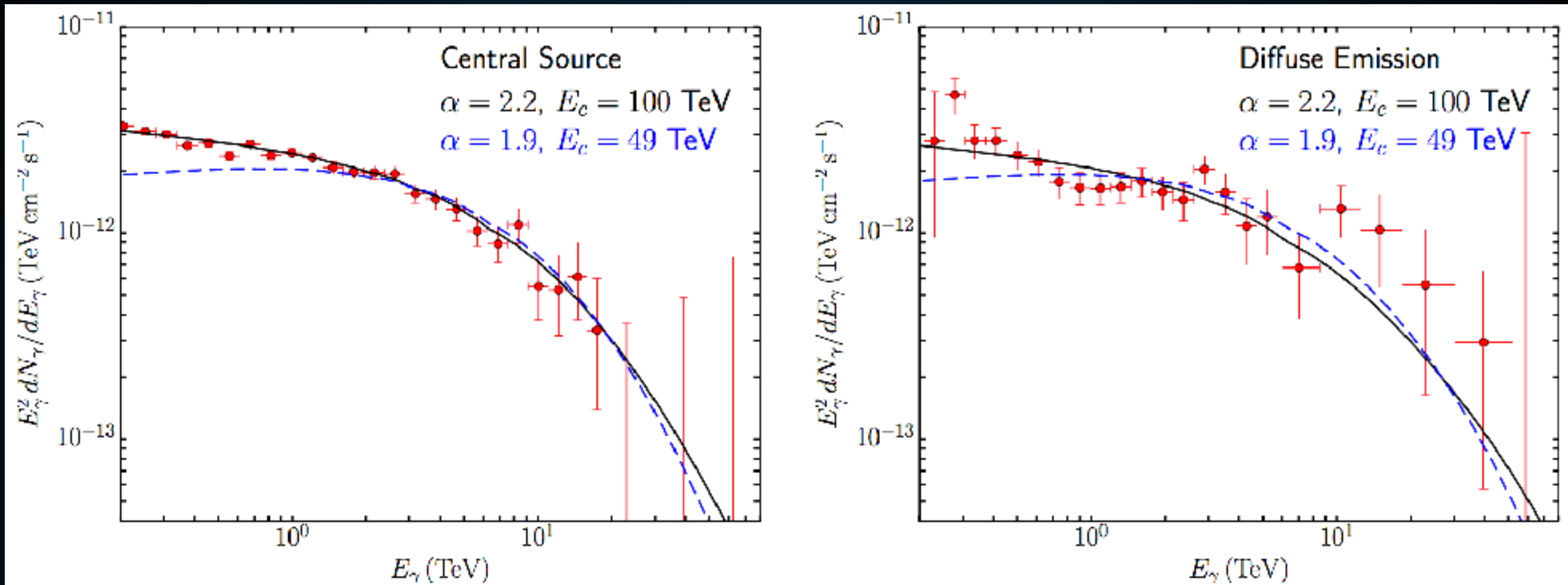


- ▶ The TeV halo spectrum from Geminga naturally reproduces the HESS observations.
- ▶ Slightly softer spectra preferred.
- ▶ Some evidence that Geminga spectrum is particularly hard.
- ▶ Hadronic diffuse background contamination?



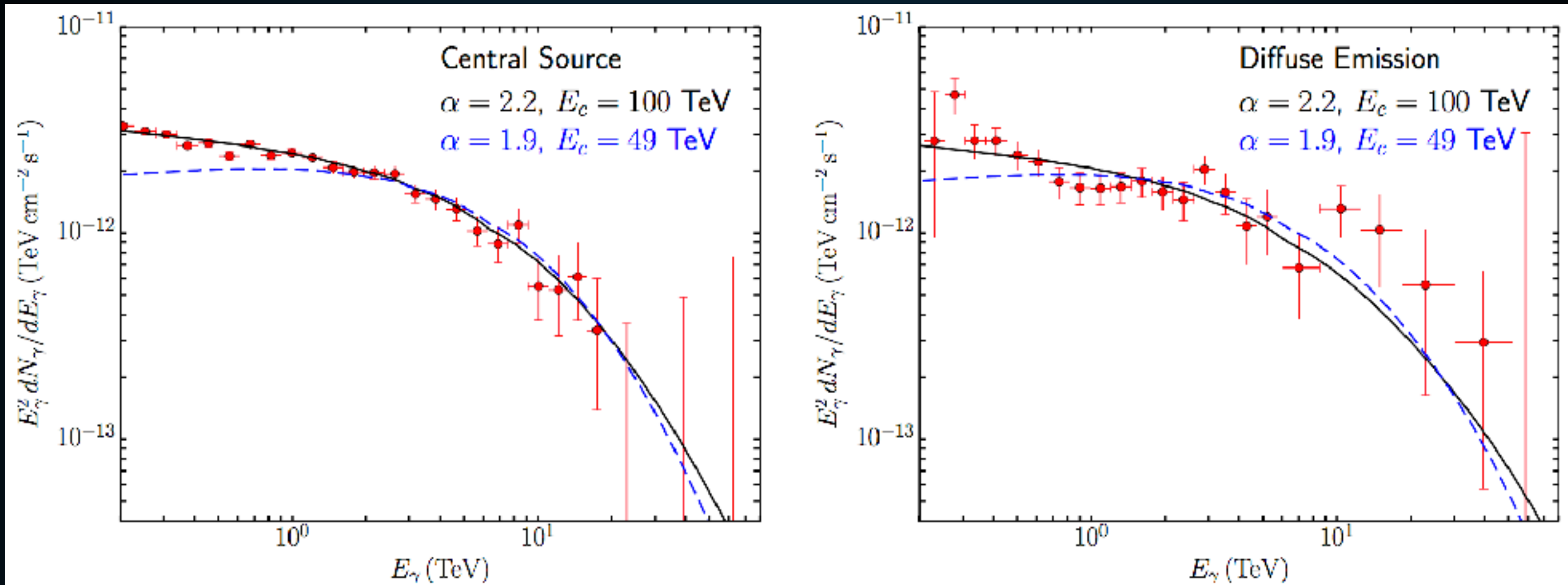
- ▶ **Significant star (pulsar) formation in the Galactic center**
- ▶ **Pulsars formed in the central parsec will be kicked into surrounding medium.**
- ▶ **Source of diffuse gamma-rays in the Galactic center.**

# INTENSITY OF TEV HALO EMISSION IN GALACTIC CENTER



- ▶ Using standard values for the propagation of these sources:
  - ▶ TeV Halos survive 10 Myr (but become very dim)
  - ▶ Pulsar kicks  $\sim 400 \text{ km/s}$
  - ▶ Birth rate between 100-750 pulsars/Myr
- ▶ We reproduce the intensity and morphology of the HESS emission.

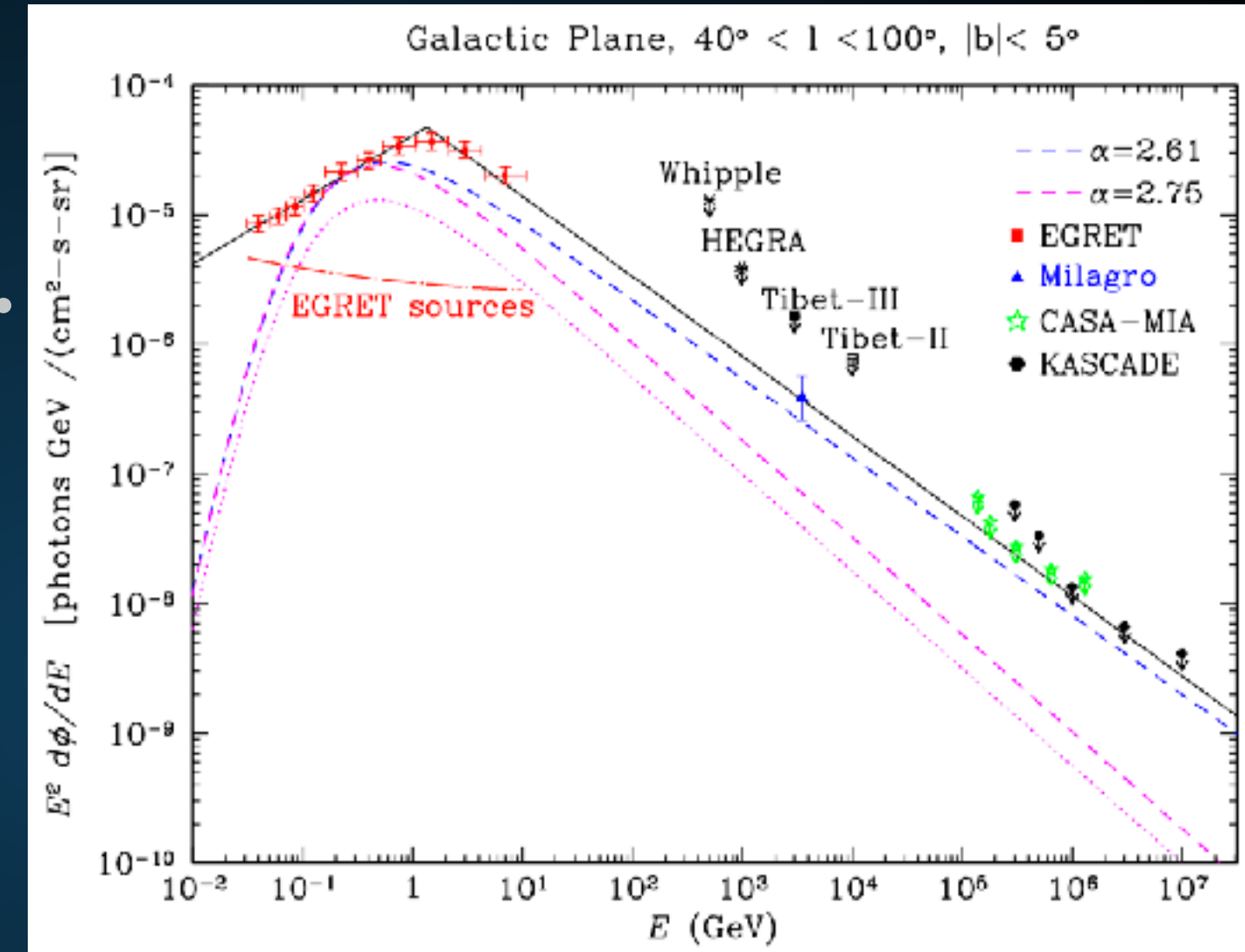
# INTENSITY OF TEV HALO EMISSION IN GALACTIC CENTER



- ▶ Our model implies that TeV halos must form a substantial fraction of the HESS Pevatron emission.
- ▶ Implies 100-300 observable pulsars in the Galactic center, providing a handle on the missing pulsar problem ([1310.7022](#), [1311.4846](#)).

- ▶ Milagro detects bright diffuse TeV emission along the Galactic plane.

- ▶ Difficult to explain with pion decay, due to steeply falling local hadronic CR spectrum.

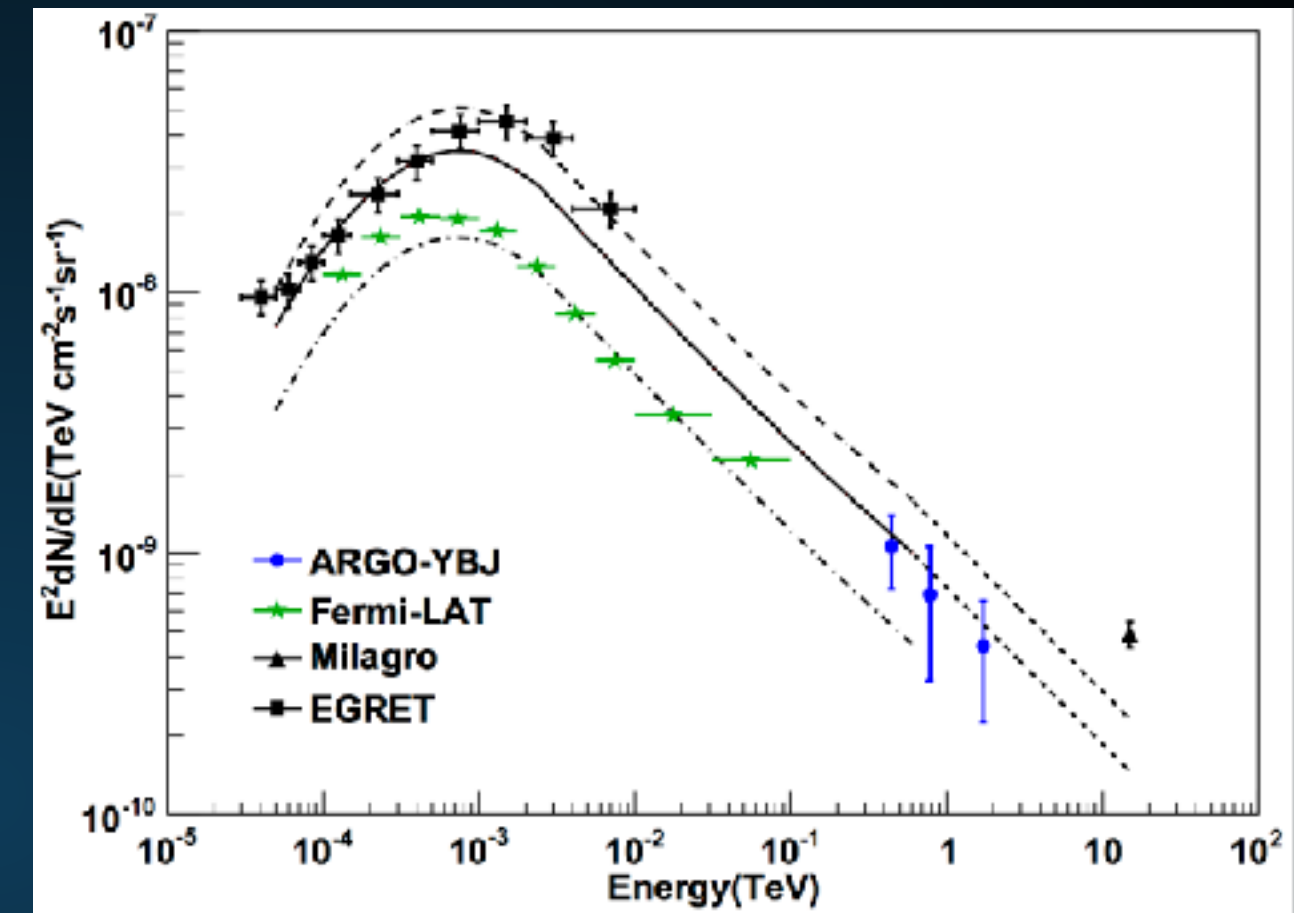


- ▶ Can harden gamma-ray emission to some extent using radially dependent diffusion constants (1504.00227).

- ▶ Recent ARGO-YBJ observations are in tension with Milagro result.

- ▶ Tension can be alleviated if the gamma-ray spectrum in the region is very hard.

- ▶ TeV halos can produce this emission!



- ▶ Use a generic model for pulsar luminosities:

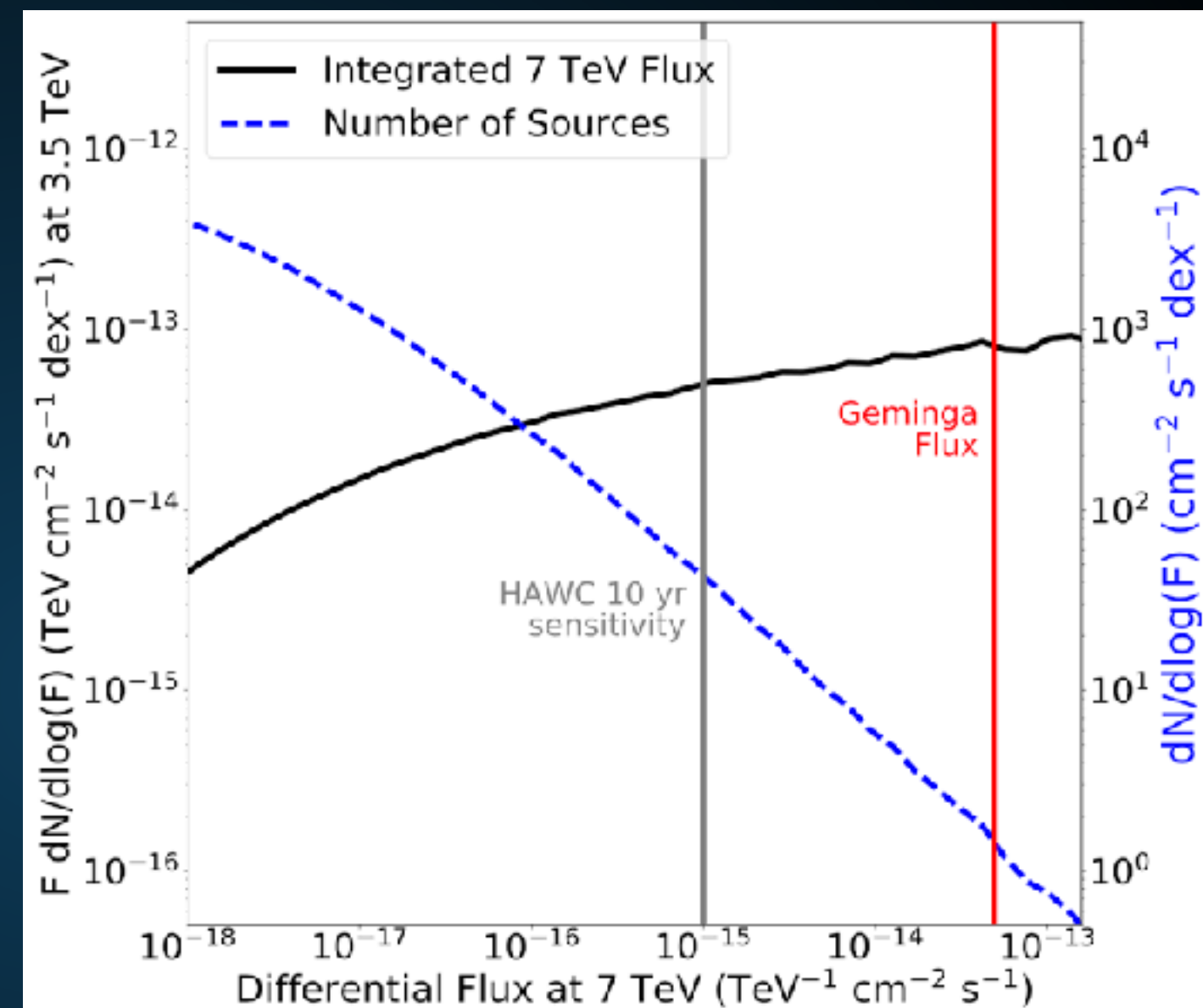
- ▶  $B_0 = 10^{12.5} \text{ G}$  ( $10^{0.3} \text{ G}$ )

- ▶  $P_0 = 0.3 \text{ s}$  ( $0.15 \text{ s}$ )

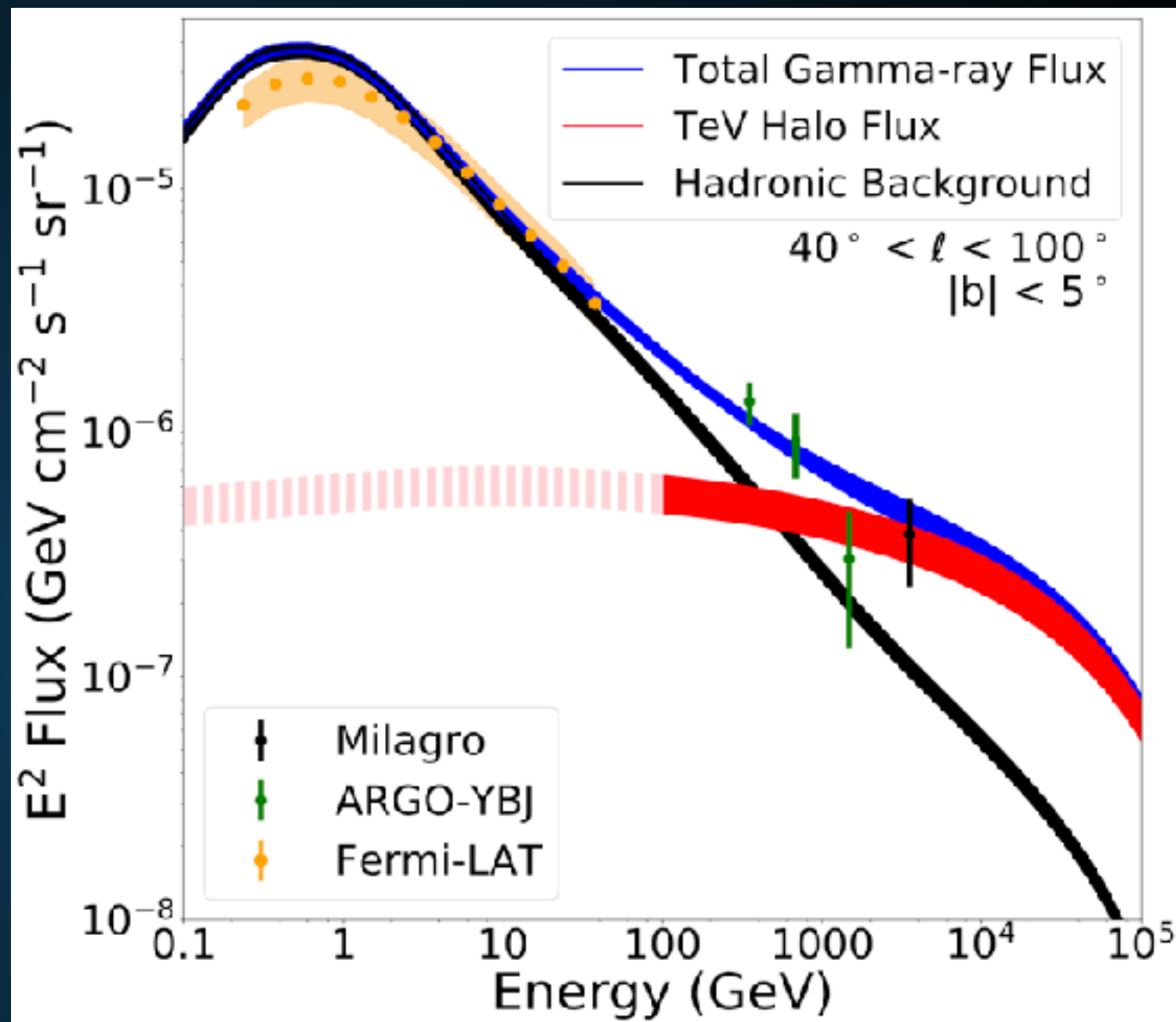
- ▶ Spindown Timescale of  $\sim 10^4 \text{ yr}$  (depends on  $B_0$ )

- ▶ Galprop model for supernova distances

- ▶ Naturally expect O(1) source as bright as Geminga
- ▶ HAWC eventually observes O(50) sources.



- ▶ Use Geminga as a template to calculate TeV halo intensity.
- ▶ Use Geminga spectrum with complete (diffuse) cooling.
- ▶ Hadronic background from Galprop models tuned to Fermi-LAT emission.
- ▶ TeV halos naturally explain the intensity and spectrum of the TeV excess.





# TeVPA 2017

[tevpa2017.osu.edu](http://tevpa2017.osu.edu)

- ▶ August 7–11, Columbus, OH
- ▶ Registration and abstract submission are open
- ▶ Pre-meeting mini-workshops on Sunday, August 6

## CONCLUSIONS (1/2)

---

- ▶ **TeV observations open up a new window into understanding Milky Way pulsars.**
- ▶ **Early indications:**
  - ▶ **Positron Excess is due to pulsar activity**
  - ▶ **TeV halos produce most of the TeV sources observed by ACTs and HAWC**
  - ▶ **TeV halos dominate the diffuse TeV emission in our galaxy.**

## CONCLUSIONS (2/2)

---

- ▶ Additional implications:
  - ▶ Young pulsar braking index
  - ▶ Galactic cosmic-ray diffusion
  - ▶ Source of IceCube neutrinos

---

# Extra Slides

## X-RAY HALOS

- ▶ An X-Ray halo with an identical morphology as the TeV halo must exist.

$$\begin{aligned} U &= \frac{1}{8\pi} \beta^2 = \frac{(10 \mu G)^2}{8\pi} \\ &= 4 \times 10^{-12} \frac{\text{erg}}{\text{cm}^3} \\ \int_0^{10 \text{ pc}} U dV &= 5 \times 10^{47} \text{ erg} \\ \hookrightarrow \text{Magnetic Flux} &\approx 5 \times 10^{38} \frac{\text{erg s}}{\text{s}} \end{aligned}$$

$$\begin{aligned} \text{ISRF} &= I \frac{\text{eV}}{\text{cm}^3} \\ \int \text{ISRF} dV &= 8 \times 10^{47} \text{ erg} \\ \hookrightarrow \text{Flux} &= 8 \times 10^{38} \frac{\text{erg s}}{\text{s}} \end{aligned}$$

$$E_{\text{sync, critical}} = 22 \text{ eV} \left( \frac{B}{5 \mu G} \right) \left( \frac{E_e}{10 \text{ TeV}} \right)^2$$

- ▶ However, the signal has a low surface brightness and peaks at a low energy.

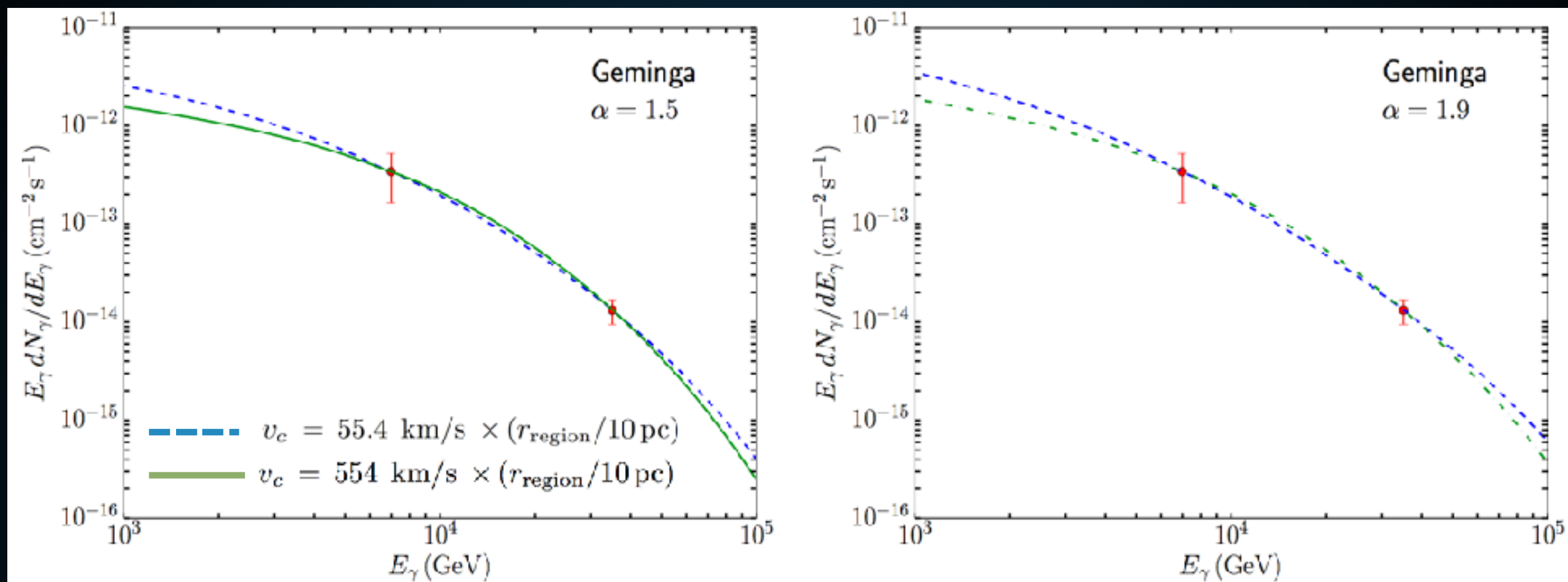
## X-RAY PULSAR WIND NEBULAE

---



- ▶ **Larger magnetic fields make compact PWN easier to observe**
- ▶ **Synchrotron dominated**
- ▶ **Higher energy peak**
- ▶ **More distant sources easier to see.**
- ▶ **Significant observation times require careful HAWC analysis.**

# GEMINGA SPECTRUM INDICATIVE OF CONVECTION



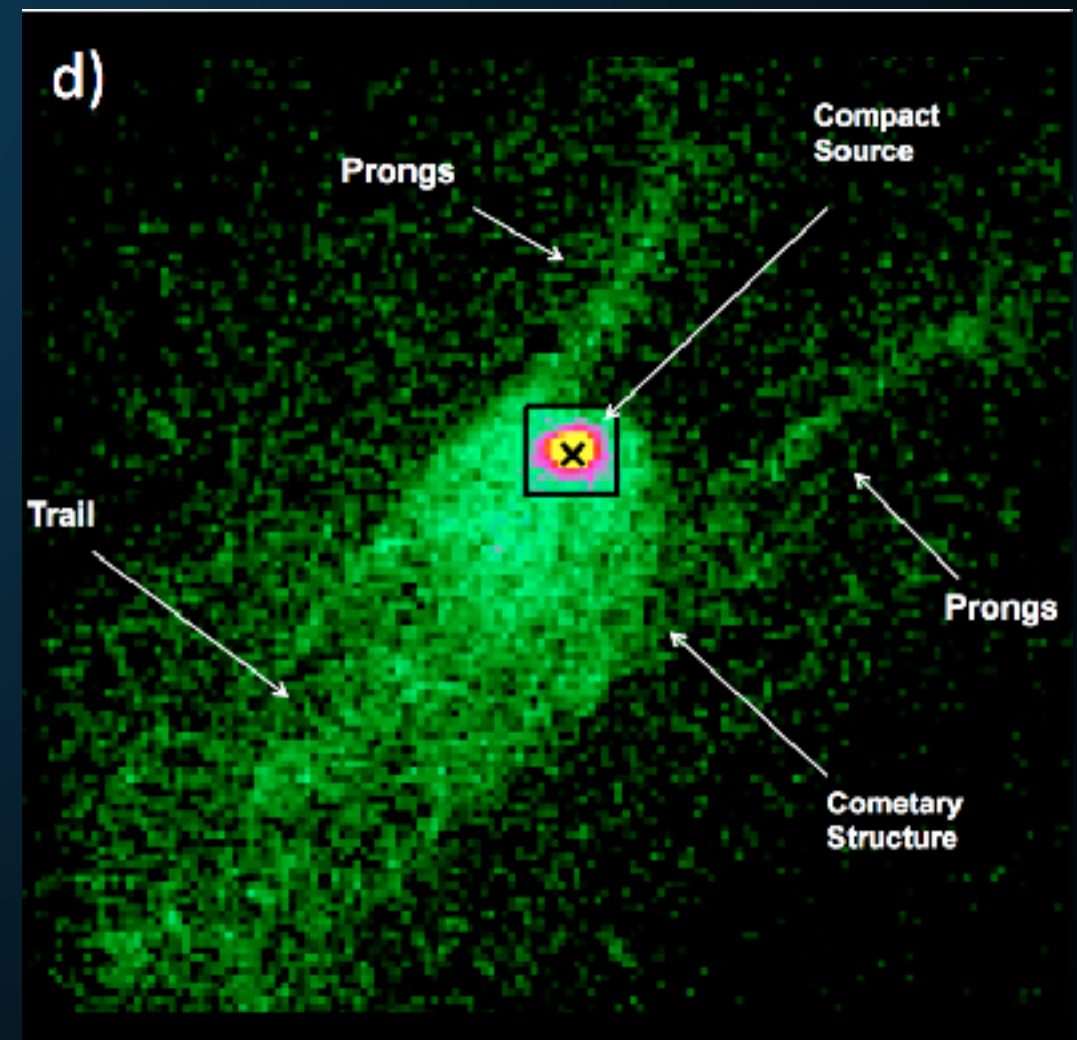
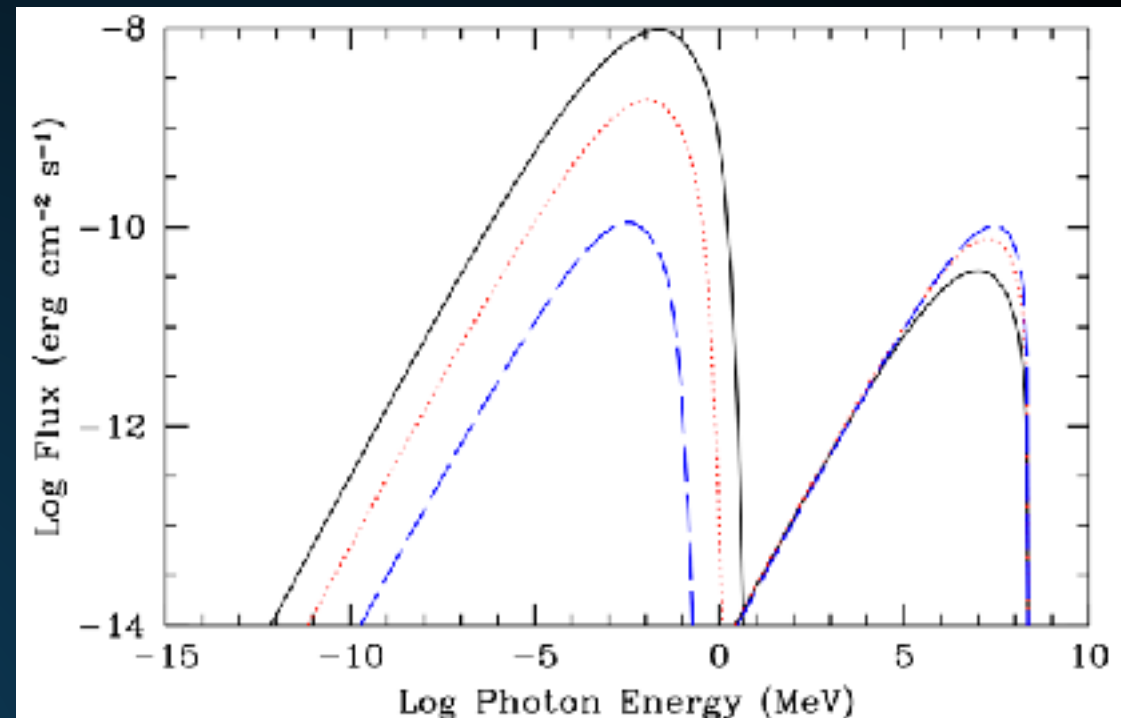
- ▶ **Geminga spectrum is fit better with convective models.**
- ▶ **Energy-independent diffusion provides identical results**
- ▶ **Best-fit spectral-index (-2.23 +/- 0.08) prefers high convection**

- ▶ Cooling dominated by  $20 \mu\text{G}$  magnetic field.

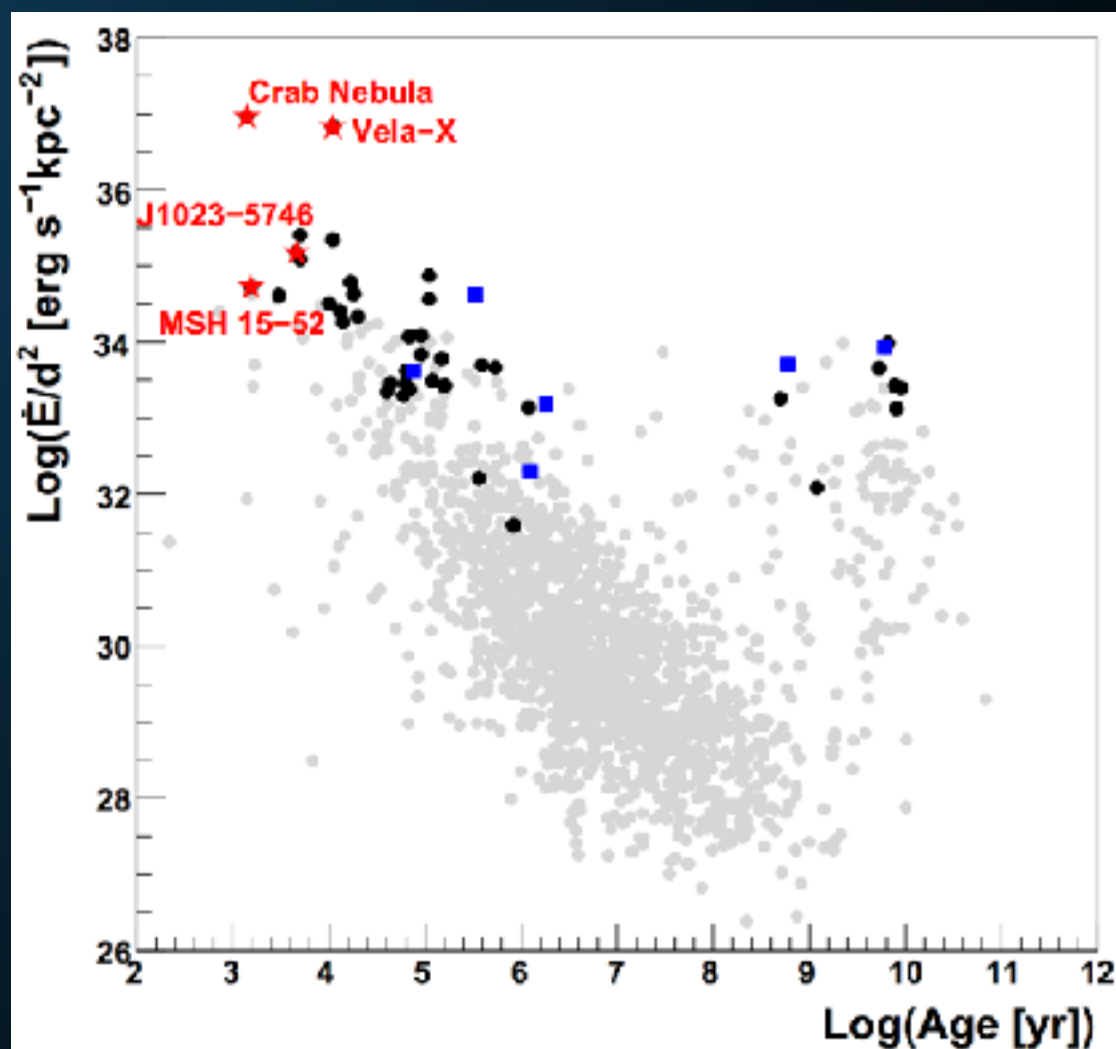
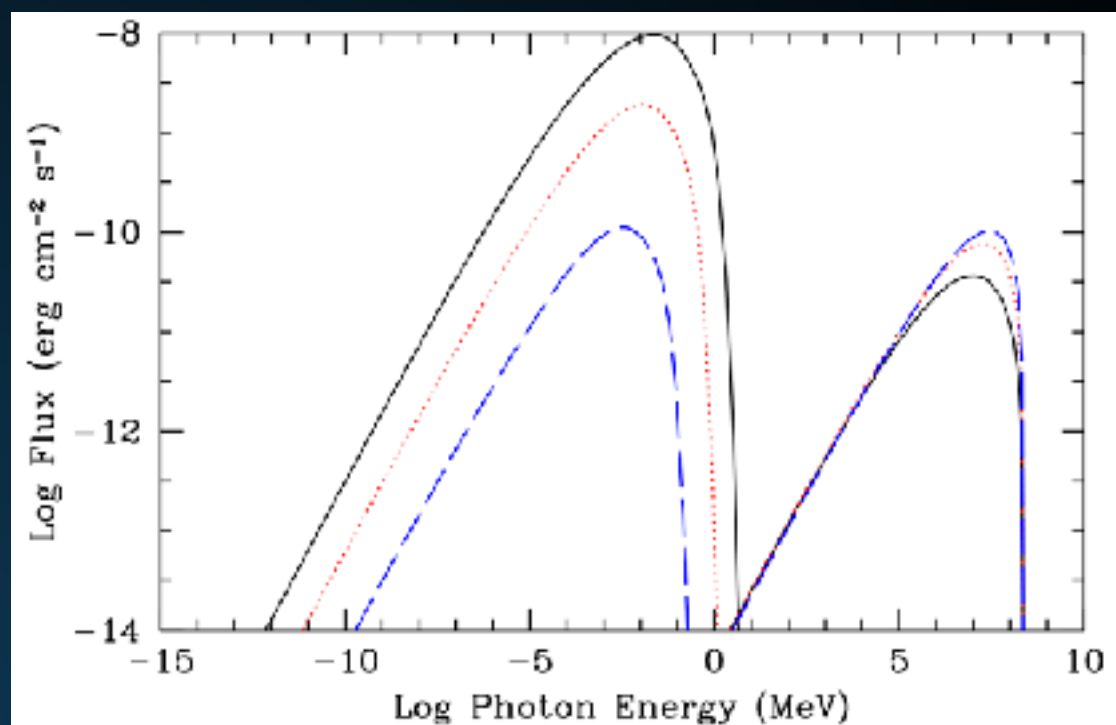
- ▶ Energy loss time:  $\sim 40$  years

- ▶ Distance Traveled:  $\sim 6$  pc for standard diffusion constant. Real diffusion must be slower.

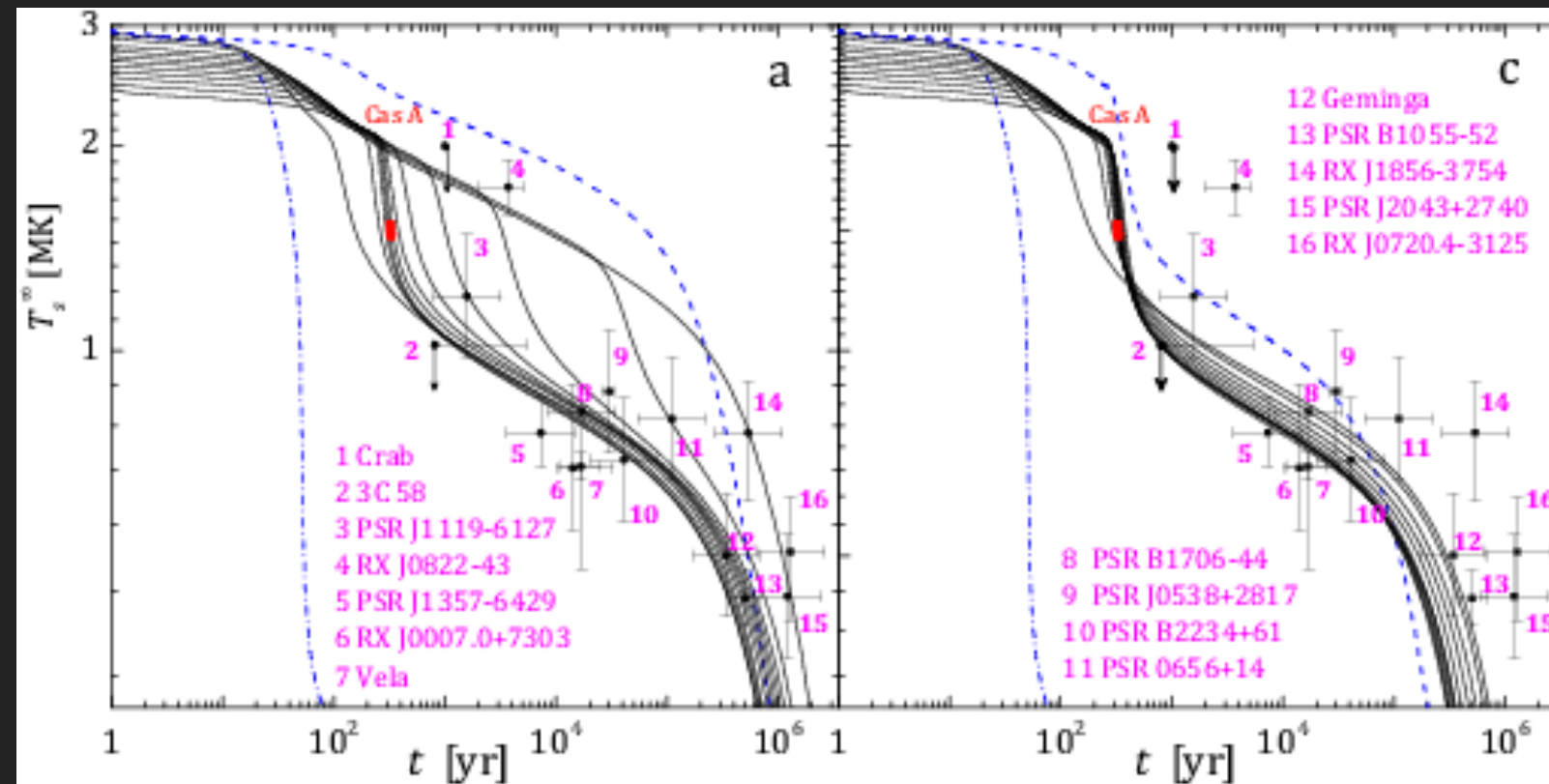
- ▶ The spectrum changes as a function of distance and time.



- ▶ Gamma-Ray produced through ICS should accompany synchrotron emission.
- ▶ Synchrotron observations imply very hard GeV gamma-ray spectrum.
- ▶ Conclusively prove leptonic nature of emission.

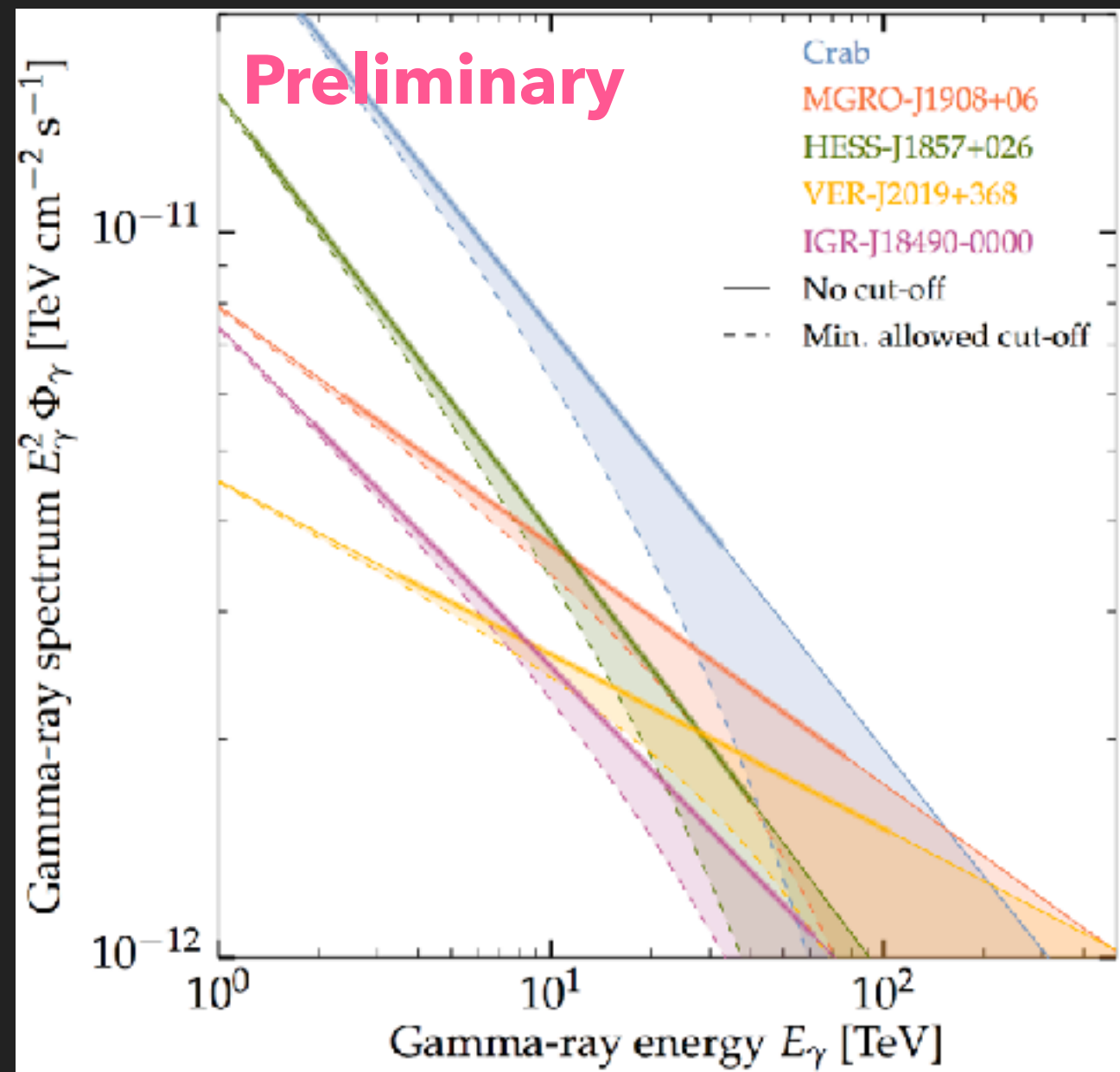


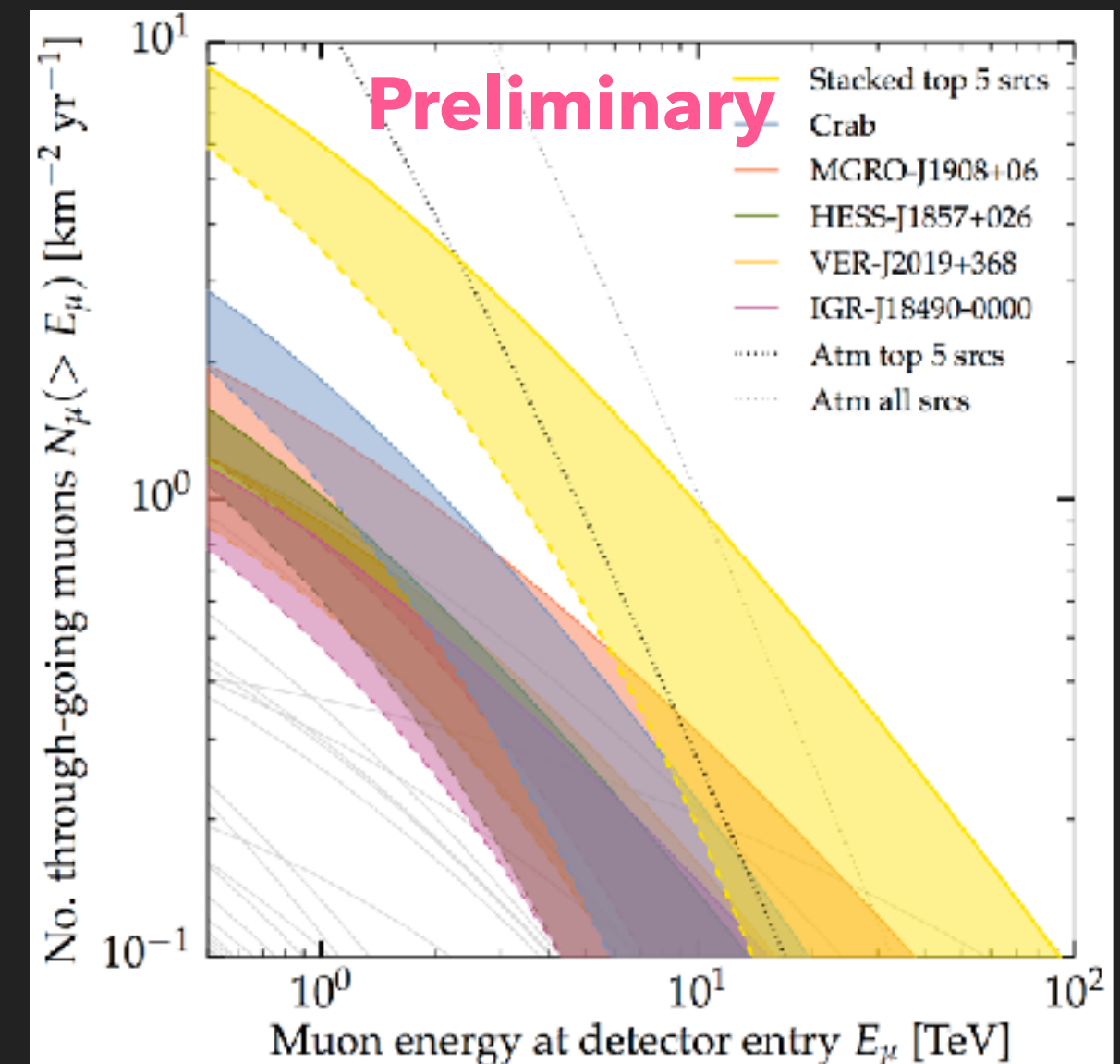
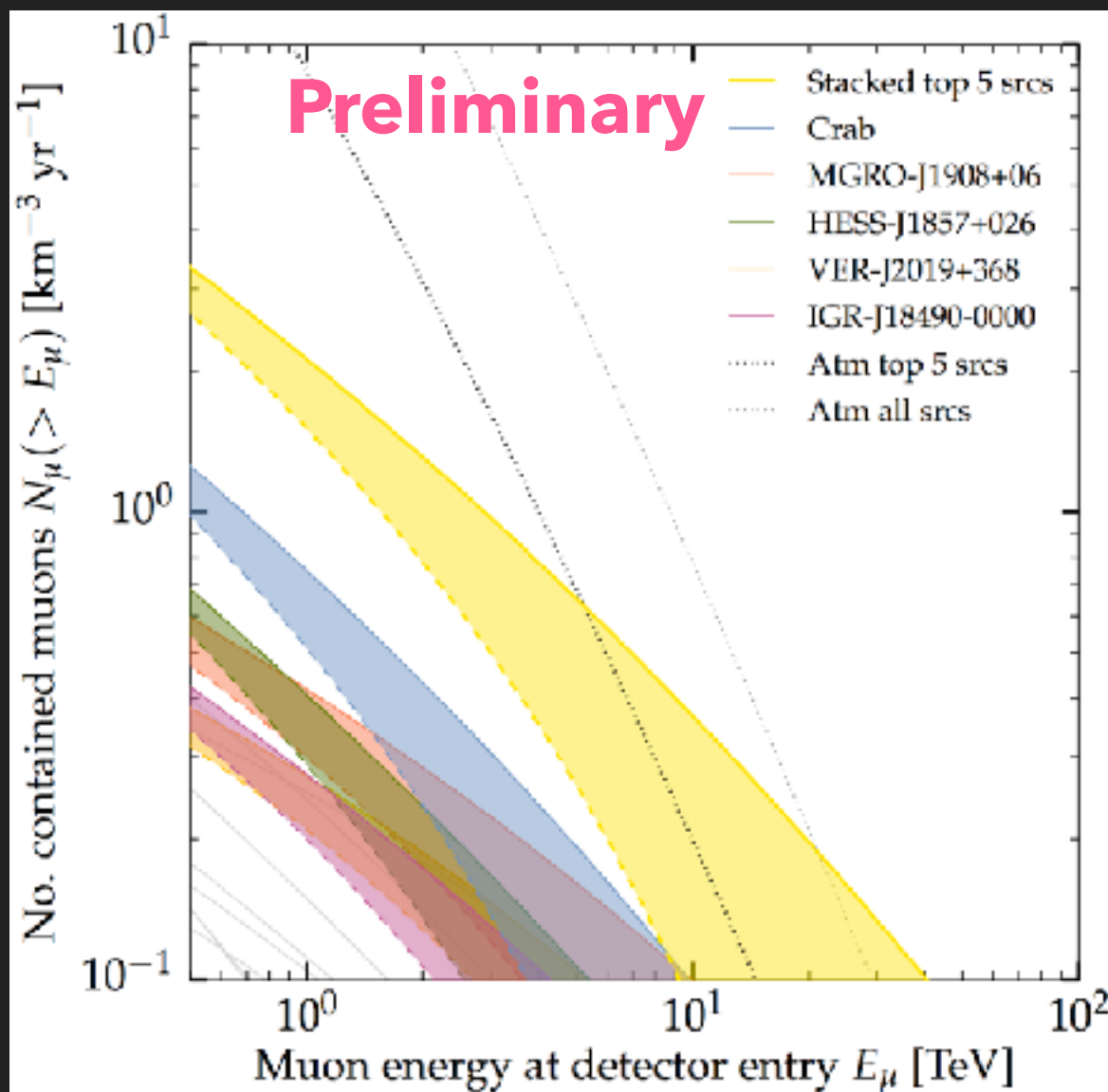
# THERMAL PULSAR EMISSION



- ▶ Hot neutron stars can also be observed via their isotropic thermal emission.
- ▶ X-Ray observations can be sensitive to  $\sim 2$  kpc for  $10^6$  K NS.
- ▶ Cooler NS extremely hard to see.
- ▶ Could potentially detect a system which has recently ceased producing TeV particles.

- ▶ HAWC sources are potential IceCube neutrino sources.
- ▶ Spectral measurements of HAWC sources are imperative to calculating the expected neutrino flux.
- ▶ Here we produce an analysis taking into account a 20% uncertainty in total flux, as well as spectral uncertainty due to an exponential cutoff.





- ▶ If these sources are hadronic, their stacked neutrino flux is detectable in current IceCube data.
- ▶ Alternatively, can place a strong constraint on the hadronic fraction of the brightest HAWC sources.